8-2023

Phenotypic and Transcriptomic Characterization of Rice SnRK1 Mutants Developed by CRISPR/Cas9 Mutagenesis

Maria Clara Faria Chaves
University of Arkansas, Fayetteville

Phenotypic and Transcriptomic Characterization of Rice SnRK1 Mutants Developed by CRISPR/Cas9 Mutagenesis.

A thesis submitted in partial fulfillment
of the requirements for the degree of
Master of Science in Crop, Soil and Environmental Sciences

by

Maria Clara Faria Chaves
University of Sao Paulo
Bachelor of Science in Agronomy, 2019

August 2023
University of Arkansas

This thesis is approved for recommendation to the Graduate Council.

Vibha Srivastava, Ph. D.
Thesis Director

Clemencia Rojas, Ph.D.
Committee Member

Joshua Sakon, Ph. D.
Committee Member

Ehsan Shakiba, Ph.D.
Committee Member

Abstract

SnRK1 is a heterotrimeric protein kinase that is composed of a catalytic subunit (α) and two regulatory subunits (β and βγ), and it has a main role in regulating energy homeostasis in the plant by modulating anabolic and catabolic process. SnRK1 phosphorylates and alters the activities of enzymes involved in metabolism and regulates gene expression by altering the activity of chromatin-remodeling enzymes or the transcription factors. Rice contains three functional paralogs of *SnRK1α*: *SnRK1αa* (LOC_Os03g17980), *SnRK1αb* (LOC_Os08g37800), and *SnRK1αc* (LOC_Os05g45420). This study focused on the function of these SnRK1 paralogs by evaluating the phenotypic and transcriptomic characteristics and the disease response of the knockout mutants developed by CRISPR/Cas9 mediated targeted mutagenesis. These knockout lines consisted of the double-mutant *snrk1αa+b* lines and the single mutant *snrk1αc* lines.

The phenotypic characterization of early-stage seedlings in ½ MS media showed that *snrka+b* mutants had lower seedling length compared with the WT but *snrk1αc* mutants were similar to the WT. The *snrk1αc* mutants showed phenotypic differences in the late developmental stages in the greenhouse, mainly in the yield parameters such as number of seeds per panicle and total weight of seeds per plant. This is in agreement with previous studies that showed that *SnRK1αa* and *SnRK1αb* are primarily expressed in the early seedling stages and *SnRK1αc* is significantly expressed in the later vegetative and reproductive phases.

Transcriptomic analysis on 7 days old seedlings showed that the defense response and the secondary metabolic process were upregulated in WT Kitaake seedlings exposed to extended darkness mimicking starvation. In contrast, the dark-exposed *snrk1αa+b* mutant showed downregulation of these biological processes and upregulation of light-induced processes such as ribosome biogenesis, translation, and DNA replication. However, not many biological processes

were found to be significantly up or down regulated in the *snrk1αc* mutant. Therefore, stress response during early stages of seedling growth is controlled by SnRK1αa and/or SnRK1αb, and SnRK1*α*c does not play a major role in the seedling growth or stress response during early phases of the development.

Next, the study examined the response of *snrk1* mutants against three different diseases: rice blast caused by *Magnaporthe oryzae*, sheath blight caused by *Rhizoctonia solani*, and bacterial panicle blight caused by *Burkholderia glumae*. Previous studies have shown that mutation in the *SnRK1* gene increases susceptibility to pathogens. However, in our experiments we did not observe an increase of susceptibility in the *snrk1αa+b* or *snrk1αc* mutants to bacterial panicle blight and sheath blight diseases. However, regarding blast fungus caused by *M. oryzae*, we noted that *snrk1* mutants were more susceptible, which is in accordance with the literature and our transcriptomic results that shows downregulation of defense response in snrk1 mutants.

Acknowledgments

First and foremost, I would like to express my sincere gratitude to my advisor Dr. Vibha Srivastava for her guidance, wisdom, and support throughout my master's degree. During the last two years, she was always available to provide guidance, answer questions, provide constructive criticism and offer encouragement. I am ever grateful to her for unwavering support and providing me with the experience and skills to apply in my career. Dr. Vibha Srivastava exceptional dedication to my growth as a researcher and constant encouragement shaped my academic and professional trajectory, and I am truly grateful for that. I want to extend my gratitude to my committee members, particularly Dr. Ehsan Shakiba for his support, encouragement, and guidance since the beginning of my academic career, Dr. Clemencia Rojas for her valuable input in my disease test experiments and her willingness to promptly respond to my questions, and Dr. Josh Sakon whose knowledge was valuable in building the foundation of my understanding in biochemistry which was essential for my research. I am very grateful to the committee members and my advisor for the expertise and mentorship which will be essential for my academic and professional life.

I am immensely grateful to both the past and present members of Dr. Vibha Srivastava's lab for their invaluable assistance and support throughout my research. I also want to acknowledge the assistance of all the staff and Professors of the University of Arkansas and the Crop Soil and Environmental Sciences department who contributed to the completion of this work. I want to express my gratitude to Johanna Echeverri Rico, a member of Dr. Clemencia Rojas' lab, for all her help, collaboration, and expertise for providing the data utilized in the initial bacterial panicle blight experiment presented in chapter 4. I want to extend my gratitude to Dr. Alejandro Rojas and his student Sherif Sharfadine for their invaluable guidance, help and

support in conducting sheath blight experiments. I extend my heartfelt appreciation to Dr. Martin Egan and his student Rinalda Proko for their unwavering assistance and expertise in facilitating experiments involving the *Magnaporthe oryzae* pathogen. I am extremely grateful for their collaboration, knowledge and patience which contributed significantly to the success of my research.

Finally, I would like to thank my family, my partner and my friends for their constant support, love, and motivation.

Table of Contents

Chapter I – Literature review

1. Introduction

1.1.Rice production and importance

Rice is an important crop in Arkansas and worldwide. The rice grain provides 20% of daily calories to the world's population (World Rice Statistics http://www.irri.org; FAOSTAT, http://apps.fao.org) and is consumed by more than three billion people every day throughout the world (Birla et al., 2017). Rice is grown in all the six continents (Asia, Africa, Oceania, Europa and North and South America), it is considered a stable food and part of cultural identities in many countries, where it provides food security (Muthayya et al., 2014). China is the largest rice producer in the world, followed by India in second place and Bangladesh in third place (Statista., 2023). In addition, rice is a vital source of carbohydrates, which the body needs in order to produce energy. It is also an important source of additional nutrients like proteins, vitamins, and minerals (Zhou et al., 2020). More than 60% of the rice produced in the Americas is grown in Brazil and the United States. In the U.S most of the rice grain produced is exported, where the four main rice-growing regions are the Arkansas Non-Delta, Mississippi River Delta, Gulf Coast, and Sacramento Valley of California (Chauhan et al., 2017). The main rice production state in the United States is Arkansas, which last year it was planted 1,106,000 acres of rice and it was produced 80,340,000 hundredweight (CWT), making a total value of production of $ 1,373,814,000 dollars (USDA, 2022). Rice, being a staple crop globally, relies on achieving optimal grain quality and yield. In order to enhance rice production, it is crucial to understand the genetic and molecular mechanisms underlying these traits.

1.2. SnRK1

Plants, like most organisms, need nutrients, water, and energy to survive. Adverse environmental conditions, such as lack of nutrients, sugar starvation, extreme temperatures, drought, or flooding, affect energy balance consequently impacting plant growth and development. Under stressful conditions, plants have mechanisms which trigger responses towards adaptation and survival. One mechanism is the signaling pathway regulated by sucrose non-fermenting (SNF) related protein kinase 1 (SnRK1), a protein that plays a central role in the regulation of metabolism and energy homeostasis (Baena-Gonzalez et al., 2007).

The SnRK1 is the plant ortholog of the evolutionarily conserved SNF1/AMPK protein kinase family that is essential for sensing energy status and adjusting growth. According to Emanuelle et al. (2015), the Snf1-related kinase 1 (SnRK1) is activated by starvation and energy-depleting stressful environments, activating catabolism, and inhibiting anabolism to preserve cellular energy homeostasis. The SnRK1 kinases regulate transcriptional networks by phosphorylating regulatory proteins and metabolism by phosphorylating certain metabolic enzymes engaged in alternate carbon sources consumption, gluconeogenesis, and respiration in yeast (Hedbacker & Carlson, 2008).

Several researchers observed that SnRK1 is activated under stress conditions, such as sugar starvation (Baena-Gonzalez et al., 2007), drought (Bledsoe et al., 2017), hypoxia (Chen et al., 2017) and nutrient deficiency (Nunes et al., 2013). Additionally, studies demonstrated that SnRK1 is related to plant survival against many pathogens, such as *Xanthomonas oryzae pv. oryzae* strain PXO99, *Magnaporthe oryzae* isolate VT5M1, *Cochliobolus miyabeanus strain* Cm988, and *Rhizoctonia solani* AG-1 IA in rice (Filipe et al., 2018) and geminiviruses in *Nicotiana benthamiana* (Hao et al., 2003). SnRK1 is also involved in carbohydrate metabolism

by saving energy and promoting nutrient remobilization when the plant is under starving conditions. (Jossier et al., 2009; Kanegae et al., 2005).

1.3.SnRK1 structure

Different from SNF1 and AMPK, the hetero-trimeric SnRK1 complex contains three subunits (Figure 1.1), catalytic α subunit, and regulatory β and βγ subunits (Broeckx et al., 2016; Emanuelle et al., 2015; Jamsheer et al., 2021; Polge & Thomas, 2006). The catalytic α subunits contain N-terminal catalytic (kinase) domain (CD), which contains the activation loop (T loop) that is required for significant kinase activity, followed by Ubiquitin-Associated Domain (UBA) and a C-terminal regulatory domain (CTD) (Figure 1.2), which are engaged in complex interactions (with the β and βγ subunits) as well as kinase activity regulation. The regulatory β subunits not only serve as complex scaffolds, but they also have an impact on kinase activity, localization, and substrate selectivity. The regulatory βγ subunit in mammals serves as the complex's energy sensor, controlling kinase activity by binding adenylate (ATP, ADP, and AMP) (Broeckx et al., 2016).

1.4.SnRK1 genes in rice

Rice contains three functional paralogs of *SnRK1α*: *SnRK1αa* (LOC_Os03g17980), *SnRK1αb* (LOC_Os08g37800), and *SnRK1αc* (LOC_Os05g45420) (Figure 1.3). *SnRK1αa* and *SnRK1αb* are highly homologous to each other and have an important role in seedling stages and endosperm development (Figure 1.4). On the other hand, *SnRK1αc* is highly expressed in reproductive stages (Figure 1.4) (Takano et al., 1998). A fourth paralog, *SnRK1αd* (LOC_Os07g09610) was recently reported (Wang et al., 2021), which is highly diverged and

weakly expressed in plants (Jamsheer et al., 2019). Therefore, contribution of *SnRK1αd* in SnRK1 signaling is believed to be limited. This research is focused on the catalytic *α* subunit in rice plants.

1.5. SnRK1: a global regulator of gene expression

Another important aspect of SnRK1 protein that researchers have noted is that SnRK1 is a global regulator of gene expression. Different studies observed that SnRK1 regulates over 1000 genes in stress conditions (Baena-Gonzalez et al., 2007; Cho et al., 2012; Pedrotti et al., 2018; Wang et al., 2021) and normal conditions (Henninger et al., 2022; Wang et al., 2021). SnRK1 activation causes the repression or induction of several of genes, which are connected to anabolic and catabolic processes (Peixoto & Baena-Gonzalez 2022). Baena-Gonzalez et al. (2007) reported that Arabidopsis *SnRK1α/KIN10* regulates 278 genes which contribute to plant survival under sugar starvation and stressful conditions. The results indicated that *SnRK1α/KIN10* activates genes related to catabolic pathways involved in the degradation of energy sources such as starch, sucrose, amino acid, lipid, and protein to produce energy for the plant. This discovery was also reported by Cho et al. (2012), who observed that in both Arabidopsis (*Arabidopsis thaliana*) and rice (*Oryza sativa*), SnRK1 regulates specific stress-inducible genes by binding directly to target gene chromatin inside the nucleus. Interestingly, trehalose-6-phosphate (T6P) that is a signaling molecule and positively correlates with sugar levels, was found to suppress SnRK1 activity. This observation supports our understanding that SnRK1 regulates plant growth during starvation (low sugar). It was also observed that SnRK1 is involved in seedling establishment genes in Arabidopsis (Henninger et al., 2022) and it is necessary to repress starvation induced genes under normal environments (Wang et al., 2021).

The accessibility of DNA regulatory elements is altered by chromatin remodeling, which has an impact on transcriptional activity of an organism. Studies have observed the connection between SnRK1 and chromatin remodeling (Cho et al., 2012; Wang et al., 2021). Chromatin is a complex of DNA and proteins that make the chromosomes. Histones pack the DNA in a compact form to fit in the nucleus inside the cell and play an essential role in gene expression, by influencing DNA transcription (Gross et al., 2015). The chromatin regulator JMJ705, which is stimulated by stress signals, encodes a histone lysine demethylase that reverses trimethylation of H3K27me3 (a mark that indicates the tri-methylation of lysine 27 on histone H3 protein in the DNA). In other words, JMJ705 removes the methyl group from the histone proteins and the transcription of genes associated with histones containing this mark is activated. Wang et al. (2021) discovered that the *SnRK1αc* (LOC_Os05g45420), under starvation, activates JMJ705 by phosphorylation. Upon activation, JMJ705 demethylates H3K27me3 associated with genes that respond to starvation, including starvation-responsive transcription factors. Another study found that, by chromatin modification, SnRK1 participates in transcriptional programming during the transition phase in legume seeds. It was observed that SnRK1 regulates the activity of chromatin remodeling proteins and modulates the expression of genes related in the abscisic acid pathway (Radchuk et al, 2006; Radchuk et al, 2010).

1.6. SnRK1's role in senescence

Senescence is a natural process of plant development and growth; however, it is often induced by stressful environments. SnRK1 is involved in extending leaf lifetime, delaying leaf senescence, and modulating numerous senescence-related physiological, genetic, and molecular mechanisms in plants (Baena-González et al., 2007; Chen et al., 2017; Cho et al., 2012; Wang et

al., 2019). SnRK1 participates in leaf senescence through different processes. Wang et al. (2019) noticed that positive regulators of leaf senescence, such as *SAG13* and *WRKY53* genes, were downregulated in Arabidopsis transgenic lines overexpressing maize SnRK1 genes (*ZmSnRK1.1, ZmSnRK1.2 and ZmSnRK1.3*). A mechanism SnRK1 uses to extend a leaf's lifetime is by positively regulating autophagy activation (Chen et al., 2017). Accordingly, Baena-Gonzalez et al. (2007) and Wang et al. (2019) noted delayed leaf senescence in *SnRK1* overexpression lines of Arabidopsis. Wang et al. (2019) also reported that lines overexpressing SnRK1 led to enhanced biomass and accumulated significantly more chlorophyll when compared with the wild type under normal conditions.

1.7. SnRK1's role in carbohydrate metabolism

Plants are autotrophic organisms, which means they produce their own food to survive. In photosynthesis, plants utilize carbon dioxide, light, and water to produce monosaccharide glucose, and the excess glucose is stored in polysaccharides called starch. Several reports studied the role of SnRK1 in carbohydrate metabolism. It was noticed that when plants are under low carbon conditions, they activate the SnRK1 enzyme to promote energy saving and nutrient remobilization strategies (Baena-Gonzalez et al., 2007; Kanegae et al., 2005; McKibbin et al., 2006). McKibbin et al. (2006) investigated the SnRK1 activity and its involvement in sugar metabolism in transgenic potato (*Solanum tuberosum* cv. Prairie). The *SnRK1* overexpressing lines had lower glucose levels and higher starch content when compared with the wild type. These results are in accordance with those presented by Wang et al. (2019), who observed that transgenic Arabidopsis lines overexpressing SnRK1 exhibited more starch in the leaves and seeds when compared with the control. This finding is consistent with that of Kanegae et al.

(2005), who studied the role of rice (*Oryza sativa*) *SnRK1* genes in sugar metabolism and noticed that the *SnRK1* silencing lines did not accumulate starch. Additionally, Baena-Gonzalez et al. (2007) demonstrated that the SnRK1 enzyme has a regulatory role in starch allocation at night.

Glucose is a key source of energy for almost all living things. Free glucose molecules, on the other hand, cannot be stored, because large concentrations of glucose disrupt the cell's osmotic balance, potentially ending in cell death. The solution is to store glucose in starch units, a huge osmotically inactive polymer. Starch is a polysaccharide found in all plants and researchers found that SnRK1 regulates carbohydrate metabolism and participates in starch biosynthesis (Bledsoe et al., 2017; Kanegae et al., 2005; Jossier et al., 2009; McKibbin et al., 2006; Nunes et al., 2013). Previous research examined the relation between T6P and SnRK1 in carbon partitioning (Bledsoe et al., 2017; Nunes et al., 2013). Nunes et al. (2013) observed that in Arabidopsis, T6P accumulates and inhibits SnRK1 when sugar is abundant, limiting expression of genes associated in the stress survival response and promoting expression of genes involved in the feast response, including growth processes. On the other hand, in sugar starvation conditions, SnRK1 is activated, and starch is synthesized, thus, enabling plant survival under stress environments. This outcome is contrary to that observed by Bledsoe et al. (2017), who discovered that starch biosynthesis was inhibited in maize under drought stress. It was reported that when the T6P concentration drops, multiple potential SnRK1 target genes are transcribed, causing a metabolic shift from biosynthesis to catabolism. A similar result was found by Jossier et al. (2009), who observed that overexpression of SnRK1 caused lower starch content in Arabidopsis. Molecular, biochemical, and genetic studies demonstrated different mechanisms SnRK1 uses to regulate carbohydrate metabolism in plant growth and development (Baena-Gonzalez et al., 2007; Jossier et al., 2009; Kanegae et al., 2005; McKibbin et al., 2006).

McKibbin et al. (2006) noticed that SnRK1 in potatoes (*Solanum tuberosum* cv. Prairie) regulates genes encoding sucrose synthase and ADP glucose pyrophosphorylase, the enzymes participating in starch biosynthesis. These results reflect those of Kanegae et al. (2005), who found that SnRK1 in rice (*Oryza sativa*), during the development of caryopsis, promotes expression of genes which are involved in conversion of sucrose to starch. Jossier et al. (2009) discovered a different mechanism used by SnRK1. It was found that SnRK1 is involved in the abscisic acid (ABA) hormone pathway by intermediating with glucose signaling. They observed that Arabidopsis seedlings overexpressing *SnRK1* exhibited hypersensitive response to ABA and this response was enhanced even further when glucose was added to the medium. It thus suggests that SnRK1 could connect sugar and ABA signaling pathways (Jossier et al., 2009). Other papers also noticed the connection between SnRK1 and ABA pathways (Belda-Palazón et al., 2020; Radchuk et al, 2006; Radchuk et al, 2010). Furthermore, a recent study discovered that SnRK1 is involved in the regulation of sorbitol, a common sugar alcohol that plays an important role in carbohydrate metabolism, plant development and tolerance to stress in rosacea tree fruits, such as apples (Meng et al., 2023). They noted that sucrose decreases SnRK1 expression while sorbitol increases it. They also found that SnRK1 phosphorylates the TF bZIP39, which increases the expression of two essential sorbitol metabolism-related genes, SORBITOL DEHYDROGENASE 1 (SDH1) and ALDOSE-6-PHOSPHATE REDUCTASE (A6PR).

1.8. SnRK1 regulates TOR signaling

TOR (Target of Rapamycin) is part of the phosphatidylinositol 3-kinase-related protein kinase family. TOR is activated under nutrient-rich conditions to promote anabolic processes, such as cell division, protein synthesis and plant growth and represses catabolism, showing a

reverse action of the SnRK1. TOR alters genes related to metabolism, cell cycle, signaling, and transcription through the phosphorylation of direct targets and transcriptional reprogramming (Margalha et al., 2019). The conserved protein kinases SnRK1 and TOR are co-regulated to control cellular metabolism, growth, and stress responses in plants. Both kinases control many similar downstream targets and are responsive to nutrition and energy status (Peixoto & Baena-Gonzales, 2021). In response to low-energy conditions, SnRK1 is activated that negatively regulates TOR to repress its activity (Nukarinen et al., 2016; Belda-Palazón et al., 2020). On the other hand, under normal conditions SnRK1 also interacts with TOR for promotion of plant growth and development (Jamsheer et al., 2021). Therefore, SnRK1 and TOR activities are necessary to regulate energy homeostasis and stabilize stress responses with plant growth and development.

1.9. SnRK1 and stress conditions

SnRK1, which is integral to each stage of a plant's life, from seedling to senescence, uses different mechanisms to assist in plant survival during stressful conditions. For example, SnRK1 regulates genes involved in stress- related adaptation (Baena-Gonzalez et al., 2007; Cho et al., 2012; Filipe et al., 2018). SnRK1 coordinates transcriptional networks to promote energy-producing pathways and suppress energy-consuming pathways (Cho et al., 2012; Tsai & Gazzarrini, 2012). SnRK1 also positively regulates FUSCA3 (a transcription factor associated with regulation of plant development) stability through physical interaction and phosphorylation (Tsai & Gazzarrini, 2012). Additionally, SnRK1 modulates a range of downstream genes and sugar signals which are crucial to coordinate biochemical and physiological responses (Chen et al., 2017; Jossier et al., 2009; Wang et al., 2019).

1.10.a. Responses to abiotic stress

Abiotic stress is the main cause of yield loss in crops worldwide. Many researchers have revealed the role of SnRK1 in plants under adverse environmental situations, such as sugar starvation, nutrient deprivation, hypoxic, flooding and drought (Baena-Gonzalez et al., 2007; Bledsoe et al., 2017; Chen et al., 2017; Cho et al., 2012, Nunes et al., 2013). To preserve cellular energy homeostasis in stressful conditions, SnRK1 promotes catabolism and suppresses anabolism using different approaches. SnRK1controls expression of genes involved in abiotic stress resistance through its direct involvement with target gene chromatins inside the nucleus (Cho et al., 2012; Wang et al., 2021) or coordinating transcription networks, contributing to the induction of plant resistance to abiotic stress (Baena-Gonzalez et al., 2007). Prior studies noticed that SnRK1 regulates the expression of genes involved in plant survival by interacting with the trehalose-6-phosphate (T6P) (T6P), a sugar signal in plants (Nunes et al., 2013). Moreover, the SnRK1 protein increases plant tolerance under stress by enhancing the phosphorylation of ATG1 (autophagy-related gene 1) to activate autophagy by initiating autophagosome formation (Chen et al., 2017). Another research found that, in Arabidopsis, SnRK1 inhibits anthocyanin biosynthesis by repressing MBW, a transcription factor complex that regulates anthocyanin biosynthesis (Broucke et al., 2023). These findings imply that anthocyanin production may be energetically costly, which could increase energy deficit under stressful conditions (Broucke et al., 2023).

The work of Baena-Gonzalez et al. (2007) demonstrated the function of SnRK1 in Arabidopsis growth and development in stressful conditions. This study noticed that *SnRK1α/KIN10* overexpression lines survived under limited sugar supply and that *SnRK1α/KIN10* silenced lines senesced before flowering. This finding is consistent with that of

Chen et al. (2017), who found that *SnRK1α/KIN10* overexpression lines were more resistant to stressful conditions such as drought, nutrient starvation, and hypoxia, when compared to the wild type. Similar results were observed by Nunes et al. (2013), who studied the effects of SnRK1 in Arabidopsis under nitrogen deficiency and cold temperature conditions. It was found that the plants overexpressing SnRK1, in response to warm temperatures, were unable to rapidly boost their growth. Nunes et al. (2013) also noted the SnRK1 activity increased 30% when plants were under nitrogen deficiency. Bledsoe et al. (2017) observed that SnRK1 enhanced drought tolerance in maize. A further important discovery was that, in Arabidopsis, *SnRK1α/KIN10* overexpression lines enhanced autophagic activity, indicating that *SnRK1α/KIN10* is a positive regulator of autophagy activation (Chen et al., 2017).

1.10.b Responses to biotic stress

Biotic stress is caused from the interaction between plants and pathogenic organisms, such as viruses, bacteria, fungi, nematodes, and pests. Like humans, plants have an immune system which is composed of mechanisms and responses to inhibit pathogen activity and prevent disease. Many researchers studied the relationship between the SnRK1 and pathogens such as bacteria, fungi, and viruses. Filipe et al. (2018) investigated the effect of SnRK1α's overexpression and silencing in both rice (*Oryza sativa*) growth and tolerance to the pathogens: *Xanthomonas oryzae* strain PXO99, *Magnaporthe oryzae* isolate VT5M1, *Cochliobolus miyabeanus* strain Cm988, and *Rhizoctonia solani* AG-1 IA in rice. The results indicated *SnRK1α* silencing enhanced rice susceptibility to the pathogens, whereas *SnRK1α* overexpression enhanced the resistance of the lines. There are similarities between these results and those described by Kim et al. (2015), who studied the function of SnRK1 in rice resistance against the

fungal pathogen *Magnaporthe oryzae*, and *Xanthomonas oryzae pv. oryzae* (Xoo). It was noticed that the *SnRK1αa* (LOC_Os03g17980) activation line improved the rice resistance against the pathogens studied, whereas the SnRK1α eletion line increased rice susceptibility to infections. This finding is consistent with that of Hao et al. (2003) who noticed that SnRK1 overexpression in *Nicotiana benthamiana* led to superior resistance against two different geminiviruses: AL2 from *Tomato golden mosaic virus* (TGMV; genus *Begomovirus*) and L2 from *Beet curly top virus* (BCTV; genus *Curtovirus*). Another research found that *SnRK1* gene silencing enhanced the phytotoxic effects of the toxin Deoxynivaleno produced by *Fusarium* (Perochon et al., 2019).

Plants use signaling molecules, sugars, hormones, transcription factors, and protein kinases as part of their defense system. SnRK1 is part of the stress and energy signaling, and it is involved in different mechanisms related to plant defense against pathogens. Perochon et al. (2019) discovered that SnRK1 in wheat (*Triticum aestivum*) enhances resistance against *Fusarium* mycotoxin by interacting with TaFROG (*Triticum aestivum Fusarium* Resistance Orphan Gene). These results reflect those of Filipe et al. (2018) and Kim et al. (2015), who found that SnRK1 protein in rice (*Oryza sativa*) activates genes correlated with plant immune system. Filipe et al. (2018) also found that SnRK1 enhances the action of both salicylic acid pathway and jasmonate regulated defense response, which are the two plant immunity mechanisms. Hao et al. (2003) also confirmed that SnRK1 is an important component of a plant's immune system. They observed that Geminivirus AL2 and L2 proteins enhance susceptibility in *N. benthamiana* by inactivating SnRK1 protein.

In conclusion, the sucrose non-fermenting related protein kinase 1 (SnRK1) is a central regulator of plant growth, development, and stress responses by regulating genes, and interacting with molecular and cellular mechanisms in plants (Baena-Gonzalez et al., 2007; Chen et al.,

2017; Cho et al., 2012; Jossier et al., 2009; Nunes et al., 2013; Perochon et al., 2019; Tsai & Gazzarrini, 2012). SnRK1 provides plant plasticity and survival when under abiotic and biotic stressful environments by regulating metabolism and energy homeostasis (Bledsoe et al., 2017; Chen et al., 2017; Cho et al., 2012; Filipe et al., 2018; Hao et al., 2003; Kim et al., 2015; Perochon et al., 2019, Wang et al., 2019). Additionally, SnRK1 is involved in sugar signaling, starch biosynthesis and carbohydrate metabolism (Baena-Gonzalez et al., 2007; Jossier et al., 2009; Kanegae et al., 2005; McKibbin et al., 2006; Nunes et al., 2013; Wang et al., 2019).

References

Baena-González, E., Rolland, F., Thevelein, J. M., & Sheen, J. (2007). A central integrator of transcription networks in plant stress and energy signalling. Nature, 448(7156), 938–942. https://doi.org/10.1038/nature06069

Belda-Palaz On, B., Onica Costa, M., Beeckman, T., Rolland, F., Baena-Gonz Alez, E., & Niyogi, K. (2022). ABA represses TOR and root meristem activity through nuclear exit of the SnRK1 kinase. https://doi.org/10.1073/pnas

Birla, D. S., Malik, K., Sainger, M., Chaudhary, D., Jaiwal, R., & Jaiwal, P. K. (2017). Progress and challenges in improving the nutritional quality of rice (Oryza sativa L.). Critical Reviews in Food Science and Nutrition, 57(11), 2455–2481. https://doi.org/10.1080/10408398.2015.1084992

Bledsoe, S. W., Henry, C., Griffiths, C. A., Paul, M. J., Feil, R., Lunn, J. E., Stitt, M., & Lagrimini, L. M. (2017). The role of T6P and SnRK1 in maize early kernel development and events leading to stress-induced kernel abortion. BMC Plant Biology, 17(1). https://doi.org/10.1186/s12870-017-1018-2

Broeckx, T., Hulsmans, S., & Rolland, F. (2016). The plant energy sensor: evolutionary conservation and divergence of SnRK1 structure, regulation, and function. In Journal of experimental botany (Vol. 67, Issue 22, pp. 6215–6252). https://doi.org/10.1093/jxb/erw416

Broucke, E., Dang, T. T. V., Li, Y., Hulsmans, S., Van Leene, J., De Jaeger, G., Hwang, I., Van den Ende, W., & Rolland, F. (2023). SnRK1 inhibits anthocyanin biosynthesis through both transcriptional regulation and direct phosphorylation and dissociation of the MYB/bHLH/TTG1 MBW complex. The Plant Journal : for Cell and Molecular Biology. https://doi.org/10.1111/tpj.16312

Chauhan, B. S., Jabran, K., & Mahajan, G. (2017). Rice Production Worldwide. Springer International Publishing AG. https://doi.org/10.1007/978-3-319-47516-5

Chen, L., Su, Z. Z., Huang, L., Xia, F. N., Qi, H., Xie, L. J., Xiao, S., & Chen, Q. F. (2017). The AMP-activated protein kinase kin10 is involved in the regulation of autophagy in arabidopsis. Frontiers in Plant Science, 8. https://doi.org/10.3389/fpls.2017.01201

Cho, Y. H., Hong, J. W., Kim, E. C., & Yoo, S. D. (2012a). Regulatory functions of SnRK1 in stress-responsive gene expression and in plant growth and development. Plant Physiology, 158(4), 1955–1964. https://doi.org/10.1104/pp.111.189829

Cho, Y. H., Hong, J. W., Kim, E. C., & Yoo, S. D. (2012b). Regulatory functions of SnRK1 in stress-responsive gene expression and in plant growth and development. Plant Physiology, 158(4), 1955–1964. https://doi.org/10.1104/pp.111.189829

Emanuelle, S., Doblin, M. S., Stapleton, D. I., Bacic, A., & Gooley, P. R. (2016). Molecular Insights into the Enigmatic Metabolic Regulator, SnRK1. In Trends in Plant Science (Vol. 21, Issue 4, pp. 341–353). Elsevier Ltd. https://doi.org/10.1016/j.tplants.2015.11.001

Emanuelle, S., Hossain, M. I., Moller, I. E., Pedersen, H. L., Van De Meene, A. M. L., Doblin, M. S., Koay, A., Oakhill, J. S., Scott, J. W., Willats, W. G. T., Kemp, B. E., Bacic, A., Gooley, P. R., & Stapleton, D. I. (2015). SnRK1 from Arabidopsis thaliana is an atypical AMPK. Plant Journal, 82(2), 183–192. https://doi.org/10.1111/tpj.12813

Filipe, O., De Vleesschauwer, D., Haeck, A., Demeestere, K., & Höfte, M. (2018). The energy sensor OsSnRK1αa confers broad-spectrum disease resistance in rice. Scientific Reports, 8(1). https://doi.org/10.1038/s41598-018-22101-6

Gross, D. S., Chowdhary, S., Anandhakumar, J., & Kainth, A. S. (2015). chromatin. Current Biology, 25(24), R1158-R1163. https://doi.org/10.1016/j.cub.2015.10.059

Hao, L., Wang, H., Sunter, G., & Bisaro, D. M. (2003). Geminivirus AL2 and L2 proteins interact with and inactivate SNF1 kinase. Plant Cell, 15(4), 1034–1048. https://doi.org/10.1105/tpc.009530

Hedbacker, K., & Carlson, M. (n.d.). SNF1/AMPK pathways in yeast. http://www.ncbi.nlm.nih.gov/entrez/query.fcgi?CMD=search&DB=pubmed

Henninger, M., Pedrotti, L., Krischke, M., Draken, J., Wildenhain, T., Fekete, A., Rolland, F., Müller, M. J., Fröschel, C., Weiste, C., & Dröge-Laser, W. (2022). The evolutionarily conserved kinase SnRK1 orchestrates resource mobilization during Arabidopsis seedling establishment. Plant Cell, 34(1), 616–632. https://doi.org/10.1093/plcell/koab270

Jamsheer K, M., Kumar, M., & Srivastava, V. (2021). SNF1-related protein kinase 1: the many-faced signaling hub regulating developmental plasticity in plants. Journal of Experimental Botany, 72(17), 6042–6065. https://doi.org/10.1093/jxb/erab079

Jamsheer, M. K., Jindal, S., & Laxmi, A. (2019). Evolution of TOR–SnRK dynamics in green plants and its integration with phytohormone signaling networks. In Journal of Experimental Botany (Vol. 70, Issue 8, pp. 2239–2259). Oxford University Press. https://doi.org/10.1093/jxb/erz107

Jossier, M., Bouly, J. P., Meimoun, P., Arjmand, A., Lessard, P., Hawley, S., Grahame Hardie, D., & Thomas, M. (2009). SnRK1 (SNF1-related kinase 1) has a central role in sugar and ABA signalling in Arabidopsis thaliana. Plant Journal, 59(2), 316–328. https://doi.org/10.1111/j.1365-313X.2009.03871.x

Kanegae, H., Miyoshi, K., Hirose, T., Tsuchimoto, S., Mori, M., Nagato, Y., & Takano, M. (2005). Expressions of rice sucrose non-fermenting-1 related protein kinase 1 genes are differently regulated during the caryopsis development. Plant Physiology and Biochemistry, 43(7), 669–679. https://doi.org/10.1016/j.plaphy.2005.06.004

Kim, Y. A., Moon, H., & Park, C. J. (2019). CRISPR/Cas9-targeted mutagenesis of Os8N3 in rice to confer resistance to Xanthomonas oryzae pv. oryzae. Rice, 12(1). https://doi.org/10.1186/s12284-019-0325-7

Margalha, L., Confraria, A., & Baena-González, E. (2019). SnRK1 and TOR: Modulating growth–defense trade-offs in plant stress responses. In Journal of Experimental Botany (Vol. 70, Issue 8, pp. 2261–2274). Oxford University Press. https://doi.org/10.1093/jxb/erz066

Martínez-Barajas, E., Delatte, T., Schluepmann, H., de Jong, G. J., Somsen, G. W., Nunes, C., Primavesi, L. F., Coello, P., Mitchell, R. A. C., & Paul, M. J. (2011). Wheat grain development is characterized by remarkable trehalose 6-phosphate accumulation pregrain filling: Tissue distribution and relationship to SNF1-related protein kinase1 activity. Plant Physiology, 156(1), 373–381. https://doi.org/10.1104/pp.111.174524

Meng, D., Cao, H., Yang, Q., Zhang, M., Borejsza-Wysocka, E., Wang, H., Dandekar, A. M., Fei, Z., & Cheng, L. (2023). SnRK1 kinase-mediated phosphorylation of transcription factor bZIP39 regulates sorbitol metabolism in apple. Plant Physiology (Bethesda). https://doi.org/10.1093/plphys/kiad226

McKibbin, R. S., Muttucumaru, N., Paul, M. J., Powers, S. J., Burrell, M. M., Coates, S., Purcell, P. C., Tiessen, A., Geigenberger, P., & Halford, N. G. (2006). Production of high-starch, low-glucose potatoes through over-expression of the metabolic regulator SnRK1. Plant Biotechnology Journal, 4(4), 409–418. https://doi.org/10.1111/j.1467-7652.2006.00190.x

Muthayya, S., Sugimoto, J. D., Montgomery, S., & Maberly, G. F. (2014). An overview of global rice production, supply, trade, and consumption. Annals of the New York Academy of Sciences, 1324(1), 7–14. https://doi.org/10.1111/nyas.12540

National Agricultural Statistics Service, Arkansas Crop Production. U.S. Department of Agriculture. Retrieved from https://www.nass.usda.gov/Statistics_by_State/Arkansas/Publications/Crop_Releases/Crop_Production_Monthly/2022/arcropsep22.pdf

Nukarinen, E., Ngele, T., Pedrotti, L., Wurzinger, B., Mair, A., Landgraf, R., Börnke, F., Hanson, J., Teige, M., Baena-Gonzalez, E., Dröge-Laser, W., & Weckwerth, W. (2016). Quantitative phosphoproteomics reveals the role of the AMPK plant ortholog SnRK1 as a metabolic master regulator under energy deprivation. Scientific Reports, 6. https://doi.org/10.1038/srep31697

Pathak, B., Maurya, C., Faria, M. C., Alizada, Z., Nandy, S., Zhao, S., Jamsheer K, M., & Srivastava, V. (2022). Targeting TOR and SnRK1 Genes in Rice with CRISPR/Cas9. Plants, 11(11). https://doi.org/10.3390/plants11111453

Pedrotti, L., Weiste, C., Nägele, T., Wolf, E., Lorenzin, F., Dietrich, K., Mair, A., Weckwerth, W., Teige, M., Baena-González, E., & Dröge-Laser, W. (2018). Snf1-RELATED KINASE1-controlled C/S1-bZIP signaling activates alternative mitochondrial metabolic pathways to

ensure plant survival in extended darkness. Plant Cell, 30(2), 495–509. https://doi.org/10.1105/tpc.17.00414

Peixoto, B., & Baena-González, E. (2022). Management of plant central metabolism by SnRK1 protein kinases. Journal of Experimental Botany, 73(20), 7068–7082. https://doi.org/10.1093/jxb/erac261

Peixoto, B., Moraes, T. A., Mengin, V., Margalha, L., Vicente, R., Feil, R., Hohne, M., Sousa, A. G. G., Lilue, J., Stitt, M., Lunn, J. E., & Baena-Gonzalez, E. (2021). Impact of the SnRK1 protein kinase on sucrose homeostasis and the transcriptome during the diel cycle. Plant Physiology, 187(3), 1357–1373. https://doi.org/10.1093/plphys/kiab350

Perochon, A., Váry, Z., Malla, K. B., Halford, N. G., Paul, M. J., & Doohan, F. M. (2019). The wheat SnRK1α family and its contribution to Fusarium toxin tolerance. Plant Science, 288. https://doi.org/10.1016/j.plantsci.2019.110217

Radchuk, R., Emery, R. J. N., Weier, D., Vigeolas, H., Geigenberger, P., Lunn, J. E., Feil, R., Weschke, W., & Weber, H. (2010). Sucrose non-fermenting kinase 1 (SnRK1) coordinates metabolic and hormonal signals during pea cotyledon growth and differentiation. Plant Journal, 61(2), 324–338. https://doi.org/10.1111/j.1365-313X.2009.04057.x

Radchuk, R., Radchuk, V., Weschke, W., Borisjuk, L., & Weber, H. (2006). Repressing the expression of the SUCROSE NONFERMENTING-1-RELATED PROTEIN KINASE gene in pea embryo causes pleiotropic defects of maturation similar to an abscisic acid-insensitive phenotype. Plant Physiology, 140(1), 263–278. https://doi.org/10.1104/pp.105.071167

Statista. (2023). Top countries of destination for US rice exports 2011. Retrieved July 5, 2023, from https://www.statista.com/statistics/255945/top-countries-of-destination-for-us-rice-exports-2011/

Takano, M., Kajiya-Kanegae, H., Funatsuki, H., & Kikuchi, S. (1998). Rice has two distinct classes of protein kinase genes related to SNF1 of Saccharomyces cerevisiae, which are differently regulated in early seed development. Molecular & General Genetics, 260(4), 388–394. https://doi.org/10.1007/s004380050908

Tsai, A. Y. L., & Gazzarrini, S. (2014). Trehalose-6-phosphate and SnRK1 kinases in plant development and signaling: The emerging picture. In Frontiers in Plant Science (Vol. 5, Issue APR). Frontiers Research Foundation. https://doi.org/10.3389/fpls.2014.00119

United States Department of Agriculture. (2022). United States Department of Agriculture

US Department of Agriculture (2022). Arkansas state overview. National Agricultural Statistics Service.

Wang, J., Guan, H., Dong, R., Liu, C., Liu, Q., Liu, T., Wang, L., & He, C. (2019). Overexpression of maize sucrose non-fermenting-i-related protein kinase 1 genes, ZmSnRK1s, causes alteration in carbon metabolism and leaf senescence in Arabidopsis thaliana. Gene, 691, 34-44. https://doi.org/10.1016/j.gene.2018.12.039

Wang, W., Lu, Y., Li, J., Zhang, X., Hu, F., Zhao, Y., & Zhou, D.-X. (2021). SnRK1 stimulates the histone H3K27me3 demethylase JMJ705 to regulate a transcriptional switch to control energy homeostasis. The Plant Cell, 33(12), 3721–3742. https://doi.org/10.1093/plcell/koab224

Xia, L.; Zou, D.; Sang, J.; Xu, X.; Yin, H.; Li, M.; Wu, S.; Hu, S.; Hao, L.; Zhang, Z. Rice Expression Database (RED): An integratedRNA-Seq-derived gene expression database for rice.J. Genet. Genom.2017,44, 235–241

Zhou, H., Xia, D., & He, Y. (2020). Rice grain quality—traditional traits for high quality rice and health-plus substances. Molecular Breeding, 40(1), 1–17. https://doi.org/10.1007/s11032-019-1080-6

Tables and Figures

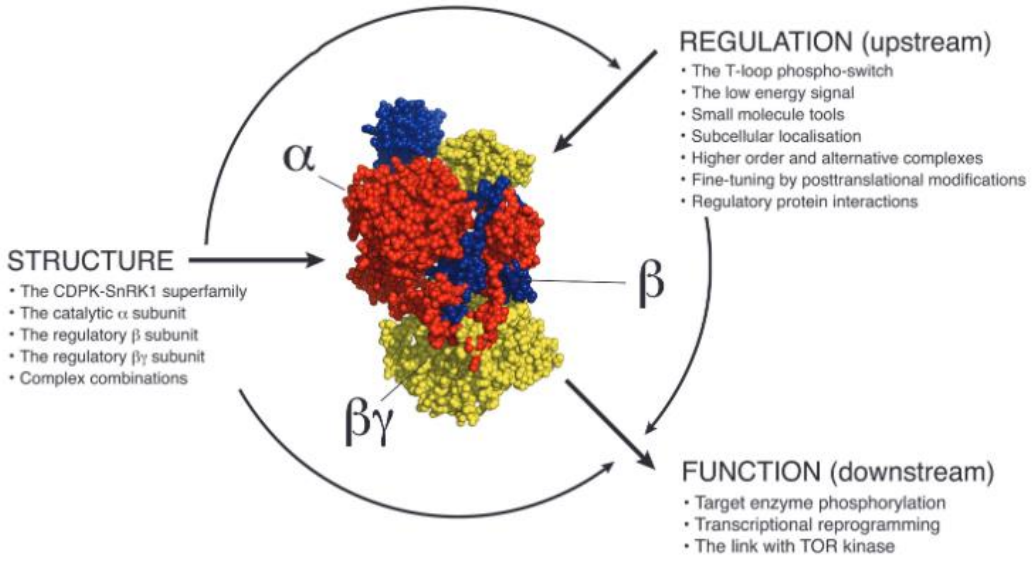

Figure 1.1 SnRK1 heterotrimeric complex structure, upstream regulation, and downstream function. Source: Broeckx et al., 2016.

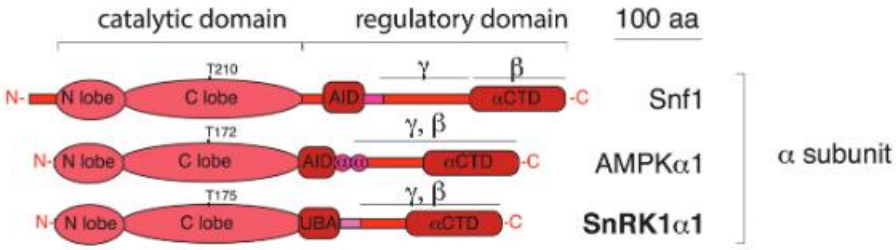

Figure 1.2 Linear structure of the SnRK1 alpha subunit in yeast (*S. cerevisiae*) SNF1, mammalian (*H. sapiens*) AMPK, and plant (*A. thaliana*). Source: Broeckx et al., 2016.

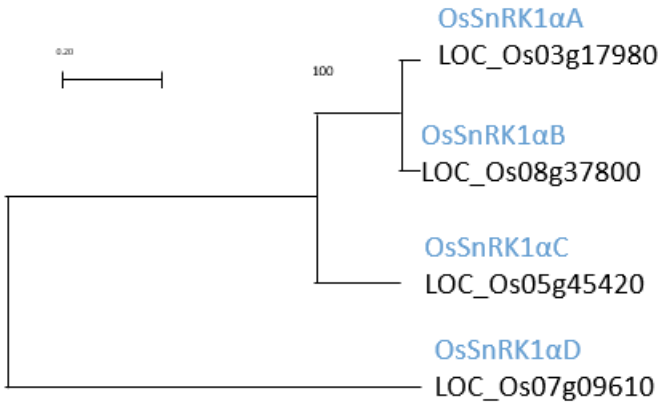

Figure 1.3. Neighbor joining-based phylogenetic reconstruction of rice *SnRK1α* subunits (Pathak et al., 2022).

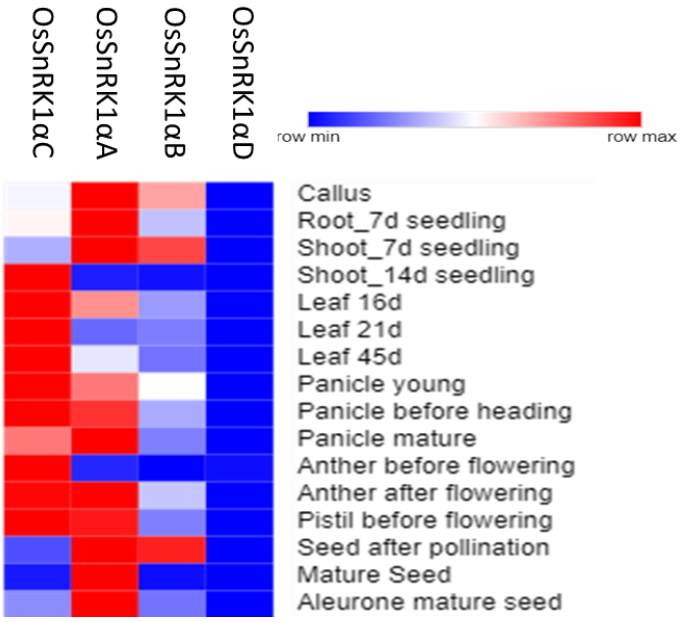

Figure 1.4. Expression level (FPKM) of rice *SnRK1α* subunits indifferent tissue and developmental stages (Pathak et al., 2022).

Chapter II – Phenotypic assessment of SnRK1 mutants

2.1. Introduction

SnRK1 is a key regulator of plant metabolism that regulates the equilibrium between energy generation and consumption in the cell. Under stress, SnRK1 is activated, which changes gene expression and metabolism to favor catabolism over anabolism towards ultimately restoring energy balance and homeostasis (Henninger et al., 2021; Nukarinen et al., 2016). Under stress conditions, SnRK1 activates genes related to catabolic pathways, such as degradation of cell walls, carbohydrates, sucrose, amino acids, lipids, and proteins that produce different types of metabolites and energy sources (Baena-Gonzalez et al., 2007). In addition to its well-known role in stress reactions, SnRK1 is being linked in an increasing number of studies to the homeostatic regulation of metabolism during normal conditions in plant organs and developmental stages (Peixoto & Baena-Gonzalez, 2022).

Previous studies observed that SnRK1 controls seedling growth in rice, pea, and Arabidopsis. Radchuk et al. (2006) explored the role of SnRK1 in pea embryos repressing SnRK1 activity by antisense technology. The transgenic lines exhibited premature germination along with abnormalities in maturation, decreased sucrose conversion into storage products, reduced dry weight and changed cotyledon surface, shape, and symmetry. It was also observed that the mutant pea seeds had lower growth and fresh weight. This finding is consistent with that of Tsai & Gazzarrini (2012), who observed that Arabidopsis seeds overexpressing *SnRK1α*/*KIN10* showed cotyledon defects and delayed germination. Lu et al. (2007) observed that *SnRK1αc* (LOC_Os05g45420) mutant, when compared with the WT, had lower seed germination, seedling growth, including reduced shoot and root growth, and impaired starch mobilization during germination. However, no difference was observed in the *SnRK1αb* (LOC_Os08g0484600)

mutant, which indicates that *SnRK1αc* and not *SnRK1αb* plays a significant role in regulating rice seed germination and seedling growth. Additionally, Baena-Gonzalez et al. (2007) observed that, in low light and limited energy availability, Arabidopsis *SnRK1α*/*KIN10* overexpression lines showed increased primary root growth and development in comparison with the WT. This result corroborates with those of Henninger et al. (2021), who found that double mutation in the *SnRK1α* catalytic site in Arabidopsis (*SnRK1α*/*KIN10* and *SnRK1α*/*KIN11*) resulted in reduced seedling growth and fresh biomass under darkness.

Studies also found that SnRK1 is essential for plant growth and the proper development of reproductive organs, including flowers and seeds. It regulates the synthesis and accumulation of starch, which is a critical energy source for the developing embryo. Tsai & Gazzarrini (2012) observed that the SnRK1 affects the development of the cotyledon, silique, and floral tissues, implying that this protein controls lateral organ development in Arabidopsis. They also observed that SnRK1 overexpression results in late flowering and late senescence. Peixoto et al. (2021) also noted that *SnRK1α* overexpression lines showed delayed flowering in Arabidopsis and the mutant lines showed early flowering. Studies also found the importance of SnRK1 in grain filling and maturation stages. Radchuk et al. (2006) observed that SnRK1 mutant lines exhibited seed abortion in various stages of the pea plant. Another study showed the importance of SnRK1 in seed filling. Hu et al. (2022) found that SnRK1 is essential for controlling the transport of nonstructural carbohydrates during rice grain filling. It was observed that *SnRK1αc* (LOC_Os05g45420) mutation in rice resulted in low grain filling, low seed setting rate, and lower 1000 grain weight when compared with the wild type. Liang et al. (2021) observed that tomato plants overexpressing the *SnRK1α* subunit (*PpSnRK1α*) showed higher total dry and fresh weight but lower growth of hypocotyls and primary roots when compared with the WT.

To regulate plant growth and development, SnRK1 uses different molecular, biochemical, and genetic mechanisms. Studying rice seedlings Lu et al. (2007) noted that *SnRK1αc* (LOC_Os05g45420) is a positive regulator of the expression of sugar-responsive genes (MYBS1 and αAmy3), including those involved in sugar transport and metabolism. It was also observed that SnRK1 activity is regulated by sugars at the posttranscriptional level and not in mRNA level. In Arabidopsis seedlings, Baena-Gonzalez et al. (2007) observed that SnRK1 activity is inhibited by sugars and activated under starvation conditions. It was also observed that SnRK1 regulates gene expression, including its interaction with transcription factors and chromatin remodeling complexes. Tsai & Gazzarrini (2012) noted that the timing of the development of lateral organs and changes between distinct stages of plant growth is regulated by the interaction of *SnRK1α/*KIN10 with the transcription factor FUSCA3, which also controls embryo development and stress responses. Henninger et al. (2022) observed that in Arabidopsis seedlings, SnRK1 activates the transcription factor BASIC LEUCINE ZIPPER63 (bZIP63) by phosphorylation, which is essential for seedling formation. Moreover, it has been demonstrated that the SnRK1s' catalytic and regulatory subunits have a role in the metabolism and signaling of hormones (Baena-Gonzalezet al., 2007; Jossier et al., 2009; Radchuk et al., 2006; Radchuket al., 2010). Finally, in pea seedlings, Radchuk et al. (2006) observed that SnRK1 mutants showed defects in the seeds that are similar to abscisic acid (ABA) insensitive mutants. Radchuk et al. (2010) found evidence that SnRK1 is required to produce ABA during the early stages of seedling development. Additionally, they observed that SnRK1 also regulates the processes of seed germination and seedling growth by controlling cytokinin auxin transport.

In a study by Hu et al, (2022) SnRK1 was found to control the expression of genes related to carbohydrate transport and metabolism. Further, mutation in SnRK1 (*SnRK1αc*:

LOC_Os05g45420) resulted in reduced nonstructural carbohydrate transfer from the sheath to the panicle, resulting in reduced grain filling and grain yield. Concurring this observation, Hu et al, (2022) observed that trehalose-6-phosphate (T6P) reduces SnRK1 activity. Other studies also observed that T6P signaling affects SnRK1 activity, in which these pathways interact with each other and coordinate the allocation of carbon and energy resources in response to environmental signals, such as nutrient availability and stress. (Baena-Gonzales & Lunn, 2020; Peixoto & Baena-Gonzales, 2022; Peixoto et al.,2021). Peixoto et al. (2021) observed that T6P signaling inhibits SnRK1 in Arabidopsis. The levels of T6P display diel oscillations and play a significant role in regulating basal SnRK1 activities throughout the regular day-night cycle (Peixoto et al., 2021). Accordingly, Peixoto et al. (2021) found that the regulation of SnRK1 activity is governed by both the circadian clock and variations in the light-dark cycle, which indicates a multifaceted interplay between SnRK1 and sucrose metabolism. Li et al. (2020) showed that SnRK1 phosphorylates and activates Opaque2, a transcription factor that regulates storage protein accumulation in corn kernels. Another study discovered that SnRK1 is necessary to suppress the starvation-induced gene expression pathway under energy-sufficient conditions (Wang et al., 2021). According to the study, SnRK1 is essential for maintaining energy balance by controlling the activity of JMJ705, a histone demethylase that in turn controls the transcription of genes related to energy metabolism. Liang et al. (2021) investigated the role of SnRK1 in regulation of photosynthesis and carbon metabolism in tomatoes. By overexpressing the *SnRK1α* subunit (PpSnRK1α) of tomato plants, expression of genes related to carbon metabolism were increased, as well as photosynthesis rate and starch content in the leaves.

Little is known about how SnRK1 functions to coordinate carbon absorption, storage, plant development and growth in rice plants. Hence, this study focuses on performing phenotypic

evaluations of SnRK1 catalytic α-subunit mutants on early seedlings stages and mature rice plants. Our main objective is to carryout phenotypic assessment of mature plants of rice *SnRK1αa*, *SnRK1αb*, and *SnRK1αc* mutants in the greenhouse along with the seed derived wild-type (WT) comparing yield parameters: (a) shoot biomass; (b) shoot length; (c) root biomass; (d) root length; (e) number of seeds per panicle and (f) weight of 100 seeds. Additionally, this study will also compare the young seedling growth parameters (a) shoot length, and (b) root length of the selected mutant lines with WT in artificial media.

2.2 Material and Methods

2.2.a. Development of CRISPR mutants

This step was done previously in Dr. Vibha Srivastava's lab. CRISPR/Cas9was used as the gene editing tool to generate the SnRK1 mutants in cv. Kitaake background. Two CRISPR constructs were developed to target the catalytic site of *SnRK1α*, one for targeting *SnRK1αc* (pNS73) and the other for targeting *SnRK1αa* and *SnRK1αb* (pNS72). Since *SnRK1αa* and *SnRK1αb* have a high degree of sequence similarity, these two genes were targeted by a single CRISPR construct to generate double-mutant lines. The lines were characterized by Sanger sequencing (mutation analysis) and the seeds were collected in 2020. The results of the use of CRISPR/Cas9 to generate mutant lines are available in Figure 2.1.

For the pNS72 construct (targeting *SnRK1αa* and *SnRK1αb*), 10 T0 plants were generated, 9 harbored monoallelic or biallelic mutations in one or both target sites (sg1 and sg2). Four of the lines were sterile or died prematurely. Hence, 5 T0 lines were selected: 1-1, 1-2, 2-4, 4-1, and 4-2 (Figure 2.1). PCR and sequencing analysis showed that lines 1-1, 4-1 and 4-2 had identical mutations in both *SnRK1αa* and *SnRK1αb*. In *SnRK1αa* sg1 site, 1-1 and 4-2 lines carried

monoallelic mutations that lead to a premature stop codon in the targeted allele, on the other hand, line 4-1 did not have a mutation in sg1 site. In *SnRK1αa* sg2, lines 1-1, 4-1 and 4-2 carried identical biallelic heterozygous mutations that led to an early stop codon in allele 1 and a loss of 1 amino acid (aa) in allele 2. In *SnRK1αb* sg1, these lines did not carry any mutation. However, in *SnRK1αb* sg2, lines 1-1, 4-1 and 4-2 had biallelic homozygous mutation, with 5 base pairs deletion resulting in an early stop codon. Line 1-2 differed slightly from these lines. While line 1-2 had the same mutation in both target sites in *SnRK1αa* and in 1 allele of *SnRK1αb* sg2 (5 base pairs deletion), it had a biallelic heterozygous mutation, containing T to G substitution in allele 2, resulting in 1 amino acid substitution. The T0 line 2-4 contained the biallelic homozygous mutation of 69 base pairs insertion in *SnRK1αa* sg2 and a monoallelic mutation (1 bp insertion) in *SnRK1αb* sg1, leading to a premature stop. The *SnRK1αb* sg2 contained a biallelic heterozygous mutation (2 and 3 bp deletion), resulting in a premature stop in allele 1 and one amino acid deletion in allele 2. The double homozygous T1 lines of 1-1 and 2-4, leading to early stop codons in both *SnRK1αa* and *SnRK1αb,* were identified using PCR and sequencing analysis (Table 2.1). The seeds of the selected double-homozygous lines were bulked for future experiments.

With pNS73 construct (targeting *SnRK1αc*), 40 T0 plants were generated, only 10 of which survived. One line, T0_13-1, had monoallelic mutation in sg1 and sg2 sites, while the other nine lines had biallelic homozygous or heterozygous mutations at both target locations (Figure 2.1). The T0 lines 6-2, 6-3, 6-6, 14-1, 14-2 and 14-3 carried identical biallelic homozygous mutations that led to an early stop codon in both alleles. Lines 6-2 and 6-3 were combined and later referred to as 6-23. T0 lines 14-4 and 14-5 had biallelic heterozygous mutations leading to early stop codon and T0 line 10-1 contained biallelic homozygous mutation with 3 base pairs deletion

at sg1 and 11 base pairs deletion in sg2 site resulting in 1 amino acid deletion and an early stop codon respectively (Figure 2.1).

For the third phenotypic assessment in the greenhouse and for the transcriptomic analysis and disease response (see chapter 3 and 4 respectively), it was selected the *snrk1αa+b* double mutant lines 1-1 and 2-4 and *snrk1αc* single mutant lines 6-23 and 10-1 (Table 2.1). A protein alignment was conducted, revealing that in lines 1-1 and 2-4, the *snrk1αa* and *snrk1αb* mutation resulted in an early stop codon before the activation loop. This mutation resulted in the absence of the T-loop, UBA domain, and a truncated kinase domain for both *SnRK1αa* and *SnRK1αb* genes. In line 6-23, protein alignment showed that the *snrk1αc* mutation led to an early stop codon after the activation loop. This mutation resulted in the absence of UBA domain, and a truncated kinase domain, missing 61 amino acids. In line 10-1, the mutation in the *snrk1αc* resulted in deletion of one amino acid in the kinase domain and absence of UBA domain. Hence, line 10-1 had both the activation loop and kinase domain.

2.2.b. Seed sterilization and plant material

Seeds from WT and mutant lines were sterilized with 70% ethanol and 30% bleach and were grown on ½ Murashige and Skoog media (MS; pH: 5.7) containing 2g/L of phytagel in Petriplates. Seven days later, at V1-V2 stage, seedlings were transferred to the greenhouse in pots filled with a mixture of sphagnum peat moss and perlite (9:1). Plants were grown in randomized block design in the greenhouse. Plants were fertilized with iron chelate and Osmocote fertilizer (15N-9P-12K) and insecticide (abamectin) when necessary. When harvesting, panicles, shoot and roots were separated, and roots were washed in running tap water. shoots and roots lengths were measured with a measurement tape and expressed in centimeters. Plant parts (shoot, roots, and panicles) were dried in 37.5 °C dryer for 14 days. Dry weight

(biomass) of root and shoot, weight of 100 seeds, total weight of seeds per plant of each plant was recorded on an electronic scale and expressed in grams. The number of seeds per panicle and number of panicles per plant were manually counted for each plant and the data was recorded.

2.2.c. Seedling growth assay

Seedling growth assessment of *snrk1αa+snrk1αb* double mutant lines T1_1-1 and T1_2-4 and *snrk1αc* single mutant lines T1_6-3 and T1_10-1 was done in comparison with the seed derived WT in three different experiments. Twenty seeds per line were sterilized as described above except that the in ½ MS media contained 2% of sucrose. The seedlings were grown in a growth chamber (Percival-Scientific Inc., Perry, IA, USA) under a 16:8 h photoperiod at 26◦C (day) and 22◦C (night) temperature in a light intensity of 10–30μmol m−2s−1. Four days after planting the seeds, on S3 stage, the seedlings were transferred to Borosilicate tubes containing ½ MS media without sucrose and 1.5 grams of phytagel per liter. The seedlings were grown in the growth chamber under maximum light (200 μmol m^{-2} $sec^{-1)}$ in a controlled environment. The light was provided from 5 am to 8 pm, for a 15 h photoperiod. Root and shoot length in seedlings were measured with a measurement tape. The SnRK1 lines used, and the measurement dates are described in the table below:

SnRK1 lines	Plate date	Measurement dates
snrk1αa+b: 1-1 *snrk1αc:* 6-23	February 15 of 2022	2 days-old and 7 days-old seedlings
snrk1αa+b: 2-4 *snrk1αc:* 10-1	June 20 of 2022	3 days-old and 5 days-old seedlings
snrk1αa+b: 1-1, 2-4 *snrk1αc:* 6-23, 10-1	August 4 of 2022	4 days-old and 9 days-old seedlings

2.2.d. Phenotypic assessment of mature plants in the greenhouse

In the first experiment, the pNS73 lines (mutant lines harboring mutations in *SnRK1αc*) were subjected to phenotypic assessment along with the tissue culture wild type (WT) *Oryza sativa var. japonica* cv. Kitaake. The following parameters were measured: shoot and root biomass, shoot and root length, number of seeds per panicle, and weight of 100 seeds. For this experiment T1 plants of lines 10-1, 6-23, 14-2, 14-4, 6-6, 13-1 harboring mutations in *SnRK1αc* were chosen (Figure 2.1). Because we had limited number of seeds in each genotype, the experiment consisted of 1 replicate of 14-2, 5 replicates of 14-4, 2 replicates of 10-1, 10 replicates of 6-23, 8 replicates of 6-6, 20 replicates of 13-1 line along with 10 WT plants. It was plated on germination media 20 seeds for each line on July 20 of 2021 and the plants were transferred to the greenhouse 13 days after plating. The plants were grown in randomized block design in the greenhouse. The plants were harvested on November 10, after 113 days in the greenhouse.

The same was done for the *snrk1αa + snrk1αb* (T1) double mutant lines (pNS72 lines) in the second experiment with lines 1-1, 2-4 and 4-1 (Figure 2.1) and the seed derived WT. Twenty replicates per line were used along with the WT. It was plated on germination media 20 seeds per line on January 21 of 2022 and plants transferred to the greenhouse 7 days after plating. The plants were harvested on May 23 of 2022 after 122 days in the greenhouse.

In the third experiment, the T2 pNS72 lines harboring homozygous mutations were used along with the T2 pNS73 lines and the seed derived WT. The selected lines were *SnRK1αa+SnRK1αb* double-mutant lines T2_1-1 and T2_2-4 and *SnRK1αc* single-mutant lines T2_6-3 and T2_10-1 along with the WT (Figure 2.1). Twenty replicates per line were used along with the WT. It was plated on germination media 20 seeds per line on June 14 of 2022 and

transferred to the greenhouse 7 days after plating. The plants were harvested on October 21 of 2022 after 126 days in the greenhouse.

2.2.e Statistical analysis

Data was collected and analyzed by analysis of variance (ANOVA), and the Tukey–Kramer test (HSD) for comparisons among treatments using JMP Statistical Discovery 17 from SAS (Version 13.2.1) software.

2.3. Results

2.3.a Seedling growth assay

Early phases of seedling growth of the *snrk1αa+b* double mutant lines, 1-1 and 2-4, and the *snrk1αc* single mutant lines, 6-3 and 10-1, were compared with WT on MS1/2 media. In the first experiment, the shoot and root length of 2 and 7-days-old seedlings of the mutant lines, 1-1 and 6-3, were compared with the WT (Figure 2.2). No statistical difference was observed between the *snrk1αc* mutant (6-23 line) and the WT regarding shoot and root length in 2- and 7-days old seedlings. However, in 2 days old seedlings of *snrk1αa+b* line (1-1) had lower shoot and root length when compared to the 6-23 line and the WT (Figure 2.2a). Similarly, shorter shoot length was observed in the 7 days old seedlings of line 1-1 (Figure 2.2b). The representative images of *snrk1* mutants (Figure 2.2c) show that 1-1 line has smaller roots and shoots when compared to the 6-23 line and the WT.

Similar patterns for shoot length were observed in the second experiment, comparing the shoot length of 3 and 5-days-old seedlings of the mutant lines, 2-4 and 10-1, and the WT (Figure 2.3ab). For both 3 and 5-days-old seedlings, the 2-4 mutant had statistically lower shoot length

than the 10-1 line and the WT (Figure 2.3a); while no difference was observed regarding the root length (Figure 2.3b).

A final experiment was conducted comparing the *snrk1αab* double mutant lines 1-1 and 2-4 and the *snrk1αc* single mutant line 6-3 and 10-1 along with WT using 4 and 9-days-old seedlings (Figure 2.4ab). No statistical difference was observed between the genotypes for shoot and root length in 4 days old or 9 days old seedlings (Figure 2.2ab). Regarding the root length on 9-days-old seedlings, the 1-1, 6-23 and 10-1 lines were statistically similar to the WT, while the 2-4 line was statistically lower than the WT (Figure 2.4b). Interestingly, 1-1 and 6-23 lines had superior fresh biomass than 2-4, 10-1 and the WT (Figure 2.2b).

2.3.b. Phenotypic assessment of snrk1αc mutants in the greenhouse

In the first experiment, the phenotypic parameters shoot length and biomass, root length and biomass, number of seeds per panicle and weight of 100 seeds in mature rice plants of *snrk1αc* mutant lines were compared with the WT cv. Kitaake. The results show that the main difference was observed in shoot biomass and number of seeds per panicle between the biallelic mutants 14-2, 14-4, 10-1, 6-23 and 6-6 and the WT (Figure 2.5a-c). Lines 14-2, 14-4, 10-1, 6-23 and 6-6 harboring biallelic mutation in *snrk1αc* had significantly lower shoot biomass (Figure 2.5a) and fewer seeds per panicle (Figure 2.5c) when compared with the WT. No significant difference was observed in the 13-1 line, harboring monoallelic mutation in *snrk1αc* gene. The lines 6-23 and 6-6 had statistically lower shoot length when compared with the 13-1 line and the WT (Figure 2.5a). The lines 6-23 and 6-6 were statistically similar with the other lines harboring biallelic mutation (14-2, 14-4, 10-1) regarding shoot length (Figure 2.5a). No significant difference was observed in root biomass between the *snrk1αc* mutant lines and the WT (Figure

2.5b). The lines 6-23 and 6-6 had a significantly lower root length when compared with the WT, and the mutants harboring biallelic (14-2, 14-4, 10-1) and monoallelic (13-1) mutations were also statistically similar with the 6-23 and 6-6 lines for root length (Figure 2.5b). In addition, the WT was statistically similar with all the mutant lines for weight of 100 seed (Figure 2.5c).

2.3.c. Phenotypic assessment of snrk1αa+b mutants in the greenhouse

In the second experiment, we conducted measurements on mature rice plants of *snrk1αa+b* double mutant lines and compared them to the seed derived WT cv. Kitaake. The following parameters were measured: shoot and root biomass, shoot and root length, number of seeds per panicle, and weight of 100 seeds. The results showed no statistical difference between the 1-1, 2-4, 4-1 and the WT for shoot length (Figure 2.6a) and root biomass (Figure 2.6b). Regarding root length, 1-1 and 2-4 lines had smaller values when compared to the WT (Figure 2.6b). The graphs of shoot biomass (Figure 2.6a) and number of seeds per panicle (Figure 2.6c) show that the mutant lines were statistically similar to each other and the WT, despite 2-4 line, which showed lower values compared with the WT. All mutants had lower weight of 100 seeds compared with the WT, and the 2-4 line had the lowest value of weight of 100 seeds when compared with the other mutants and the WT (Figure 2.6c).

2.3.d Phenotypic assessment of snrk1αc and snrk1αa+b mutants in the greenhouse

In the third experiment, 1-1 and 2-4 T2 lines harboring homozygous mutations in *SnRK1αa* and *SnRK1αb* and the homozygous *snrk1αc* single mutant line 6-3 and 10-1 were selected for the phenotypic comparison with the WT plants at maturity. It was measured the following parameters: shoot and root biomass, shoot length, number of seeds per panicle, weight of 100

seeds and total weight of seeds per plant. The results showed that *snrk1αc* mutants were more compromised in yield parameters as compared to the WT. The *snrk1αa+b* mutant lines (1-1 and 2-4) and the *snrk1αc* mutants (6-23 and 10-1) had lower shoot biomass compared to the WT (Figure 2.7a) but the 6-23 line was significantly lower in shoot biomass than the other mutant lines (Figure 2.7a and Figure 2.8). Regarding the root biomass, the *snrk1αa+b* mutant lines (1-1 and 2-4) were statistically lower to the WT and similar to each other and to the *snrk1αc* 6-23 line (Figure 2.7b). No difference was observed between the 10-1 line and the WT for root biomass (Figure 2.7b). Statistical differences were observed in shoot length between the 6-23 line and the WT, while no differences were observed between the other mutants and the WT (Figure 2.7a). The yield parameters, number of seeds per panicle (Figure 2.7c) and total weight of seeds per plant (Figure 2.7c), showed similar patterns, i.e., the WT was significantly higher than the mutant lines, where the *snrk1αc* mutants (6-23 and 10-1) had lowest number of seeds per panicle and total weight of seeds per plant. Similarly, in Figure 2.8, the *snrk1* mutants have lower number of panicles when compared with the WT. The weight of 100 seeds, however, was statistically similar to each other and the WT, despite 2-4 line showing lower values compared with the WT (Figure 2.7c).

2.4. Discussion

In this study, we investigated the role of SnRK1 in the growth of rice seedlings and in mature plants by measuring several phenotypic parameters. In rice seedlings, we measured the shoot and root length and total biomass. Our study found that mutations in the *SnRK1αa* and/or *SnRK1αb* affected seedling shoot and root growth, while no effect on the seedling growth was observed in *snrk1αc* mutants. The analysis of two independent lines of *snrk1αa+b* mutants, 1-1

and 2-4, in two separate experiments showed that while both were retarded in shoot growth as compared to the WT, only 1-1 was clearly retarded in both shoot and root growth (Figure 2.2). Although, the two lines were compared in different experiments, this observation suggests that the role of SnRK1αa or SnRK1αb is more prominent in the shoot growth and the phenotypic effects appear to be stronger in *snrk1αa+b* line 1-1. This corroborates with the literature, where it is reported that *SnRK1* mutants had retarded shoot and root growth in rice (*SnRK1αb*) (Lu et al., 2007), Arabidopsis (*SnRK1α/KIN1*0 and *SnRK1α/AKIN11*) (Baena-Gonzalez et al., 2007; Henninger et al., 2021), and pea (J971809) (Radchuk et al., 2006, 2010). Similar observation was made in our study regarding shoot length in 3 and 5-days-old seedlings (Figure 2.3ab). It was observed that *snrk1αa+b* mutants 1-1 and 2-4 had lower shoot length; however, only 1-1 showed lower root length. Surprisingly, in the final experiment, no differences were found in shoot and root length of 4-days-old seedlings of *snrk1αa+b* double mutant lines T2_1-1 and T2_2-4 and the *snrk1αc* single mutant line T2_6-3 and T2_10-1 and the WT (Figure 2.4ab). In this experiment, the *snrk1αa+b* and *snrk1αc* mutants were statistically similar with the WT regarding shoot length in 9-days-old seedlings. Although, this finding is inconsistent with our previous experiments, Henninger et al. (2021) observed no difference in fresh biomass between the *snrk1* mutants and the WT in Arabidopsis seedlings. The inconsistency between our experiments may be due to the T2 seeds used for the last experiment. These seeds were derived from unhealthy plants that were treated with excessive fertilizer.

Possible explanations of our findings of lower seedling growth in SnRK1 mutants can be found in the literature. In rice, SnRK1 plays a critical role in sugar signaling during seedling stages by phosphorylating MYBS1, a transcription factor that controls genes involved in glucose metabolism (Lu et al., 2007). In the presence of glucose, SnRK1 phosphorylates MYBS1, which

then binds to a particular promoter sequence to promote the expression of genes encoding enzymes involved in glycolysis (process by which glucose is broken down into smaller molecules, producing energy in the form of ATP) and other carbohydrate metabolic pathways. As a result, there is an increase in energy production and a change in metabolism using glucose as an energy source (Lu et al., 2007). Another downstream target of SnRK1 identified by Lu et al. (2007) is aAmy3, an alpha-amylase enzyme that is involved in the breakdown of starch into glucose. In Arabidopsis, Henninger et al. (2021) discovered that SnRK1 is involved in the transcriptional control of amino acid catabolism, and that it is required for mobilization of triacylglycerol reserves from the seed to the shoot. The enzyme cyPPDK is involved in feeding amino acid derived pyruvate into gluconeogenesis pathway. They found that SnRK1 negatively regulates cyPPDK expression by phosphorylating bZIP63, a transcription factor that binds to the promoter region of cyPPDK and activates its expression. The phosphorylation of bZIP63 by SnRK1 leads to reduced binding of bZIP63 to the cyPPDK promoter and decreased cyPPDK expression, which may help to conserve energy resources during seedling establishment (Henninger et al., 2021). In accordance with this study, Baena-Gonzalez et al. (2007) also observed lower seedling establishment in SnRK1 mutants in Arabidopsis. They also noted that by regulating key enzymes and transcription factors, SnRK1 regulates catabolic pathways that give alternative sources of energy and metabolites including the breakdown of cell walls, starches, sucrose, amino acids, lipids, and proteins. Moreover, metabolite profiling of SnRK1 mutants in pea revealed that SnRK1 suppression inhibits the usage of carbon skeletons for the synthesis of amino acids. It was also found that SnRK1 is involved in the regulation of cell cycle in pea seedling by interacting with cytokine and auxin hormones (Radchuk et al., 2010). The results of these studies suggest that SnRK1 regulates sugar signaling and metabolic adaptation by

regulating transcription factors, coordinating catabolic pathways, and interacting with hormone pathways during the early growth stages of the seedlings, which has important implications for the healthy growth and development. In accordance with the literature, the findings of this study provide further evidence for the role of SnRK1 in rice seedling growth in early phases of the development.

In the next part of our study, phenotypic assessment was done on mature rice plants of *snrk1αc* and *snrk1αa+b* mutant lines compared with the wild type cv. Kitaake. Our results showed that mutant lines harboring biallelic mutations in *snrk1αc* had lower yield parameters, such as shoot length and biomass, number of seeds per panicle and total weight of seeds per plant when compared with the WT and *snrk1αa+b* mutants (Figure 2.5abc and Figure 2.7abc), however no differences of weight of 100 seeds was observed between the *snrk1αc* mutants and the WT. Interestingly, shoot biomass (Figure 2.7a) and root biomass (Figure 2.7b) was statistically lower on 6-23 mutant then the other *snrk1αc* mutant (10-1) when compared with the WT. This could be explained by the type of mutation in *snrk1αc* genes: 6-23 line have truncated kinase domain, while 10-1 have only one amino acid deletion in the kinase domain. Regarding yield traits, Hu et al. (2022) also found that *snrk1αc* mutants in rice had lower seed setting rate, however they did not observe differences in the panicle number and number of grains per panicle between the mutants and the WT. As shown in Figure 2.5c and Figure 2.7c, the *snrk1αc* mutants had a very low number of seeds per panicle. Similarly, Radchuk et al. (2006) observed that SnRK1 mutant lines demonstrated seed abortion in pea plants. The lower number of seeds per panicle and total weight of seeds per plant can be explained by the role SnRK1 plays in the regulation of carbohydrate transport during rice grain filling. During vegetative growth, sugars are stored in the chloroplasts of the plant sheaths as nonstructural carbohydrates (NSCs), such as

starch. During grain filling, these NSC are transformed into soluble sugars, such as sucrose, and transported from the sheaths into the developing seeds, resulting in lower sucrose concentrations in the sheaths. Hu et al. (2022) investigated the effects of *snrk1αc* (LOC_Os05g45420) mutation using the leaf-cutting assay. They observed that during grain filling, the low sucrose level in the sheath induces SnRK1 activity and suppresses the level of T6P (trehalose 6-phosphate). The increase in SnRK1 activity then promotes the transfer of NSCs from the sheath to the panicle. The study also found that the *snrk1αc* mutants showed higher concentrations of starch in the sheath and a lower grain filling rate. To further confirm the role of SnRK1 in the transport of carbohydrates in rice, they performed phosphoproteomics in the *snrk1αc* mutant that revealed that SnRK1 regulates the carbohydrate catabolism pathway and the transport of NSCs in rice (Hu et al., 2022). An interesting finding by Wang et al. (2021) was that the rice *SnRK1αc* (LOC_Os05g45420) is necessary not only to regulate transcription during stress conditions but also to suppress the starvation-induced transcriptional program during energy-sufficient situations. It was found that SnRK1 regulates the activity of the histone demethylase JMJ705, which in turn removes the H3K27me3 from of the chromatin of key starvation-responsive genes. The study revealed that this mechanism also operates in response to energy stress conditions, allowing plants to adapt to changing energy demands.

Our phenotypic assessment of the mature plants showed that *snrk1αa+b* mutant lines had statistically similar shoot length and root biomass when compared to the WT (Figure 2.6a and Figure 2.7a). In the third greenhouse experiment, where we compared *snrk1αa+b* mutant lines (1-1 and 2-4) with *snrk1αc* (6-23 and 10-1) and the WT, it was observed that 1-1 and 2-4 lines had lower total weight of seeds per panicle, number of seeds per panicle, and shoot biomass compared with the WT but higher values compared with 6-23 and 10-1 (Figure 2.7abc),

suggesting that mutation in *SnRK1αc* has a greater effect on later stages of growth than the mutation in *SnRK1αa* and *SnRK1αb*, which is supported by the *SnRK1α* heat map in rice (Figure 1.4). In addition, Takano et al. (1998) observed that *SnRK1αa* and *SnRK1αb* had weak expression in flowers and strongest expression in the developing seeds. This corroborates with our results (Figure 2.6c and Figure 2.7c), where *SnRK1αa+b* double mutant lines, 2-4 and 4-1, had lower weight of 100 seeds. We could suggest that this happened because *SnRK1αa* is strongly expressed in seed after pollination and mature seed stages as shown in the heat map (Figure 1.4). Another explanation is that *SnRK1αa* and *SnRK1αb* are highly expressed during the development of endosperm in the rice grain (Takano et al., 1998), which helps to explain the lower weight of 100 seeds in 2-4 and 4-1 lines.

This study looked at the effects of *SnRK1α* mutations on rice seedling growth and plant yield characteristics. According to our findings, the growth of rice seedlings was affected by mutations in the *SnRK1αa* and *SnRK1αb* genes; however, no apparent effect of *SnRK1αc* mutation occurred on seedling growth, i.e., the early phase of the plant growth. On the other hand, our study of phenotypic assessment on mature plants of *snrk1αa+snrk1αb* double homozygous (lines 1-1 and 2-4) and *snrk1αc* single mutant (lines 6-23 and 10-1) demonstrated that mutations in the *SnRK1αc* gene affected later vegetative stages and yield parameters, such as number of seeds per panicle, total weight of seeds per plant, root and shoot biomass. Our study is in line with the *SnRK1α* genes expression profile (Figure 1.4), which shows that *SnRK1αc* is highly expressed in later vegetative and reproductive stages of rice plants. On the other hand, *SnRK1αa* and *SnRK1αb* are highly expressed in young seedling stages. In addition, our study is in accordance with the literature (Lu et al., 2007; Takano et al., 1998). Takano et al. (1998) studied the differential expression of SnRK1 genes in different growth stages in rice plants. They observed

that *SnRK1αc* (LOC_Os05g45420) had homogeneous expressions in young roots, young shoots, flowers, and immature seeds, while *SnRK1αa* (LOC_Os03g17980) and *SnRK1αb* (LOC_Os08g37800) exhibited significant expression in immature seeds. Moreover, the study supports previous research indicating that SnRK1 is central not only to activate energy production and repression of energy consumption under stress but also in the repression of stress-induced genes under normal conditions. The results of this study should help us to understand the role of SnRK1 in plant growth and development. In conclusion, the study shows that SnRK1 have a substantial role in the everyday preservation of plant energy homeostasis and the coordination of transcription factors, gene expression and carbohydrate metabolic pathways in the absence of external disturbances.

References

Baena-González, E., & Lunn, J. E. (2020). SnRK1 and trehalose 6-phosphate – two ancient pathways converge to regulate plant metabolism and growth. In Current Opinion in Plant Biology (Vol. 55, pp. 52–59). Elsevier Ltd. https://doi.org/10.1016/j.pbi.2020.01.010

Baena-González, E., Rolland, F., Thevelein, J. M., & Sheen, J. (2007). A central integrator of transcription networks in plant stress and energy signalling. Nature, 448(7156), 938–942. https://doi.org/10.1038/nature06069

Henninger, M., Pedrotti, L., Krischke, M., Draken, J., Wildenhain, T., Fekete, A., Rolland, F., Müller, M. J., Fröschel, C., Weiste, C., & Dröge-Laser, W. (2022). The evolutionarily conserved kinase SnRK1 orchestrates resource mobilization during Arabidopsis seedling establishment. Plant Cell, 34(1), 616–632. https://doi.org/10.1093/plcell/koab270

Hu, Y., Liu, J., Lin, Y., Xu, X., Xia, Y., Bai, J., Yu, Y., Xiao, F., Ding, Y., Ding, C., & Chen, L. (2022). Sucrose nonfermenting-1-related protein kinase 1 regulates sheath-to-panicle transport of nonstructural carbohydrates during rice grain filling. Plant Physiology. https://doi.org/10.1093/plphys/kiac124

JMP® Pro 15. SAS Institute Inc., Cary, NC, 1989-2021.

Jossier, M., Bouly, J. P., Meimoun, P., Arjmand, A., Lessard, P., Hawley, S., Grahame Hardie, D., & Thomas, M. (2009). SnRK1 (SNF1-related kinase 1) has a central role in sugar and ABA signalling in Arabidopsis thaliana. Plant Journal, 59(2), 316–328. https://doi.org/10.1111/j.1365-313X.2009.03871.x

Li, C., Qi, W., Liang, Z., Yang, X., Ma, Z., & Song, R. (2020). A SnRK1-ZmRFWD3-Opaque2 signaling axis regulates diurnal nitrogen accumulation in maize seeds. Plant Cell, 32(9), 2823–2841. https://doi.org/10.1105/TPC.20.00352

Liang, J., Zhang, S., Yu, W., Wu, X., Wang, W., Peng, F., & Xiao, Y. (2021). PpSnRK1α overexpression alters the response to light and affects photosynthesis and carbon metabolism in tomato. Physiologia Plantarum, 173(4), 1808–1823. https://doi.org/10.1111/ppl.13523

Lu, C. A., Lin, C. C., Lee, K. W., Chen, J. L., Huang, L. F., Ho, S. L., Liu, H. J., Hsing, Y. I., & Yu, S. M. (2007). The SnRK1αa protein kinase plays a key role in sugar signaling during germination and seedling growth of rice. Plant Cell, 19(8), 2484–2499. https://doi.org/10.1105/tpc.105.037887

Peixoto, B., & Baena-González, E. (2022). Management of plant central metabolism by SnRK1 protein kinases. Journal of Experimental Botany, 73(20), 7068–7082. https://doi.org/10.1093/jxb/erac261

Peixoto, B., Moraes, T. A., Mengin, V., Margalha, L., Vicente, R., Feil, R., Hohne, M., Sousa, A. G. G., Lilue, J., Stitt, M., Lunn, J. E., & Baena-Gonzalez, E. (2021). Impact of the SnRK1 protein kinase on sucrose homeostasis and the transcriptome during the diel cycle. Plant Physiology, 187(3), 1357–1373. https://doi.org/10.1093/plphys/kiab350

Radchuk, R., Emery, R. J. N., Weier, D., Vigeolas, H., Geigenberger, P., Lunn, J. E., Feil, R., Weschke, W., & Weber, H. (2010). Sucrose non-fermenting kinase 1 (SnRK1) coordinates metabolic and hormonal signals during pea cotyledon growth and differentiation. Plant Journal, 61(2), 324–338. https://doi.org/10.1111/j.1365-313X.2009.04057.x

Radchuk, R., Radchuk, V., Weschke, W., Borisjuk, L., & Weber, H. (2006). Repressing the expression of the SUCROSE NONFERMENTING-1-RELATED PROTEIN KINASE gene in pea embryo causes pleiotropic defects of maturation similar to an abscisic acid-insensitive phenotype. Plant Physiology, 140(1), 263–278. https://doi.org/10.1104/pp.105.071167

Takano, M., Kajiya-Kanegae, H., Funatsuki, H., & Kikuchi, S. (1998). Rice has two distinct classes of protein kinase genes related to SNF1 of Saccharomyces cerevisiae, which are differently regulated in early seed development. Molecular & General Genetics, 260(4), 388–394. https://doi.org/10.1007/s004380050908

Tsai, A. Y. L., & Gazzarrini, S. (2012). AKIN10 and FUSCA3 interact to control lateral organ development and phase transitions in Arabidopsis. Plant Journal, 69(5), 809–821. https://doi.org/10.1111/j.1365-313X.2011.04832.x

Wang, W., Lu, Y., Li, J., Zhang, X., Hu, F., Zhao, Y., & Zhou, D.-X. (2021). SnRK1 stimulates the histone H3K27me3 demethylase JMJ705 to regulate a transcriptional switch to control energy homeostasis. The Plant Cell, 33(12), 3721–3742. https://doi.org/10.1093/plcell/koab224

Tables and Figures

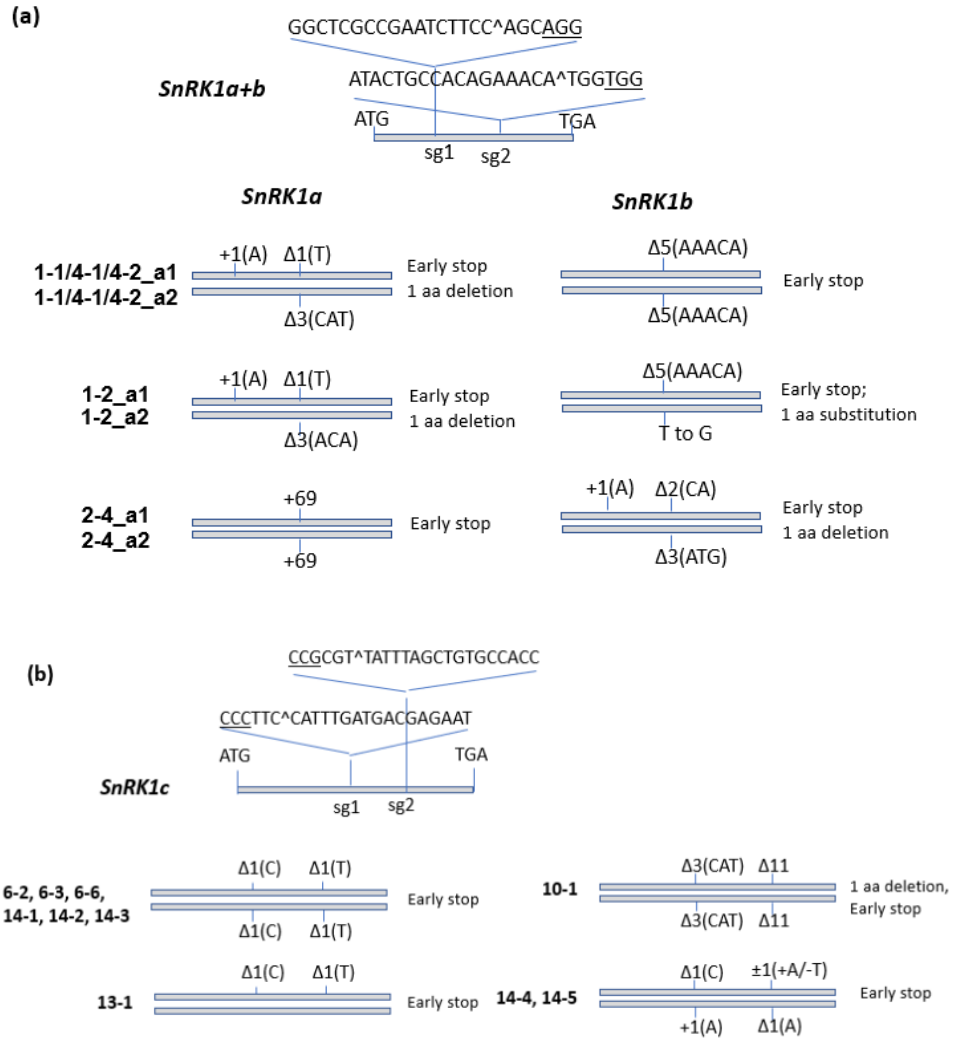

Figure 2.1 Characterization of mutations in the T0 lines. (a) pNS72 lines targeting *SnRK1αa* and *SnRK1αb*, and (b) pNS73 lines targeting *SnRK1αc*. Mutations in each allele (a1 and a2) of *SnRK1αa*, *SnRK1αb*, and *SnRK1αc* are shown as insertion (+), or deletions (Δ) and the effect of mutation is indicated. Different T0 lines showing identical mutations are grouped. In each sg site, PAM is underlined, and the predicted double-strand break site is indicated (^).

Table 2.1 Characterization of T2 homozygous *snrk1αa+b* double mutant and *snrk1αc* single mutant lines.

SnRK 1 line	**Construct**	***SnRK1αa***		***SnRK1αb***		***SnRK1αc***		**Type**
		Sg1	***Sg2***	***Sg1***	***Sg2***	***Sg1***	***Sg2***	
1-1	pNS72	+1	-1	-	-5	-	-	Early stop
2-4	pNS72	-	+69	+1/ -*	-2	-	-	Early stop
6-23	pNS73	-	-	-	-	-1	-1	Early stop
10-1	pNS73	-	-	-	-	-3	-11	Early stop

*Heterozygous

a) 2 days old seedling

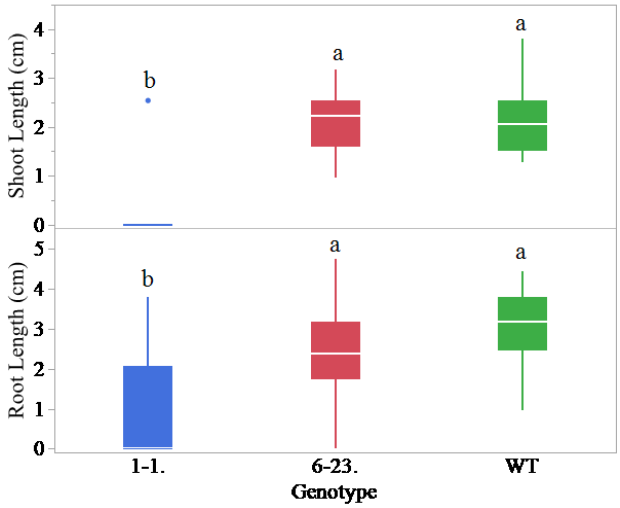

b) 7 days old seedling

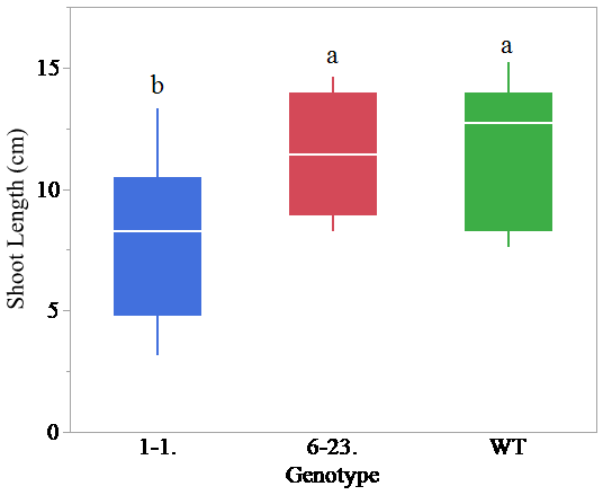

c) Image of 7 days old seedling

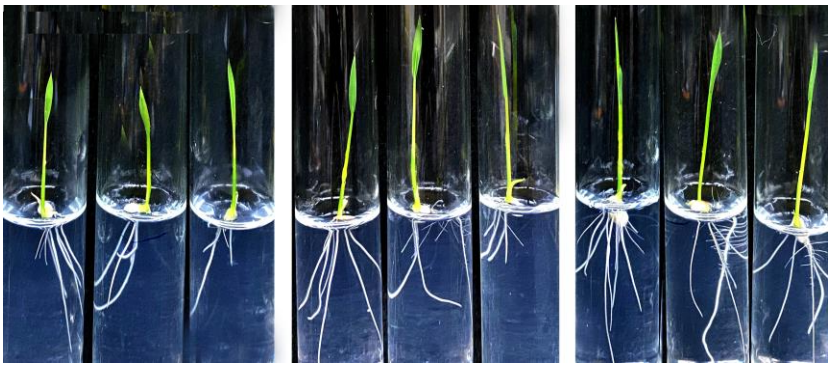

1-1 line 6-23 line WT

Figure 2.2. Phenotypic assessment of *snrk1αa+b* line 1-1 and *snrk1αc* line 6-23. (a-b) shoot length and root length in 2 days-old or 7 days-old seedlings (n=10 or 11);(c) representative 7 days-old seedlings of *snrk1αa+b* double homozygous (line 1-1) and *snrk1αc* single mutant (line 6-23) and the WT. Seedlings were grown in MS ½ media in the growth chamber under maximum light (200 µmol m−2 sec−1). Data analyzed by Tukey HSD test and statistical differences are shown by letters on each box ($p \leq 0.05$). Values having the same letter are not significantly different.

a) 3 days old seedling **b) 5 days old seedling**

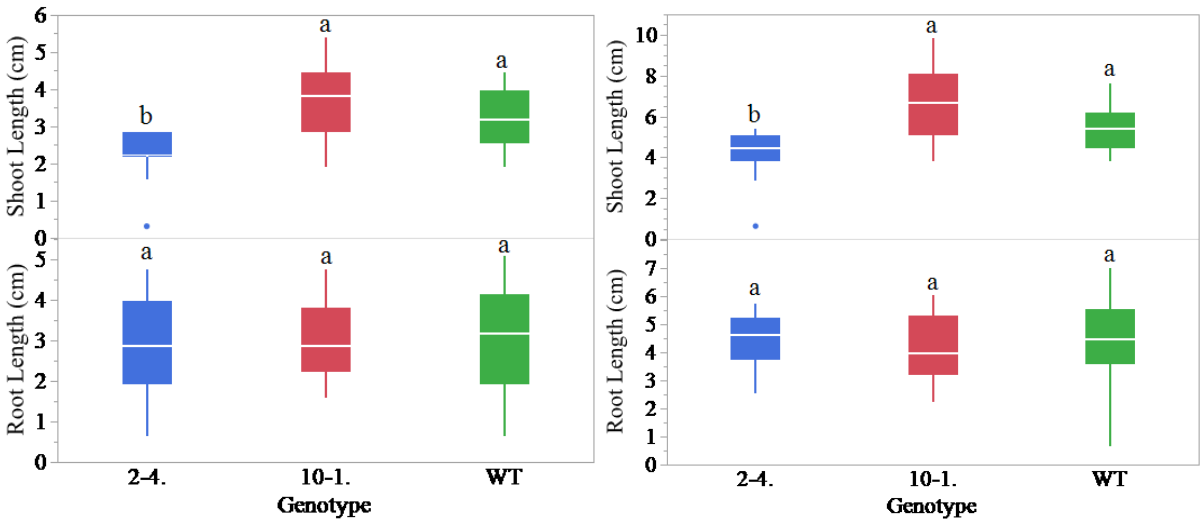

Figure 2.3. Phenotypic assessment of *snrk1αa+b* line 2-4 and *snrk1αc* line 10-1. (a-b) shoot and root length of 3 days-old or 5 days-old seedlings. (n=20). Seedlings were grown in MS1/2 media in the growth chamber under maximum light (200 µmol m−2 sec−1). Data analyzed by Tukey HSD test and statistical differences are shown by letters on each box with 0.05 significance level ($p \leq 0.05$). Values having the same letter are not significantly different.

a) 4 days old seedling

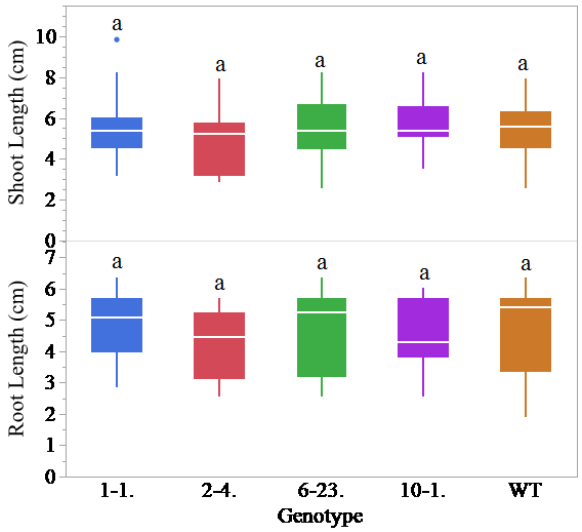

b) 9 days old seedling

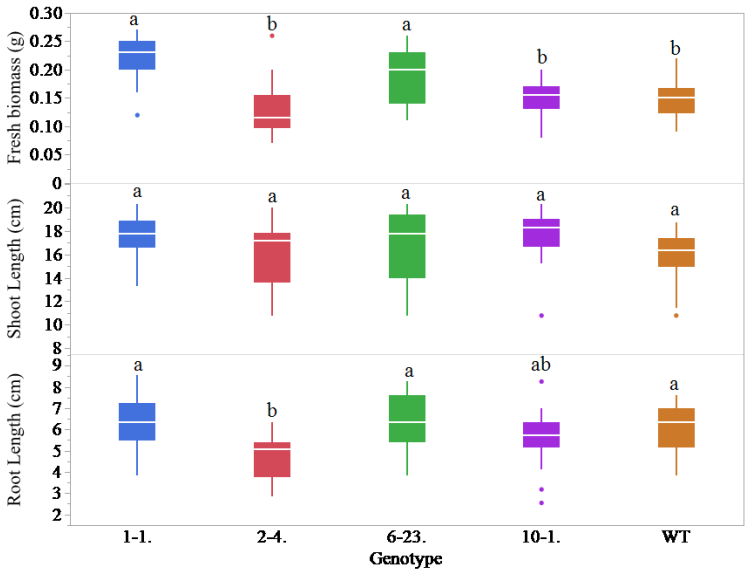

Figure 2.4. Phenotypic assessment of snrk1αa+b and snrk1*α*c mutants. (a) Shoot and root length of 4 days-old and 9 days-old the T2 seedlings of *snrk1αa+b* (lines 1-1 and 2-4) and *snrk1αc* (lines 6-23 and 10-1) (n=20); (b) Fresh biomass of *snrk1αa+b* (lines 1-1 and 2-4) and *snrk1αc* (lines 6-23 and 10-1) 9-days old seedlings in comparison with WT (n=20). Seedlings were grown in MS1/2 media in the growth chamber under maximum light (200 µmol m−2 sec−1). Data analyzed by Tukey HSD test and statistical differences are shown by letters on each box with 0.05 significance level ($p \leq 0.05$). Values having the same letter are not significantly different.

a) Shoot length and biomass

b) Root length and biomass

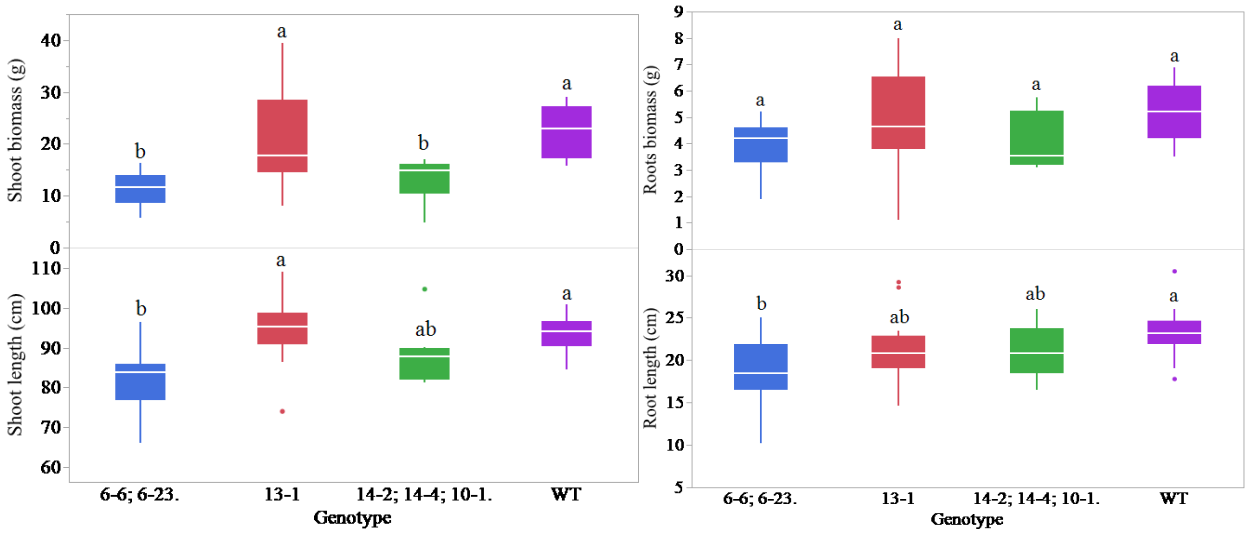

c) Number of seeds per panicle and weight of 100 seeds (g)

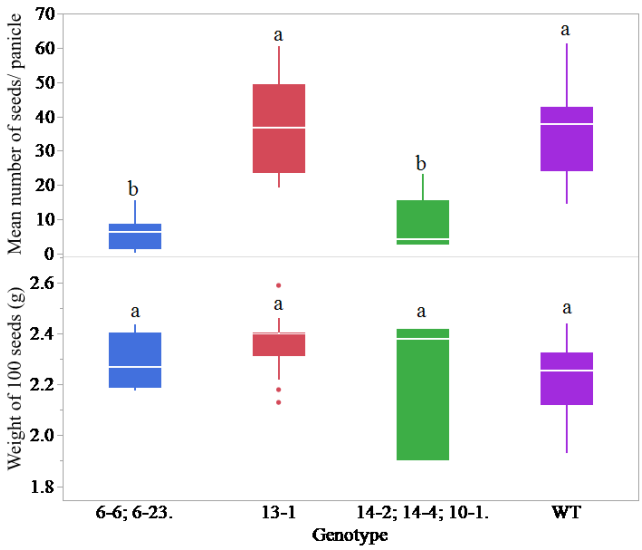

Figure 2.5 Phenotypic assessment of the greenhouse grown plants of *snrk1αc* mutants harboring biallelic (lines 6-6, 6-23, 14-2, 14-4, 10-1) or monoallelic (line 13-1) mutations at maturity. (a) shoot characteristics (length and biomass), (b) root characteristics (length and biomass), (c) Seed characteristics (number of seeds per panicle and weight of 100 seeds) in T1 plants of *snrk1αc* mutant lines (n=20). Data analyzed by Tukey HSD test and statistical differences are shown by letters on each box with 0.05 significance level ($p \leq 0.05$). Values having the same letter are not significantly different.

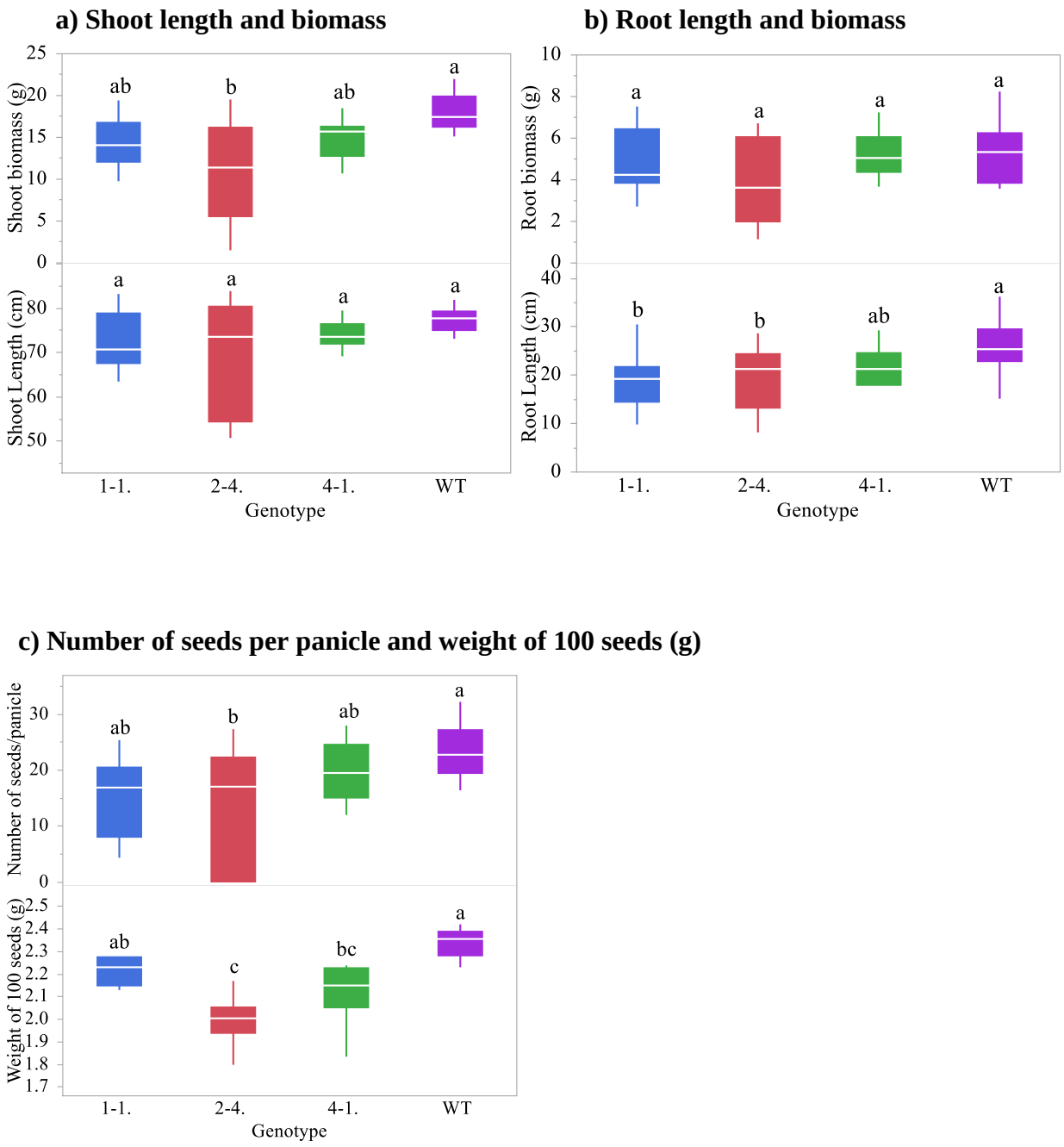

Figure 2.6 Phenotypic assessment of the greenhouse grown *snrk1αa+b* double-mutant (lines 1-1, 2-4 and 4-1) at maturity. (a) shoot characteristics (length and biomass), (b) root characteristics (length and biomass), (c) seed yield (number of seeds per panicle and weight of 100 seeds) (n=20). Data analyzed by Tukey HSD test and statistical differences are shown by letters on each box with 0.05 significance level ($p \leq 0.05$). Values having the same letter are not significantly different.

a) Shoot length and biomass

b) Root biomass

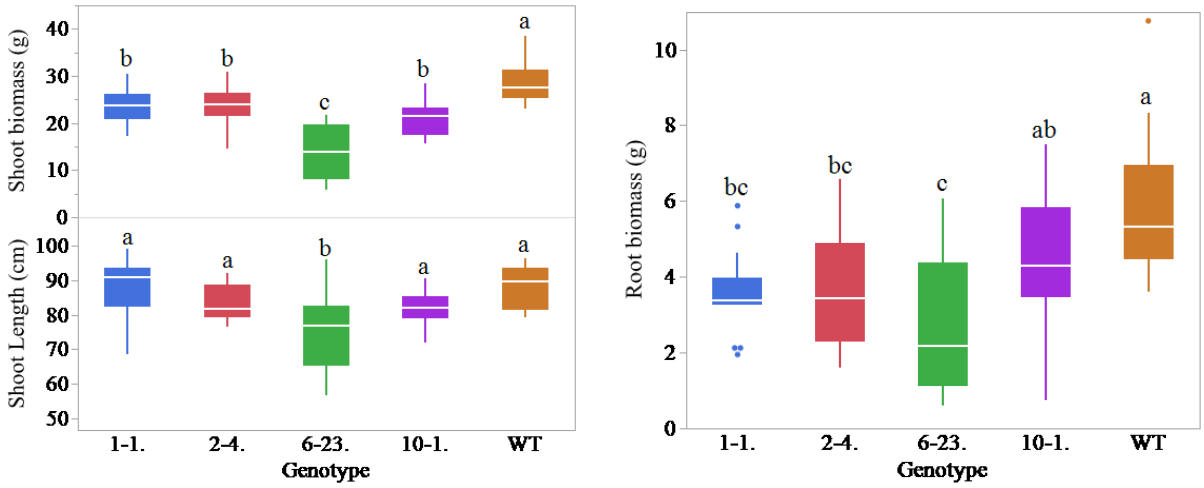

c) Grain yield

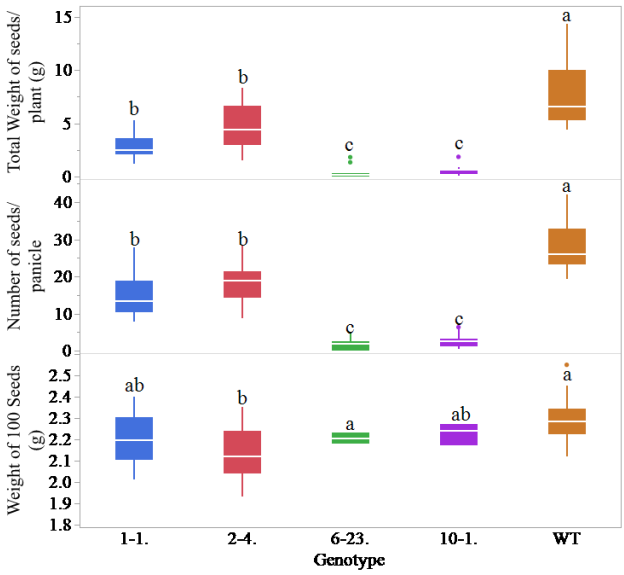

Figure 2.7 Phenotypic assessment of *snrk1αa+* double homozygous lines 1-1 and 2-4, and *snrk1αc* homozygous lines 6-23 and 10-1) in the greenhouse in comparison to WT. (a) shoot characteristics (length and biomass), (b) root biomass, (c) grain yield parameters (number of seeds per panicle, weight of 100 seeds, and total weight of seeds per plant) (n=20). Data analyzed by Tukey HSD test and statistical differences are shown by letters on each box with 0.05 significance level ($p \leq 0.05$). Values having the same letter are not significantly different.

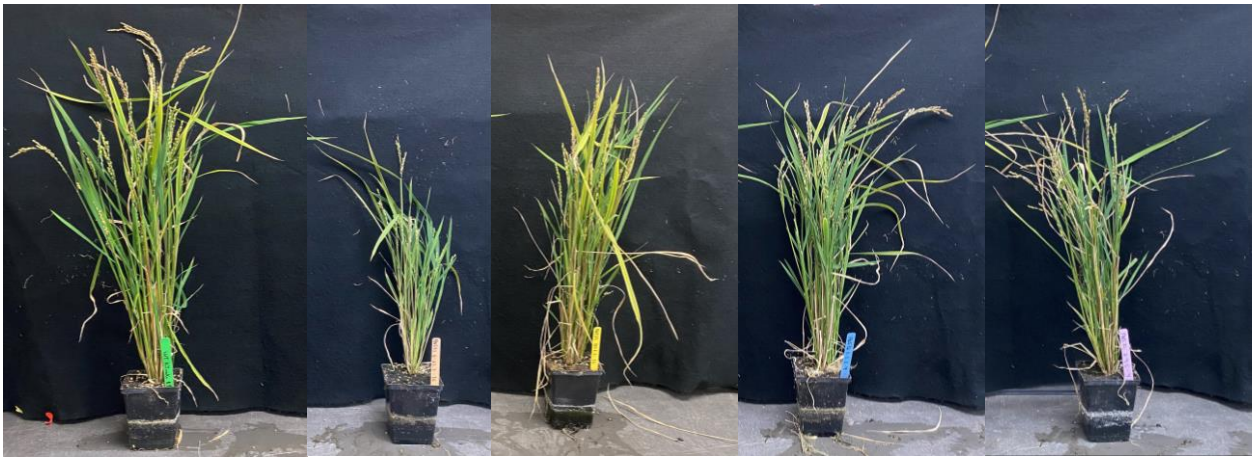

WT 6-23 line 10-1 line 1-1 line 2-4 line

Figure 2.8 Representative images of *snrk1αa+snrk1αb* double homozygous (lines 1-1 and 2-4) and *snrk1αc* single mutant (lines 6-23 and 10-1) in mature stage (R9) grown in the greenhouse in comparison to WT cv. Kitaake.

Chapter III – Transcriptomic analysis of SnRK1 mutants

4.1 Introduction

Cells in all living things need to maintain a balance between their energy supply and consumption in order to survive and grow. SnRK1 (Sucrose Non-Fermenting Related Kinase 1) plays a crucial role in the regulation of cellular metabolism and energy balance in plants. By detecting cellular energy levels, SnRK1 acts as a master regulator of gene expression, ensuring energy homeostasis. To maintain the cellular energy homeostasis and ensure the plant's survival, SnRK1 promotes catabolism and suppress anabolism (Peixoto & Baena-Gonzalez 2022) in both stress conditions (Baena-Gonzalez et al., 2007; Cho et al., 2012; Pedrotti et al., 2018; Wang et al., 2021) and normal conditions (Henninger et al., 2022; Wang et al., 2021). Once SnRK1 is activated, it triggers signaling events that result in the repression of anabolic processes such as cell wall formation, protein translation, and ribosome biogenesis (Baena-Gonzalez et al., 2007; Henninger et al, 2021; Nukarinen et al., 2016; Wang et al., 2021) and the promotion of catabolic processes involved in carbohydrate, lipid, and amino acid metabolism (Baena-Gonzalez et al., 2007; Baena-Gonzalez & Sheen, 2008; Henninger et al., 2021; Lu et al., 2007). SnRK1 regulates these biological processes in two ways: by altering the activities of enzymes involved in metabolism (Cho et al., 2012; Nukarinen et al., 2016) or by regulating gene expression (Mair et al., 2014). The role of SnRK1 in regulating gene expression is poorly understood in plants. Previous studies observed that SnRK1 can regulate gene expression by phosphorylating and altering the activity of chromatin-remodeling enzymes (Radchuk et al., 2006; Pedrotti et al., 2018; Wang et al., 2021), and by regulating the activity of transcription factors (Chan et al., 2017; Han et al., 2020; Tsai & Gazzarrini, 2012; Zhai et al., 2017), which change the expression of genes by binding to DNA. However, only few studies performed transcriptomic analysis of

snrk1 mutants in plants (Henninger et al, 2021; Pedrotti et al., 2018; Peixoto et al., 2021; Radchuk et al., 2006; Wang et al., 2021), and only one was done on the rice *snrk1* mutants (Wang et al., 2021).

4.1.a. SnRK1 role in anabolism

Transcriptomic and phosphoproteomics studies observed that SnRK1 represses a variety of anabolic activities, including the synthesis of amino acids, cell walls, lipids, proteins, sugars, and starches. The majority of repression targets are the pathways involved in protein synthesis, which is upregulated by the TOR signaling. SnRK1 was found to repress many genes involved in ribosome biogenesis, amino acid metabolism, cell cycle regulators and cell wall biosynthesis (Baena-Gonzalez et al., 2007; Henninger et al, 2021; Nukarinen et al., 2016; Wang et al., 2021). It is suggested that in low energy conditions SnRK1 promotes an energy saving program by inhibiting TOR kinase, leading to the inhibition of anabolic processes (Margalha et al., 2019; Nukarinen et al., 2016; Belda-Palazon et al., 2020; Wang et al., 2021). For example, phosphoproteomics studies observed that the phosphorylation levels of the conserved TOR targets, ribosomal protein RPS6 and translation initiation factors, were both altered in SnRK1 mutants in Arabidopsis (*SnRK1α/*KIN10 and *SnRK1α/*KIN 11) (Nukarinen et al., 2016). Wang et al. (2021) suggested that SnRK1 may need to be inactive in order for TOR signaling to occur under normal conditions. Further investigation is needed to fully understand the relationship between SnRK1 and TOR.

4.1.b. SnRK1 role in stress response

SnRK1 is a global regulator of gene expression related to stress responses. In response to stress conditions, SnRK1 activates stress related transcription processes to maintain energy homeostasis for plant survival. Numerous SnRK1 induced stress responsive genes have been identified (Baena-Gonzalez et al., 2007; Baena-Gonzalez & Sheen, 2008). Transient overexpression of SnRK1α/KIN10 in Arabidopsis protoplasts induced a transcriptional pattern resembling different starvation states and uncovered 1021 candidate SnRK1 target genes (Baena-Gonzalez et al., 2007). Wang et al. (2021) performed RNA seq studies in *snrk1αc* (LOC_Os05g45420) mutants in rice seedlings under normal and starvation conditions. They found that the mutations imitate a starvation-induced gene expression under normal conditions. Some of the genes were OsbZIP63 (BASIC LEUCINE ZIPPER PROTEIN 63), OsDIN2 (DARK INDUCIBLE 2), OsDIN9, OsMYBS1. Radchuk et al. (2006) evaluated gene expression analysis in SnRK1 antisense repressed pea seeds and observed upregulation of stress responsive genes. Similar finding was also reported by Chen et al. (2017), who found that SnRK1 is a positive regulator of autophagy, a process crucial for plant's response to stress conditions, by phosphorylating TG1 (autophagy-related gene 1) proteins in Arabidopsis.

4.1.c. Catabolism

By controlling the equilibrium between energy production and consumption during stressful and growth-promoting situations, SnRK1 plays a crucial role in plant catabolism. SnRK1 targets a wide range of genes that orchestrate transcription networks, promote catabolism, and restrict anabolism after sensing and signaling the lack of sugar and energy (Baena-Gonzalez et al., 2007). Studies observed that, under starvation conditions, SnRK1 upregulates genes that are

participate in several catabolic pathways and nutrient remobilization processes, involved in cell wall, starch, sucrose, amino acids, lipids, and proteins catabolism, providing the cell with alternative sources of energy and metabolites (Baena-Gonzalez et al., 2007; Baena-Gonzalez & Sheen, 2008; Henninger et al., 2021). Henninger et al. (2021) performed transcriptomic analysis in double mutants of *SnRK1α* catalytic site (*SnRK1α/KIN10* and *SnRK1α/KIN11*) in Arabidopsis seedlings under starvation and glucose feeding conditions and discovered that SnRK1 is required for the transcription of Branched Chain Amino Acid (BCAA) and pro catabolic genes (BCAT2, MCCA/B, and ProDH) during seedling establishment. In addition, a study found that under low sugar conditions, SnRK1 regulates starch catabolic processes in rice (Lu et al., 2007).

4.1.c. Transcription factors and Chromatin remodeling

SnRK1 has also been shown to modulate gene expression by regulating the activity of transcription factors (TF) through phosphorylation, or by regulating the activity of chromatin-modifying enzymes. By phosphorylating TFs, SnRK1 can either activate or repress their activity, leading to changes in gene expression. For example, SnRK1α/KIN10 in Arabidopsis has been shown to phosphorylate and regulate the TF FUSCA3 (FUS3), a major regulator of seed maturation, seed yield and plant growth (Chan et al., 2017; Tsai & Gazzarrini, 2012). It was also found that SnRK1α/KIN10 phosphorylates and stabilizes the TF SPEECHLESS (SPCH) to promote stomatal development, which influences plant response to environmental changes (Han et al., 2020). SnRK1α/KIN10 also regulates the activity of genes involved in glycolysis and plastidial lipid biosynthesis by controlling the TF WRINKLED1 (WRI1) (Zhai et al., 2017). In addition, Mair et al. (2014) discovered that the TF bZIP63 from Arabidopsis is a crucial regulator of the starvation response and a direct target of SnRK1 by directly binding and

controlling the cyPPDK promoter (Henninger et al, 2021). Similar to these findings, in Arabidopsis, SnRK1 regulates the TF group bZIP, which activates dark-induced genes in dark conditions (Baena-Gonzalez et al., 2007). In the same study, it was found that SnRK1 triggers several transcription cascades and controls chromatin remodeling factors in the presence of stress, darkness, and sugar deprivation. A recent study found that SnRK1phosphorylates the bZIP transcription factor bZIP39, which regulates the sorbitol metabolism in apple (Meng et al., 2023). Furthermore, in Arabidopsis, SnRK1 regulating anthocyanin biosynthesis by inhibiting the TF MBW (Broucke et al., 2023).

SnRK1 also regulates gene expression by phosphorylating and modifying the activity of chromatin-remodeling enzymes. Wang et al. (2021) found that SnRK1 phosphorylates the chromatin modifier JMJ705, which removes methyl groups from histones of key starvation responsive genes. These results reflect those of Pedrotti et al. (2018) who observed that, under starvation conditions, the TF bZIP and SnRK1 induce histone acetylation of the ETFQO promoter and facilitate transcription. Another study observed that SnRK1 is involved in chromatin modification during phase transitions in peas seeds (Radchuk et al., 2006).

The objective of this study is to identify biological processes, pathways and functions that are enriched in the set of differentially expressed genes (DEGs) between light and dark conditions through RNA-seq analysis of *snrk1* mutants and WT in rice seedlings.

4.2 Material and Methods

4.2.a. Plant material and growth conditions

For the transcriptomic experiment, 20 seedlings each of *snrk1αa+b* double mutant line T1_1-1, *snrk1αc* single mutant line T1_6-3 and the WT were plated on February 15 of 2022 in ½ MS

media with 2% sucrose and 2 grams of phytagel per liter. Four days after plating (February 19), the S3 stage germinated seeds were transferred to glass tubes containing ½ MS media without sucrose and 1.5 grams of phytagel per liter. The seedlings were grown in the growth chamber in a controlled environment with optimal light. The light was provided from 5 am to 8 pm, totaling 15 h photoperiod. On February 24, when the seedlings were at V1 stage, the seedlings were divided into 2 groups: half of them were transferred to complete darkness and the other half were grown in the normal light for 2 days. After that (February 26), each seedling (with roots), was rinsed in water, dried on tissue paper, and immediately frozen in liquid nitrogen for RNA extraction. Also, DNA was extracted from each seedling and used in PCR-sequencing to confirm mutation. The seedlings harvested from light and dark treatments were bulked, the RNA was extracted and sent for RNA sequencing along with the WT.

4.2.b. RNA extraction

For the RNA extraction protocol, each of the 12 samples, as shown in the table below (seedlings with roots) was ground in liquid nitrogen and homogenized in 1 ml of Trizol and incubated for 5 minutes to dissociate the nucleotide complex, 200 µl of chloroform was added and mixed on the shaker for 5 minutes. The samples were centrifuged at 13,000 rpm (4 °C) in an Eppendorf minicentrifuge 5415D, and the supernatant was decanted to a new tube, where it was mixed with 500 µl of isopropanol. Afterwards, the samples were incubated for 10 minutes and centrifuged for 15 minutes (same rotation and temperature as previously). Supernatant was discarded and 1 ml of 75% ethanol was added to wash the pellet. Samples were again centrifuged for 5 minutes, and the pellet was suspended in 40 µl of nuclease-free water. Once the total RNA

was extracted, the quantity and quality were checked using Nano-drop 2000 (Thermo-Fisher Inc) as shown below:

Samples	Lines	Mutation	Treatment	Number of seedlings	RNA concentration (ng/µl)
1	WT	-	Dark	4	2652.00
2	WT	-	Dark	3	2961.30
3	1-1	*snrk1αa+b*	Dark	1	1071.20
4	1-1	*snrk1αa+b*	Dark	1	1289.90
5	6-23	*snrk1αc*	Dark	3	1737.10
6	6-23	*snrk1αc*	Dark	3	999.50
7	WT	-	Light	3	2626.70
8	WT	-	Light	3	1401.20
9	1-1	*snrk1αa+b*	Light	1	1162.90
10	1-1	*snrk1αa+b*	Light	1	1162.90
11	6-23	*snrk1αc*	Light	3	1831.90
12	6-23	*snrk1αc*	Light	3	1233.50

The samples were prepared and sent for sequencing to Novogene Inc. It was sent 30 µg per sample and volume of 30 µl per sample for sequencing. Bioinformatic analysis such as differential expression analysis and gene enrichment analysis was done by Novogene Inc.

4.2.c. Gene ontology analysis

The gene ontology (GO) enrichment analysis, which shows the significant (Pvalue < 0.05) biological pathways down- or up-regulated was done for the following comparisons: *snrk1αa+b*_light vs WT_light, *snrk1αa+b*_ dark vs WT_dark, *snrk1αc*_light vs WT_light and *snrk1αc*_dark vs WT_dark. The GO:Biological Processes (BP) were divided into defense, catabolic and anabolic processes.

4.3 Results

4.3.a. WT dark and light comparison

The comparison of WT seedlings after dark and light treatment revealed that in the dark, pathways (GO: BP) related to defense and catabolic process were upregulated (Figure 3.1). The defense related processes upregulated in WT under dark conditions are: defense response (120 genes), defense response to other organism (60 genes), defense response to bacteria (40 genes), defense response to fungus (21 genes), regulation of hormone levels (55 genes), secondary metabolic process (49 genes) and regulation of jasmonic acid (JA) mediated signaling (11 genes). In addition, processes related to catabolism were also upregulated in WT seedlings in the dark: carbohydrate derivative catabolic process (16 genes), lipid catabolic process (34 genes) and small molecule catabolic process. On the other hand, in WT dark, processes related to anabolism were downregulated: ribosome biogenesis (175 genes), cytoplasmic translation (45 genes), cell cycle (121 genes), DNA replication (57 genes), photosynthesis (35 genes), mitotic cell cycle (73 genes), regulation of translation (39 genes), DNA metabolic process (112 genes), fatty acid biosynthetic process (25 genes) and positive regulation of cell proliferation (15 genes) (Figure 3.1)

4.3.b. 1-1 line dark and light comparison

Figure 3.2 shows the significant pathways that were up or down regulated in 1-1 line (*snrk1αa+b* mutant) in dark compared to light. This mutant had the opposite behavior when compared with the WT dark and light comparison: the pathways that are downregulated in the WT dark are upregulated in 1-1 dark, and the pathways that are upregulated in WT dark are downregulated in 1-1 dark. Under dark conditions, pathways related to anabolic process were upregulated and catabolic and defense process were downregulated in 1-1. The significantly

upregulated pathways were only 12, from which the following were chosen: cell differentiation (24 genes), negative regulation of proteolysis (12 genes), negative regulation of peptidase activity (12 genes), cellular developmental process (29 genes) and plant epidermis development (10 genes). Pathways related to stress response were downregulated: response to toxic substance (34 genes), response to other organism (31 genes), response to salt stress (26 genes), response to oxidative stress (42 genes), response to cold (22 genes), and jasmonic acid metabolic process (8 genes). Catabolic processes were also downregulated: generation of precursor metabolites and energy (71 genes), carbohydrate catabolic process (39 genes) and small molecule catabolic process (34 genes). Genes related to photosynthesis were also downregulated in 1-1 line in dark conditions (60 genes) (Figure 3-2).

4.3.c. 6-23 line dark and light comparison

The transcriptional responses of line 6-23 line (*snrk1αc* mutant) under dark and light conditions showed that in the dark, this mutant had significant downregulation of genes related to anabolism and photosynthesis while only 5 significant pathways upregulated (Figure 3.3). Thus, the transcriptional responses of this mutant are reminiscent of the transcriptional responses of wild type plants. . The upregulated processes in line 6-23 under dark conditions were: defense response (52 genes), multi-organism process (48 genes) and diterpenoid metabolic process (12 genes). On the other hand, the downregulated processes in 6-23 dark were: photosynthesis (50 genes), ribosome biogenesis (53 genes), cytoplasmatic translation (21 genes) and generation of precursor metabolites and energy (53 genes).

4.3.d. 1-1 line versus WT in light

When comparing the transcriptional responses under light conditions of the *snrk1αa+b* mutant (line 1-1) versus wild type, the results show that the *snrk1αa+b* mutant had catabolic and

defense processes upregulated in light, while anabolic processes were downregulated (Figure 3.4). This is similar to the transcriptome of WT dark (Figure 3.1). The defense processes upregulated in 1-1 line were: regulation of hormone levels (42 genes), response to jasmonic acid (16 genes), secondary metabolic process (28 genes), defense response (71 genes), response to water deprivation (30 genes), response to salt stress (31 genes) and response to osmotic stress (33 genes). Catabolic processes were also upregulated in 1-1 line: carbohydrate catabolic process (43 genes), lipid catabolic process (25 genes) and fatty acid catabolic process (11 genes). The top 10 processes that were downregulated were all anabolic processes: ribosome biogenesis (56 genes), cytoplasmatic translation (22 genes), cell cycle (68 genes), DNA replication (35 genes), photosynthesis (23 genes), mitotic cell cycle (41 genes), DNA metabolic process (62 genes), ribonucleoprotein complex biogenesis (71 genes), regulation of cell proliferation (10 genes) and ribosome assembly (18 genes).

4.3.e. 1-1 line versus WT in dark

When comparing the transcriptional responses under dark conditions between the *snrk1αa+b* mutant (line 1-1) and wild type, the results show that in 1-1, the defense processes were downregulated in dark, and anabolic processes were upregulated (Figure 3.5). The anabolic processes upregulated in 1-1 line in dark were: ribosome biogenesis (34 genes), cytoplasmatic translation (11 genes), cell cycle (41 genes), DNA replication (19 genes), DNA metabolic process (36 genes), ribosome assembly (10 genes), mitotic cell cycle (30 genes), meristem growth (4 genes), ribonucleoprotein complex biogenesis (38 genes) and regulation of cell proliferation (10 genes). The defense processes downregulated in 1-1 line were: defense response (72 genes), defense response to other organism (38 genes), defense response to bacterium (24 genes), response to toxic substance (54 genes), response to water deprivation (21 genes),

response to oxidative stress (52 genes), detoxification (47 genes), secondary metabolic process (45 genes) and flavonoid biosynthetic process (7 genes).

4.3.f. 6-23 line versus WT in light

When comparing the transcriptional responses under light conditions of the *snrk1αc* mutant (line 6-23) versus wild type, the results show that fewer than 25 processes were found to be significantly upregulated in 6-23 and only 4 genes were found to be upregulated in 6-23 line(Figure 3.6). This is not surprising because *SnRK1αc* gene is highly expressed in later vegetative and reproductive stages, while this transcriptomic data was generated from 7 days old seedlings. The upregulated genes related to defense processes were defense response (29 genes), defense response to other organisms (11 genes) and defense response to fungus (16 genes). The upregulated genes related to anabolic processes were regulation of developmental process (16 genes), positive regulation of growth (4 genes). The downregulated processes were: positive regulation of mitochondrial translation (2 genes) and nitrate metabolic process (2 genes).

4.3.f. 6-23 line versus WT in dark

When comparing the transcriptional responses under dark conditions of the *snrk1αc* mutant (line 1-1) versus wild type, no pathways were significantly upregulated in 6-23 (Figure 3.7), but there were pathways that show significant down regulation in 6-23 line. Those pathways are: photosynthesis (23 genes), response to toxic substance (23 genes), secondary metabolic process (14 genes) and generation of precursor metabolites and energy (30 genes).

4.4 Discussion

In this study, we sought to identify biological processes that are regulated by SnRK1 by conducting genome-wide transcriptomics analysis to light and darkness on lines containing mutations on SnRK1αa and SnRK1αb, or SnRK1αc genes. We observed that in the WT plant, pathways related to defense and catabolic process, such as defense response, secondary metabolic processes and carbohydrate catabolic processes were upregulated under dark condition whereas pathways related to anabolism, such as ribosome biogenesis, cell cycle and translation were downregulated (Figure 3.1). Our study corroborates previous transcriptomics studies of plants under starvation. Wang et al. (2007) observed that the transcriptomic profile of rice suspension cells under starvation showed downregulation of genes involved in the synthesis of macromolecules and upregulation of genes participating in the degradation of molecules such as sucrose, fatty acids and amino acids. Similarly, other studies also observed that growth under dark conditions leads to the upregulation of stress responses and catabolic pathways and downregulation of translation apparatus and cell division (Contento et al., 2004; Valencia-Lozano et al., 2022). Those findings agree with the widely accepted knowledge that under stress, plants activate a complex network of signaling pathways leading to protective responses while repressing growth processes. These transcriptional and metabolic are essential to promote survival by inducing stress responses and providing the plant with alternative sources of energy, metabolites, and nutrients (Baena-Gonzalez & Sheen, 2008).

When comparing transcriptomics profiling of WT plants in dark vs light), although the plant is under abiotic stress (starvation conditions), we observed upregulation of several defense response genes, including defense response to organisms such as fungi or bacteria. A possible explanation is that dark-induced (DIN) genes are activated under diverse stress conditions, such

as starvation, pathogens and senescence, and that abiotic and biotic stress responses control various but overlapping set of genes (Baena-Gonzalez et al., 2007; Fujita et al., 2006; Kilian et al., 2007; Smith & Stitt, 2007). Ultimately, abiotic and biotic stress conditions result in energy deprivation, which is partially translated as an energy-deficit signal that causes converging reactions regardless of its underlying cause. Ma & Bohnert (2007) clustered Arabidopsis transcript profiles for several treatments, including abiotic and biotic stress, and observed common stress response in diverse conditions such as cold, osmotic, salinity, wounding, and biotic stress.

In addition to defense response genes, wild type plants exposed to dark conditions also showed upregulation of secondary metabolic process and regulation of hormones (Figure 3.1). Secondary metabolites are substances found in specialized cells that are not essential for the survival of the cell but are vital for the environment-survival of the plant. Secondary metabolites improve plant fitness by inhibiting disease and insect attack, as well as promoting reproduction by luring pollinators or attracting seeds via flower aroma or coloring (Kliebenstein et al., 2005). Previous studies observed that secondary metabolites are implicated in response to both biotic and abiotic stresses (Kilian et al., 2007; Walley et al., 2007). The upregulation of hormone pathways in wild type seedlings in the dark can be explained by the fact that biotic and abiotic stress responses are largely mediated by hormone signaling pathways controlled by ethylene, salicylic acid, jasmonic acid, and abscisic acid (Fujita et al., 2006; Kilian et al., 2007; Walley et al., 2007).

The downregulation of photosynthesis in wild type seedlings grown in the dark is expected, since photosynthetic carbon assimilation occurs only in the light. Similar results have been obtained in dark-grown Arabidopsis (Baena-Gonzalez et al., 2007; Contento et al., 2004). Cell

cycle, DNA metabolic process and replication were also downregulated in dark. During starvation, plants show a decrease in the level of transcripts encoding proteins required for cell division, cell cycle and DNA replication to promote cessation of growth (Smith & Stitt, 2007). In addition, growth, and biosynthesis processes, such as ribosome biogenesis and translation processes were downregulated in WT dark. Nucleolins are the primary mechanism by which ribosome production is controlled and the expression of the nucleolin gene AtNUC-L2 is suppressed by carbon deprivation. Therefore, when the plant is under carbon deprivation, protein synthesis is suppressed for conserving resources and promoting plants survival (Smith & Stitt, 2007).

After analyzing the biological processes that are up and downregulated in the WT under dark condition, we analyzed how growth in the dark affects biological processes in *snrk1* mutants. In *snrk1αa+b* mutant (1-1 line) in dark, the anabolic processes were found to be upregulated and the catabolic processes were found to be downregulated (Figure 3.2). This indicates that anabolic processes such as cell differentiation and cellular development are actively repressed and catabolic processes such as carbohydrate catabolism are induced by *snrk1αa+b* in the dark. Similarly, the comparison of *snrk1αa+b* mutant with the WT in dark condition (Figure 3.5) showed upregulation of biosynthesis process and downregulation of defense processes in the mutant. Previous research showed that SnRK1 is a major regulator of gene expression in response to dark and other types of stress, and it regulates energy homeostasis by stimulating catabolic and energy preserving processes under stress conditions (Polge & Thomas, 2006). The research of Baena-Gonzalez et al. (2007) did an analysis of the extensive genome-wide transcriptional alterations induced by SnRK1 in Arabidopsis (*SnRK1α/KIN10* and *SnRK1α/KIN11* double mutants), where they found 278 genes that were co-activated by SnRK1

in dark conditions. They found that under starvation, SnRK1 activates cell wall, starch, sucrose, amino acid, lipid, and protein degradation catabolic pathways. They also found that SnRK1 is a global regulator of defense response and secondary metabolism, which is in agreement with our findings. Figure 3.5 shows downregulation of defense response and secondary metabolic process in *snrk1αa+b* mutant in dark. Broucke et al. (2023) also observed that SnRK1 is crucial in the control of secondary metabolites, especially the phenolic flavonoid anthocyanin. Their work demonstrates that SnRK1 is a negative regulator of anthocyanin production by inhibiting the TF complex MBW. By suppressing MBW, SnRK1 conserves energy for essential functions under stressful conditions. In addition, the *snrk1αa+b* mutant in dark had biosynthesis processes upregulated, which is explained by the fact that SnRK1 inhibits energy-intensive anabolic processes like protein and lipid synthesis while promoting defense response and catabolic processes like mobilization of energy reserves and amino acid catabolism (Baena-Gonzalez & Sheen, 2008; Henninger et al, 2021; Lu et al, 2007).

Figure 3.4 shows that dark-induced processes were upregulated in light grown *snrk1αa+b* mutant. These processes include lipid, carbohydrate and fatty acid catabolic processes, defense related processes, and regulation of hormone levels. Next, biosynthesis processes are downregulated: ribosome biogenesis, cytoplasmatic translation, DNA metabolic process and cell cycle. These results corroborate with previous studies, where SnRK1 is shown to repress anabolic processes, such as ribosome biogenesis, cell cycle, protein, and amino acids biosynthesis in dark (Baena-Gonzalez et al., 2007; Belda-Palazon et al., 2020; Wang et al., 2021). Nukarinen et al., (2016) discovered that SnRK1 activation is necessary for the inhibition of energy-intensive cell functions and growth by regulating target of rapamycin (TOR) complex called TORC1, a major regulator of anabolic processes. In addition, as mentioned earlier, our

transcriptomic data shows that lipid, carbohydrate, and fatty acid catabolic processes along with defense processes such as defense response and regulation of hormone levels is upregulated in *snrk1αa+b* mutant as compared to the WT in light (Figure 3.4). This suggests that SnRK1 activity is necessary for both the activation of the low energy, stress-triggered transcriptional program, and its suppression in the energy-sufficient condition, which is in accordance with the findings of Wang et al (2021). SnRK1 is also known to activate transcription factors and chromatin-modifying enzymes in both stress and normal conditions (Henninger et al, 2021; Mair et al., 2014; Wang et al., 2021), such as bZIP transcription factors and the histone demethylase JMJ705, which are involved in stress response (Pedrotti et al., 2018; Wang et al., 2021).

The dark-induced biological processes in *snrk1αc* mutant (6-23 line) were similar to that in the WT (Figure 3.3). We observed that *snrk1αc* had a similar transcriptome as that of the WT: genes related to anabolism and photosynthesis were downregulated and defense response processes were upregulated in dark. This is further supported by a comparison of *snrk1αc* with WT under dark condition where no significant pathway was upregulated; however, a few pathways such as photosynthesis, secondary metabolic process, and generation of precursor metabolites were downregulated (Figure 3.7). In the light grown *snrk1αc* mutant, defense response and growth processes were upregulated, while nitrate metabolic process was downregulated (Figure 3.6), which corroborates with previous finding that SnRK1 controls nitrate reductase activity as well as nitrogen metabolism (Sugden et al., 1999). Similarly, in comparison with the WT, defense response was upregulated in the light grown *snrk1αc* mutant, which is explained by the fact that SnRK1 is a major regulator of defense genes under stress conditions. However, not many biological processes were found to be up or down regulated in the *snrk1αc* in dark condition, during which SnRK1 is most active (Figure 3.3). This can be

explained by the fact that the plants used for the RNA-seq were 7 days old seedlings, and *SnRK1αc* is highly expressed in reproductive stages, but not in early seedlings stages (Figure 1.4) (Takano et al., 1998).

The present result is in accordance with previous studies that performed transcriptomic analysis of SnRK1 mutants in plants. Wang et al. (2021) did transcriptomic analysis in *snrk1αc* (LOC_Os05g45420) mutants of rice and observed that in darkness, 1966 genes were upregulated that include biosynthesis of enzymes, ribosomal proteins and cell cycle, and 1407 genes related to macromolecule degradation and stress signaling were downregulated. This is similar to our results that show the upregulation of growth processes and downregulation of stress response in dark-grown snrk1αa+*b* mutant in comparison to WT (Figure 3.5). In addition, Wang et al. (2021) showed that over 50% of downregulated genes in *snrk1αc* in normal conditions were repressed by dark conditions in the WT. Similarly, our results show that biosynthesis process (ribosome biogenesis, cell cycle, cytoplasmatic translation and DNA replication) that are downregulated in light-grown *snrk1αa+b* mutant (Figure 3.4), are suppressed in WT dark-grown seedlings (Figure 3.1). Henninger et al. (2021) did transcriptomic analysis in double mutants of *SnRK1α* catalytic site (*SnRK1α/KIN10* and *SnRK1α/AKIN11*) in Arabidopsis seedlings under starvation and light conditions and observed that *snrk1* double mutants in dark had over 3000 genes differently expressed compared to the WT. Henninger et al. (2021) also noted that *snrk1* double mutants had biosynthesis processes, such as biosynthesis of triacylglycerol and fatty acid, downregulated and catabolic processes, such as amino acid catabolism, upregulated in normal conditions, which is similar with the *snrk1αa+b* mutant in light and WT light comparison (Figure 3.4), where biogenesis process are downregulated and catabolic process are upregulated. Radchuk et al. (2006) did gene expression analysis of *snrk1* mutants in pea embryo under low energy conditions

and observed that SnRK1 has a main role in repressing energy consuming processes and inducing stress response.

In conclusion, this study validated the effect of *snrk1* mutations in two different rice lines by showing similar transcriptomic changes as reported in previous studies on *snrk1* mutants. We compared the biological processes that were up or downregulated in WT and *snrk1* mutants under light and dark conditions. The result of this work is consistent with earlier transcriptomic studies of SnRK1 mutants in rice, pea, and Arabidopsis, and shows that SnRK1 controls genes involved in anabolism, catabolism, defense response, and stress signaling. Under low energy conditions, SnRK1 promotes energy conservation by suppressing TOR signaling through the phosphorylation of RAPTOR (one of the components of TOR complex), leading to the inhibition of anabolic processes (Nukarinen et al., 2016). In addition, aligned with previous research, this study confirms that SnRK1 is not only important for stress conditions, but also in regulating plant growth and development in normal conditions. We also confirmed that SnRK1 is necessary to repress defense and energy saving processes under normal conditions. Hence, SnRK1 has a main role in regulating energy homeostasis and promoting plant growth, development, and survival.

References

Baena-González, E., & Sheen, J. (2008). Convergent energy and stress signaling. In Trends in Plant Science (Vol. 13, Issue 9, pp. 474–482). https://doi.org/10.1016/j.tplants.2008.06.006

Baena-González, E., Rolland, F., Thevelein, J. M., & Sheen, J. (2007). A central integrator of transcription networks in plant stress and energy signalling. Nature, 448(7156), 938–942. https://doi.org/10.1038/nature06069

Belda-Palaz On, B., Onica Costa, M., Beeckman, T., Rolland, F., Baena-Gonz Alez, E., & Niyogi, K. (2022). ABA represses TOR and root meristem activity through nuclear exit of the SnRK1 kinase. https://doi.org/10.1073/pnas

Broucke, E., Dang, T. T. V., Li, Y., Hulsmans, S., Van Leene, J., De Jaeger, G., Hwang, I., Van den Ende, W., & Rolland, F. (2023). SnRK1 inhibits anthocyanin biosynthesis through both transcriptional regulation and direct phosphorylation and dissociation of the MYB/bHLH/TTG1 MBW complex. The Plant Journal : for Cell and Molecular Biology. https://doi.org/10.1111/tpj.16312

Chan, A., Carianopol, C., Tsai, A. Y. L., Varathanajah, K., Chiu, R. S., & Gazzarrini, S. (2017). SnRK1 phosphorylation of FUSCA3 positively regulates embryogenesis, seed yield, and plant growth at high temperature in Arabidopsis. Journal of Experimental Botany, 68(15), 4219–4231. https://doi.org/10.1093/jxb/erx233

Chen, L., Su, Z. Z., Huang, L., Xia, F. N., Qi, H., Xie, L. J., Xiao, S., & Chen, Q. F. (2017). The AMP-activated protein kinase kin10 is involved in the regulation of autophagy in arabidopsis. Frontiers in Plant Science, 8. https://doi.org/10.3389/fpls.2017.01201

Contento, A. L., Kim, S. J., & Bassham, D. C. (2004). Transcriptome profiling of the response of arabidopsis suspension culture cells to Suc starvation. Plant Physiology, 135(4), 2330–2347. https://doi.org/10.1104/pp.104.044362

Fujita, M., Fujita, Y., Noutoshi, Y., Takahashi, F., Narusaka, Y., Yamaguchi-Shinozaki, K., & Shinozaki, K. (2006). Crosstalk between abiotic and biotic stress responses: a current view from the points of convergence in the stress signaling networks. In Current Opinion in Plant Biology (Vol. 9, Issue 4, pp. 436–442). https://doi.org/10.1016/j.pbi.2006.05.014

Han, C., Liu, Y., Shi, W., Qiao, Y., Wang, L., Tian, Y., Fan, M., Deng, Z., Lau, O. S., De Jaeger, G., & Bai, M. Y. (2020). KIN10 promotes stomatal development through stabilization of the SPEECHLESS transcription factor. Nature Communications, 11(1). https://doi.org/10.1038/s41467-020-18048-w

Henninger, M., Pedrotti, L., Krischke, M., Draken, J., Wildenhain, T., Fekete, A., Rolland, F., Müller, M. J., Fröschel, C., Weiste, C., & Dröge-Laser, W. (2022). The evolutionarily

conserved kinase SnRK1 orchestrates resource mobilization during Arabidopsis seedling establishment. Plant Cell, 34(1), 616–632. https://doi.org/10.1093/plcell/koab270

Kilian, J., Whitehead, D., Horak, J., Wanke, D., Weinl, S., Batistic, O., D'Angelo, C., Bornberg-Bauer, E., Kudla, J., & Harter, K. (2007). The AtGenExpress global stress expression data set: Protocols, evaluation and model data analysis of UV-B light, drought and cold stress responses. Plant Journal, 50(2), 347–363. https://doi.org/10.1111/j.1365-313X.2007.03052.x

Kliebenstein, D. ., Rowe, H. ., & Denby, K. . (2005). Secondary metabolites influence Arabidopsis/Botrytis interactions: variation in host production and pathogen sensitivity. The Plant Journal : for Cell and Molecular Biology, 44(1), 25–36. https://doi.org/10.1111/j.1365-313X.2005.02508.x

Li, C., Qi, W., Liang, Z., Yang, X., Ma, Z., & Song, R. (2020). A SnRK1-ZmRFWD3-Opaque2 signaling axis regulates diurnal nitrogen accumulation in maize seeds. Plant Cell, 32(9), 2823–2841. https://doi.org/10.1105/TPC.20.00352

Lu, C. A., Lin, C. C., Lee, K. W., Chen, J. L., Huang, L. F., Ho, S. L., Liu, H. J., Hsing, Y. I., & Yu, S. M. (2007). The SnRK1αa protein kinase plays a key role in sugar signaling during germination and seedling growth of rice. Plant Cell, 19(8), 2484–2499. https://doi.org/10.1105/tpc.105.037887

Ma, S., & Bohnert, H. J. (2007). Integration of Arabidopsis thaliana stress-related transcript profiles, promoter structures, and cell-specific expression. Genome Biology, 8(4). https://doi.org/10.1186/gb-2007-8-4-r49

Mair, A., Pedrotti, L., Wurzinger, B., Anrather, D., Simeunovic, A., Weiste, C., Valerio, C., Dietrich, K., Kirchler, T., Agele, T. N. ¨, Jesús, J. J., Carbajosa, V., Hanson, J., Baena-Gonzálezgonz´gonzález, E., Chaban, C., Weckwerth, W., Dröge, W., Dröge-Laser, D., & Teige, M. (n.d.). SnRK1-triggered switch of bZIP63 dimerization mediates the low-energy response in plants. https://doi.org/10.7554/eLife.05828.001

Margalha, L., Confraria, A., & Baena-González, E. (2019). SnRK1 and TOR: Modulating growth–defense trade-offs in plant stress responses. In Journal of Experimental Botany (Vol. 70, Issue 8, pp. 2261–2274). Oxford University Press. https://doi.org/10.1093/jxb/erz066

Meng, D., Cao, H., Yang, Q., Zhang, M., Borejsza-Wysocka, E., Wang, H., Dandekar, A. M., Fei, Z., & Cheng, L. (2023). SnRK1 kinase-mediated phosphorylation of transcription factor bZIP39 regulates sorbitol metabolism in apple. Plant Physiology (Bethesda). https://doi.org/10.1093/plphys/kiad226

Nukarinen, E., Ngele, T., Pedrotti, L., Wurzinger, B., Mair, A., Landgraf, R., Börnke, F., Hanson, J., Teige, M., Baena-Gonzalez, E., Dröge-Laser, W., & Weckwerth, W. (2016). Quantitative phosphoproteomics reveals the role of the AMPK plant ortholog SnRK1 as a

metabolic master regulator under energy deprivation. Scientific Reports, 6. https://doi.org/10.1038/srep31697

Pedrotti, L., Weiste, C., Nägele, T., Wolf, E., Lorenzin, F., Dietrich, K., Mair, A., Weckwerth, W., Teige, M., Baena-González, E., & Dröge-Laser, W. (2018). Snf1-RELATED KINASE1-controlled C/S1-bZIP signaling activates alternative mitochondrial metabolic pathways to ensure plant survival in extended darkness. Plant Cell, 30(2), 495–509. https://doi.org/10.1105/tpc.17.00414

Peixoto, B., & Baena-González, E. (2022). Management of plant central metabolism by SnRK1 protein kinases. Journal of Experimental Botany, 73(20), 7068–7082. https://doi.org/10.1093/jxb/erac261

Peixoto, B., Moraes, T. A., Mengin, V., Margalha, L., Vicente, R., Feil, R., Hohne, M., Sousa, A. G. G., Lilue, J., Stitt, M., Lunn, J. E., & Baena-Gonzalez, E. (2021). Impact of the SnRK1 protein kinase on sucrose homeostasis and the transcriptome during the diel cycle. Plant Physiology, 187(3), 1357–1373. https://doi.org/10.1093/plphys/kiab350

Polge, C., & Thomas, M. (2007). SNF1/AMPK/SnRK1 kinases, global regulators at the heart of energy control? In Trends in Plant Science (Vol. 12, Issue 1, pp. 20–28). https://doi.org/10.1016/j.tplants.2006.11.005

Radchuk, R., Radchuk, V., Weschke, W., Borisjuk, L., & Weber, H. (2006). Repressing the expression of the SUCROSE NONFERMENTING-1-RELATED PROTEIN KINASE gene in pea embryo causes pleiotropic defects of maturation similar to an abscisic acid-insensitive phenotype. Plant Physiology, 140(1), 263–278. https://doi.org/10.1104/pp.105.071167

Smith, A. M., & Stitt, M. (2007). Coordination of carbon supply and plant growth. In Plant, Cell and Environment (Vol. 30, Issue 9, pp. 1126–1149). https://doi.org/10.1111/j.1365-3040.2007.01708.x

Sugden C, Donaghy PG, Halford NG, Hardie DG.. 1999. Two SNF1-related protein kinases from spinach leaf phosphorylate and inactivate 3-hydroxy-3-methylglutaryl-coenzyme A reductase, nitrate reductase, and sucrose phosphate synthase in vitro. Plant Physiology 120, 257–274.

Takano, M., Kajiya-Kanegae, H., Funatsuki, H., & Kikuchi, S. (1998). Rice has two distinct classes of protein kinase genes related to SNF1 of Saccharomyces cerevisiae, which are differently regulated in early seed development. Molecular & General Genetics, 260(4), 388–394. https://doi.org/10.1007/s004380050908

Tsai, A. Y. L., & Gazzarrini, S. (2012). AKIN10 and FUSCA3 interact to control lateral organ development and phase transitions in Arabidopsis. Plant Journal, 69(5), 809–821. https://doi.org/10.1111/j.1365-313X.2011.04832.x

Valencia-Lozano, E., Herrera-Isidrón, L., Flores-López, J. A., Recoder-Meléndez, O. S., Barraza, A., & Cabrera-Ponce, J. L. (2022). Solanum tuberosum Microtuber Development under Darkness Unveiled through RNAseq Transcriptomic Analysis. International Journal of Molecular Sciences, 23(22), 13835–. https://doi.org/10.3390/ijms232213835

Walley, J. W., Coughlan, S., Hudson, M. E., Covington, M. F., Kaspi, R., Banu, G., Harmer, S. L., & Dehesh, K. (2007). Mechanical stress induces biotic and abiotic stress responses via a novel cis-element. PLoS Genetics, 3(10), 1800–1812. https://doi.org/10.1371/journal.pgen.0030172

Wang, H. J., Wan, A. R., Hsu, C. M., Lee, K. W., Yu, S. M., & Jauh, G. Y. (2007). Transcriptomic adaptations in rice suspension cells under sucrose starvation. Plant Molecular Biology, 63(4), 441–463. https://doi.org/10.1007/s11103-006-9100-4

Wang, W., Lu, Y., Li, J., Zhang, X., Hu, F., Zhao, Y., & Zhou, D.-X. (2021). SnRK1 stimulates the histone H3K27me3 demethylase JMJ705 to regulate a transcriptional switch to control energy homeostasis. The Plant Cell, 33(12), 3721–3742. https://doi.org/10.1093/plcell/koab224

Zhai, Z., Liu, H., & Shanklin, J. (2017). Phosphorylation of WRINKLED1 by KIN10 results in its proteasomal degradation, providing a link between energy homeostasis and lipid biosynthesis. Plant Cell, 29(4), 871–889. https://doi.org/10.1105/tpc.17.00019

Tables and figures

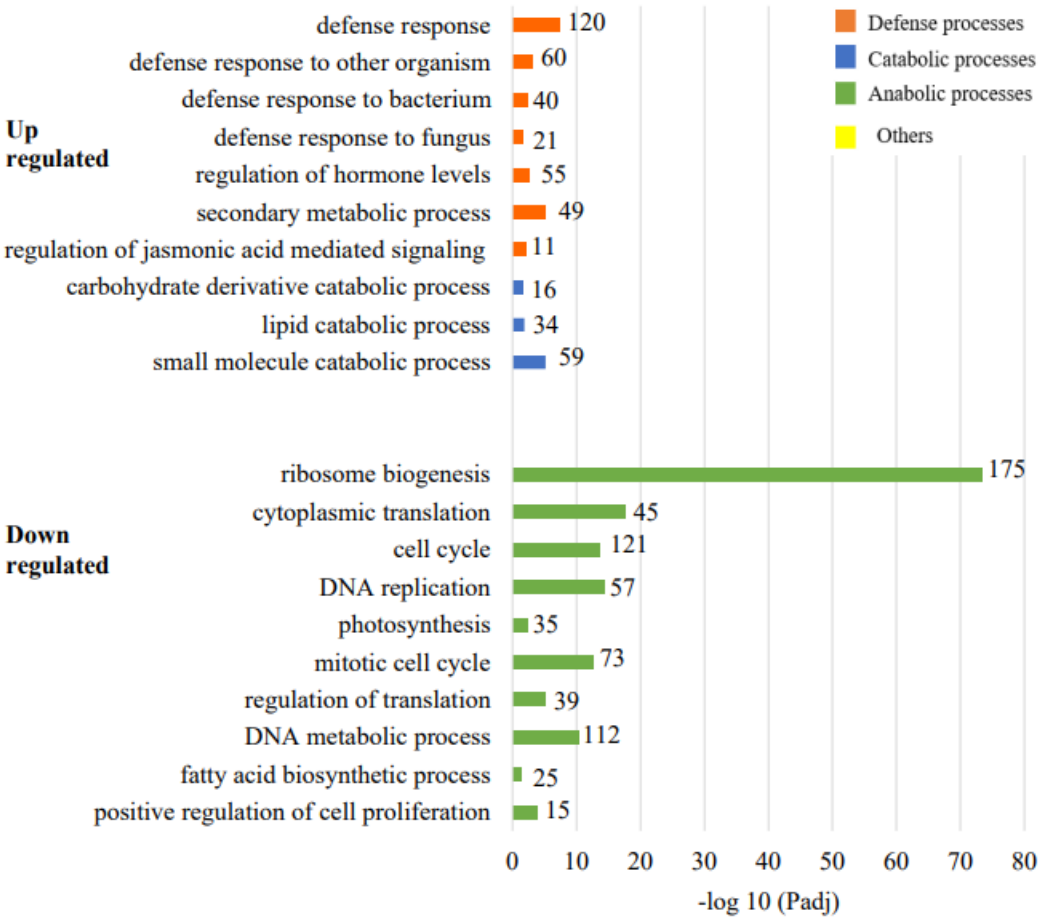

Figure 3.1. Differentially expressed biological processes in 7d-old WT seedlings grown under dark condition (p-value < 0.05). Pathways are divided into defense response (orange bars), catabolic process (blue bars), anabolic process (green bars) and other types of pathways (yellow bars). The number of differentially expressed genes in each pathway are indicated.

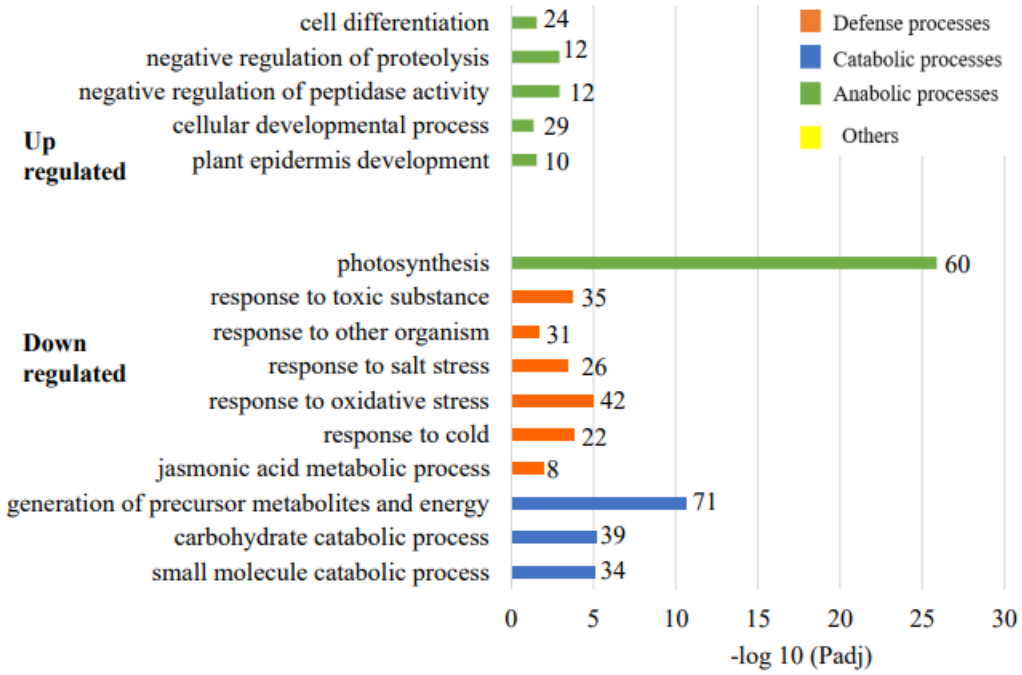

Figure 3.2. Differentially expressed biological processes in 7d-old *snrk1αa+b* mutant seedlings grown under dark condition (p-value < 0.05). Pathways are divided into defense response (orange bars), catabolic process (blue bars), anabolic process (green bars) and other types of pathways (yellow bars). The number of differentially expressed genes in each pathway are indicated with significance.

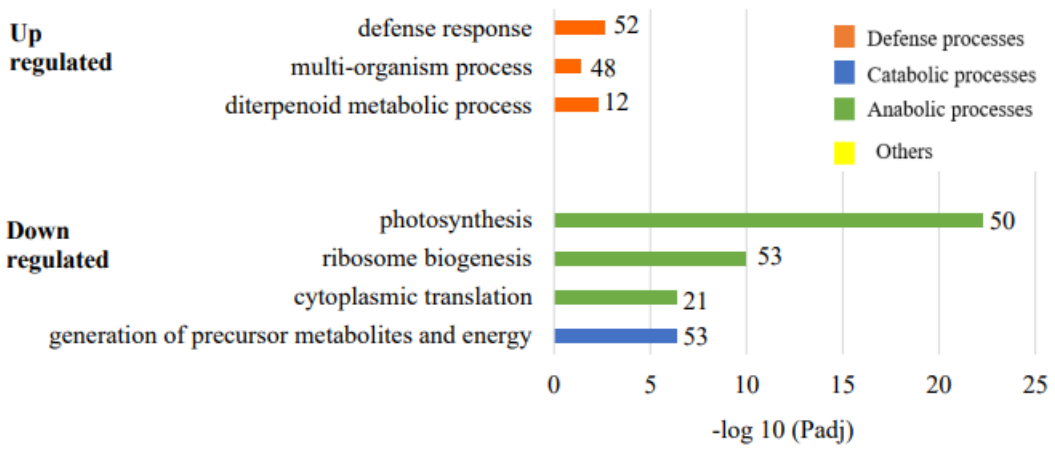

Figure 3.3. Differentially expressed biological processes in 7d-old *snrk1αc* mutant seedlings grown under dark condition (p-value < 0.05). Pathways are divided into defense response (orange bars), catabolic process (blue bars), anabolic process (green bars) and other types of pathways (yellow bars). The number of differentially expressed genes in each pathway are indicated with significance.

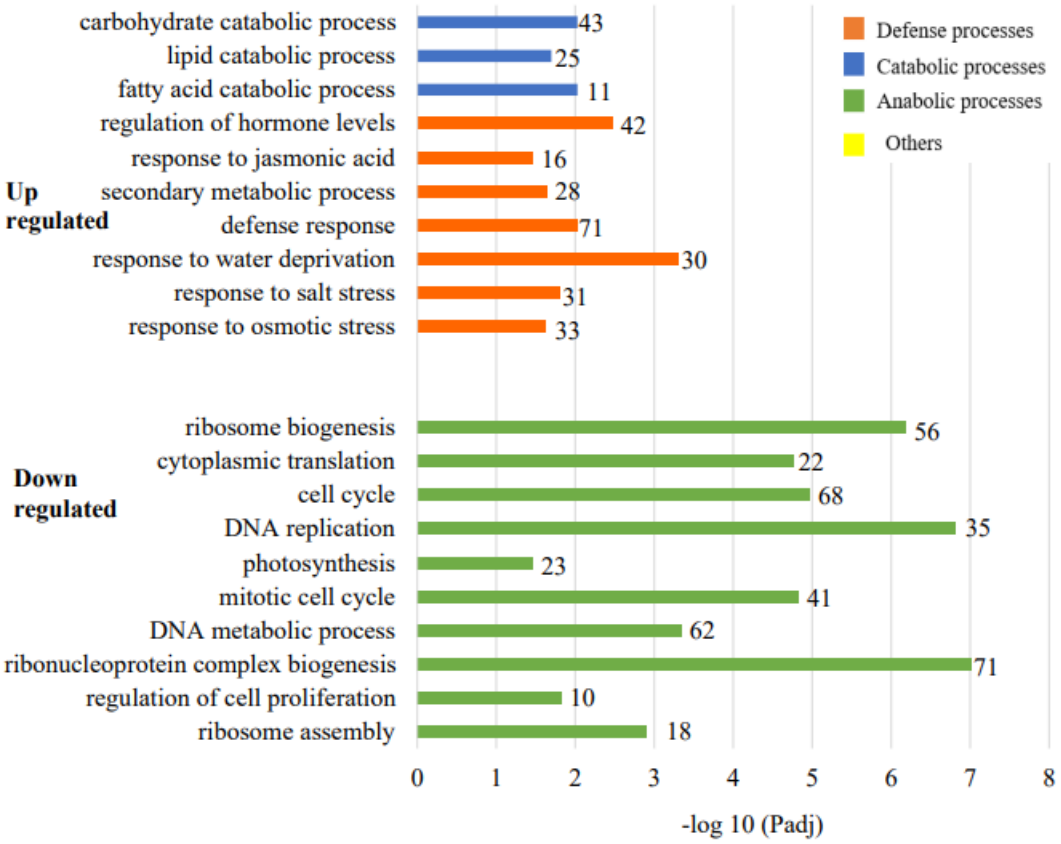

Figure 3.4. Differentially expressed biological processes in 7d-old *snrk1αa+b* mutant seedlings grown under light condition in comparison to the WT (p-value < 0.05). Pathways are divided into defense response (orange bars), catabolic process (blue bars), anabolic process (green bars) and other types of pathways (yellow bars). The number of differentially expressed genes in each pathway are indicated with significance.

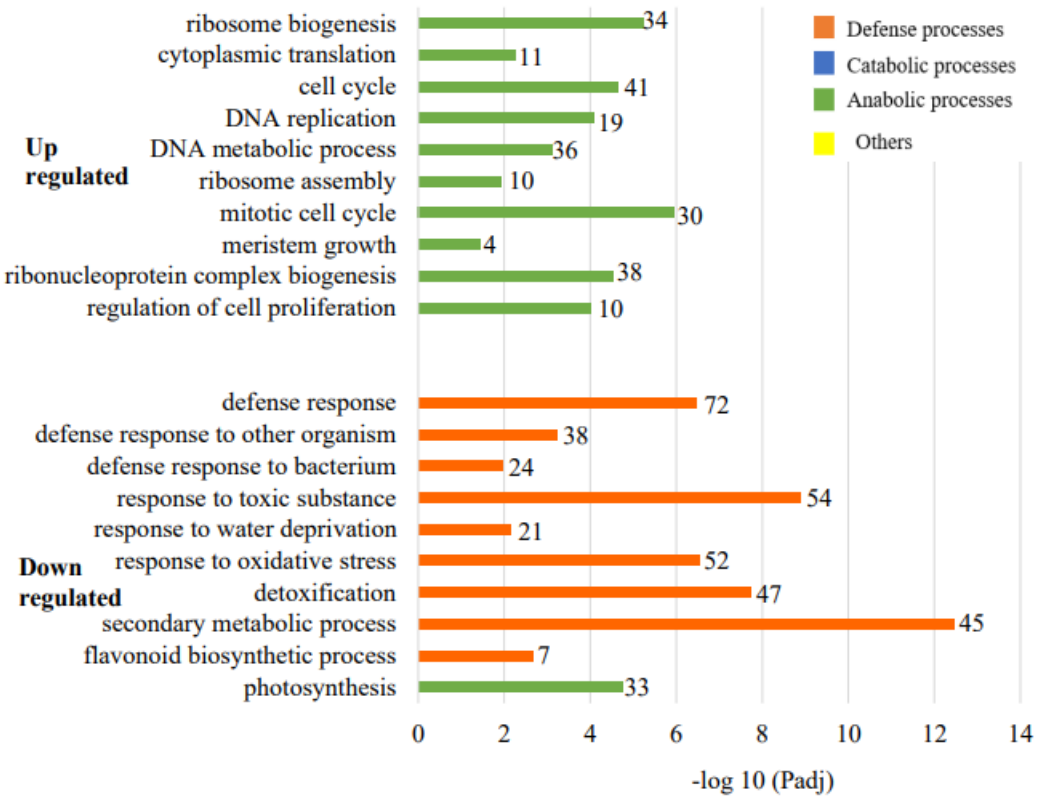

Figure 3.5 Differentially expressed biological processes in 7d-old *snrk1αa+b* mutant seedlings grown under dark condition in comparison to the WT (p-value < 0.05). Pathways are divided into defense response (orange bars), catabolic process (blue bars), anabolic process (green bars) and other types of pathways (yellow bars). The number of differentially expressed genes in each pathway are indicated with significance.

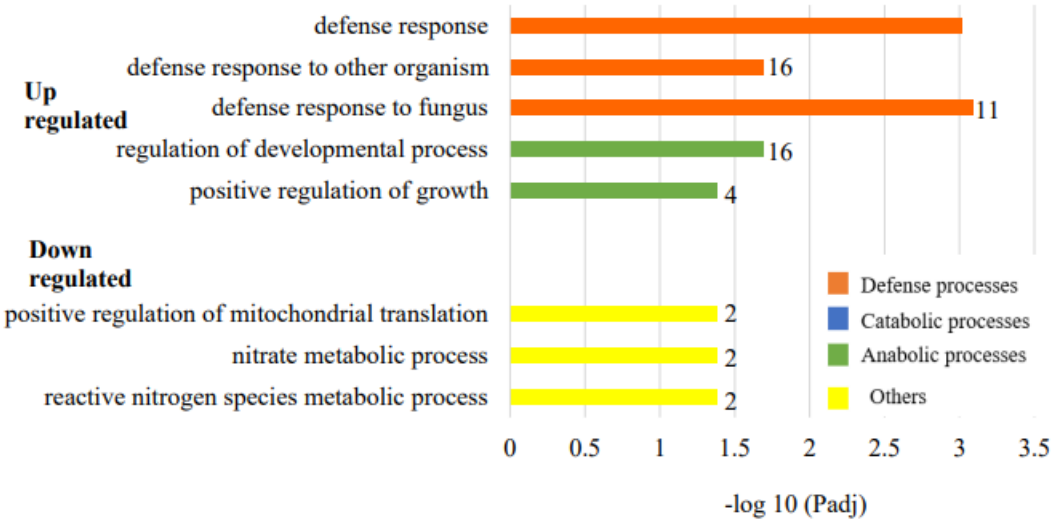

Figure 3.6 Differentially expressed biological processes in 7d-old *snrk1αc* mutant seedlings grown under light condition in comparison to the WT (p-value < 0.05). Pathways are divided into defense response (orange bars), catabolic process (blue bars), anabolic process (green bars) and other types of pathways (yellow bars). The number of differentially expressed genes in each pathway are indicated with significance.

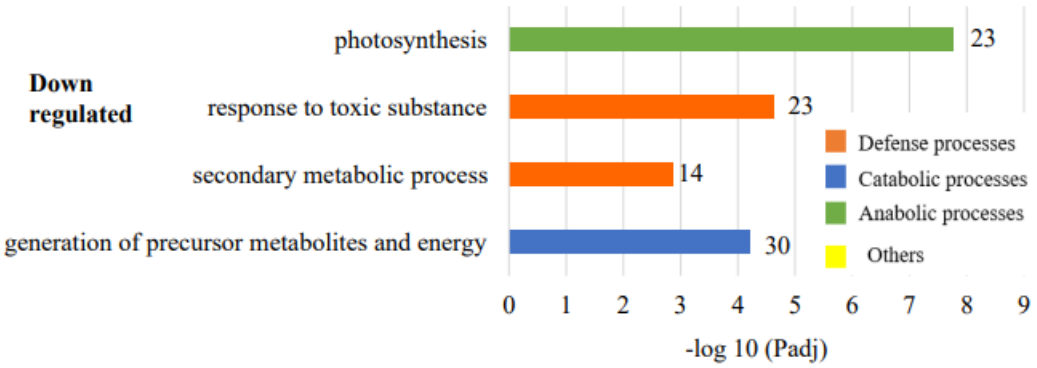

Figure 3.7 Differentially expressed biological processes in 7d-old *snrk1αc* mutant seedlings grown under dark condition in comparison to the WT (p-value < 0.05). Pathways are divided into defense response (orange bars), catabolic process (blue bars), anabolic process (green bars) and other types of pathways (yellow bars). The number of differentially expressed genes in each pathway are indicated with significance.

Chapter IV – Disease Response of SnRK1 mutants

4.1 Introduction

Rice is consumed by more than three billion people every day throughout the world (Birla et al., 2017). One of the main yield limitations for rice is the presence of pathogens. Diseases can significantly affect rice crops, causing yield losses, low grain quality, and decreased farmer profitability. In addition, with the advancement of global warming, the increase of temperature can create conditions to favor the growth of pathogens and enhance plant diseases leading to the decrease of yield. Crop yield losses caused by diseases can be influenced by a several factors, including host resistance to the pathogen. The method that is most efficient and environment-friendly to control plant pathogens is to use resistant varieties (Chaloner et al., 2021).

Plants with R genes (Resistance genes) are resistant to particular diseases by identifying and reacting to molecules originating from pathogens known as effectors, through a process known as effector-triggered immunity (ETI). ETI is a quick and powerful immune response that activates a number of defense pathways, causing the creation of defense-related proteins and the triggering of cell death in order to limit the pathogen. R genes are very varied amongst plant species and can offer either general or targeted resistance against various disease types (Zaidi et al., 2018). The R genes play a major role in defensive pathways, including hormonal control, reactive oxygen species generation, secondary metabolite synthesis, and cell wall modification (Kumar et al., 2021). On the other hand, plants with S genes (Susceptibility genes) are more prone to being infected by particular diseases. Pathogen effectors may directly target S genes or may do so indirectly by interfering with host cellular functions. Through the detection of pathogen effectors by R genes, which results in the activation of ETI and the containment of the

pathogen, the plant's immune system is able to overcome the sensitivity imparted by S genes (Zaidi et al., 2018). Despite significant advancements in our understanding of plant-pathogen interactions, we still have a limited understanding of the molecular pathways that result in either resistance or susceptibility in crops against pathogens.

As mentioned previously, SnRK1 is a kinase that is essential for controlling plant's development, growth, and responses to stress. It has been confirmed to be involved in plant-pathogen interactions such as fungi, bacteria and viruses (Hulsman et al., 2016). In addition, SnRK1 can control the metabolic processes that produce defense-related substances including salicylic acid and jasmonate, which are necessary for inducing plant immune responses. As demonstrated previously, phytohormones like salicylic acid, jasmonic acid, and ethylene are important in mediating plant protection during a pathogen attack (Meng et al, 2019). SnRK1 was also recently found to regulate secondary metabolic processes, such as anthocyanin biosynthesis (Broucke et al., 2023). Moreover, SnRK1 can control plant metabolism at the same time to supply the resources and energy required for the plant to mount an immune response (Filipe et al., 2018; Hao et al., 2003; Hulsmans et al., 2016; Kim et al., 2015). As a result, to improve plant immunity to pathogens and to further our understanding of the molecular mechanisms underlying plant resistance, it is critical to understand SnRK1 signaling in plant-pathogen interactions.

There is currently no rice variety completely resistant to *Burkholderia glumae*, *Rhizoctonia solani*. *Magnaporthe oryzae* necessitates ongoing research to find new genes or quantitative trait loci (QTLs) that give broad spectrum resistance as well as to comprehend the underlying mechanisms (Kumar et al., 2021). In addition, little is known about the interaction between these pathogens and rice plants. Consequently, understanding the molecular basis of rice

sheath blight caused by *Rhizoctonia Solani*, bacterial panicle blight caused by *Burkholderia Glumae* and rice blast caused by *Magnaporthe Oryzae* resistance, is a crucial step in creating tolerant varieties and efficient disease control methods (Zhang et al., 2017). Building techniques for stress resistance breeding requires a clear understanding of the molecular mechanisms driving disease and stress responses in rice.

4.1.a. Bacterial panicle blight caused by Burkholderia glumae

Bacterial panicle blight of rice, which is caused by *Burkholderia glumae*, is a disease that is becoming a bigger issue for the world's rice production (Ham et al., 2011). This disease has been documented in over 18 countries distributed across Africa, Asia, Latin America, and North America and it can cause a decrease of up to 75% of crop yield (Fory et al., 2014; Francis et al., 2013). *Burkholderia glumae* is a seed-borne rice bacteria and its symptoms include sterility of panicles, discoloration of growing grains, grain rot and grain abortion (Gunasena et al., 2022; Ortega & Rojas, 2021). Bacterial panicle blight disease cycle is not fully understood. This condition occurs because, when the pathogen carrier seedlings survive the post-germination phase, the plant is largely asymptomatic, when the bacteria is kept as an endophyte, during its vegetative phase until grain production, at which point the disease symptoms reappear (Ham et al., 2011; Li et al., 2016; Ortega & Rojas, 2021). The disease cycle begins with primary infections caused by contaminated seed, soil, and irrigation water, where the bacteria penetrate through natural openings in the plant and through glume hairs (Li et al., 2016). The bacteria seem to persist on the leaves and sheath after seed germination and spread upward as the plant grows. If the bacterial population reaches a certain level and the environmental conditions are

right, they infect rice panicles during flowering. Secondary infections follow as a result of contact with infected panicles and rain splash (Nandakumar et al., 2009; Tsushima et al., 1996).

It is difficult to effectively control this bacterial disease. There are currently no scouting techniques to identify and forecast the onset of the disease. Therefore, the coordinated utilization of various management options is a key component of the effective and sustainable control of the Bacterial panicle blight disease (BPB). Plant quarantine is the first line of defense to keep the BPB pathogens out of a disease-free region, which is the most efficient method to prevent BPB of rice. Another efficient method of limiting this illness is the use of pathogen-free or certified seed. Farmers are advised not to utilize the seeds obtained from fields that were contaminated with BPB the year prior in order to minimize the spread of the disease. Furthermore, there are no cultural practices that could lessen the prevalence and severity of BPB in rice. The susceptibility of rice plants to the BPB disease seems to increase with high nitrogen fertility levels, hence it is possible to lessen the harm done by BPB by avoiding high nitrogen rates (Wamishe et al., 2014). Early planting or the adoption of early maturing rice cultivars to avoid the hottest portions of the growing season is another successful strategy to lessen the damage caused by the illness under the Southern US rice producing systems. The occurrence and severity of the disease can be decreased by avoiding high seeding rates (Zhou, X. G., 2019).

According to the Wamishe et al (2021), there are no approved chemical solutions for either seed treatment or spray application in the United States for bacterial panicle blight in rice. The effectiveness of tested seed treatments has varied or has significantly reduced seed germination. Even though some foliar antibiotic is efficient and available in other countries, the U.S. does not allow their usage due to environmental issues. Foliar treatments, such as copper-based fungicides, have not proven successful in the field. Scientists are still looking for methods of chemical control

for *Burkholderia glumae*. Oxolinic acid (5-ethyl-5,8-dihydro-8-oxo-[1,3]dioxolo[4,5-g]quinoline-7-carboxylic acid, Starner®), the first chemical to be reported to be particularly effective for controlling the BPB disease in rice, has been a significant BPB control strategy in Japan for more than 20 years (Hikichi et al., 1989). In Korea, the forecasting system BGRcast, which used temperature and humidity to estimate the possibility of a BPB outbreak, was used to plan applications of this antibiotic (Lee et al., 2015). However, populations of *B. glumae* that are resistant to oxolinic acid have been identified (Hikichi et al., 1998; Hikichi et al., 2001; Maeda et al., 2007; Maeda et al., 2004), which restricts the use of this antibiotic compounds for BPB management. Neither the USA nor many other nations have labeled oxolinic acid for use on rice.

Bacterial Panicle Blight is a serious disease that is made worse by a variety of infections as well as a lack of effective methods to control. The best alternative may be to growing disease-resistant varieties, however there are not any commercially available rice cultivars with enough BPB resistance at the moment (Mizobuchi et al., 2016; Pinson et al., 2010; Shahjahan et al., 2000) and they lack desired commercial traits (Sayler et al., 2006; Ham and Groth, 2011; Karki et al., 2012). Quantitative features are extremely reliant on environmental and experimental conditions, and efforts to include resistant qualities using traditional breeding techniques have been hampered by the significant heterogeneity in disease phenotyping, such as in BPB, among rice cultivars (Mizobuchi et al., 2016). Since no source of total resistance has yet been identified, more investigation is required to explore new sources of resistance (Zhou, X. G., 2019).

4.1.b. Sheath blight caused by Rhizoctonia solani

The soil-borne pathogen *Rhizoctonia solani* has a wide host range, such as soybeans, sorghum, corn, and sugarcane, and it causes several economically significant illnesses in a

variety of host species, including rice. It causes sheath blight in rice, one of the most significant and pervasive diseases in the world. In conditions that supports severe sheath blight, susceptible cultivars may experience up to 50% grain loss (Okubara et al., 2014). When vulnerable cultivars are grown under ideal circumstances, such as warm temperatures (28 to 32°C), high humidity (95% or above), and dense stands with a densely developed canopy, the infection spreads fast. Sclerotia begin to germinate, and the mycelia start to grow under these ideal conditions, which causes lesions and damage in sheaths and leaves. Additionally, *Rhizoctonia solani* causes post-emergence seedling damping off and root rot, which can cause poor stand establishment, low biomass, uneven plant height, and lower germination in rice plants (Ajayi-Oyetunde & Bradley, 2018).

The disease cycle starts with infected plant detritus, which has two major sources of inoculum: sclerotia and mycelia. Sclerotia, which falls on the soil during or after harvest, acts as structures for survival from one cropping season to the next. In rice growing farms, they can survive in the soil for two years, and they typically tend to accumulate in the field over time. Also, the water movement by rain and irrigation, and soil work help spread the pathogen in the field. The fungus starts infecting plants when sclerotium floats on the water surface and encounters the host, which the fungus is attracted to by chemicals released by the rice plant. The sclerotia or mycelia penetrates the host tissue using natural openings, by appressoria or by realizing enzymes which destroy the plant cell wall. Symptoms start to appear as the fungus enters and colonizes the plant tissue. As the fungi grows in the plant, it infects the higher leaf sheaths, leaf blades, and panicles (Kumar et al, 2009; Lee & Rush, 1983).

Because of the broad host range, extensive population diversity and molecular components of this pathogen, effective management needs an integrated disease control method.

Management methods to control seedling damping off and sheath blight caused by *Rhizoctonia solani* includes fungicides treatment of seeds, use of moderately resistant varieties, rotation to a non-host crop, and the use of certified seeds. Moreover, excessive seeding rates and excessive nitrogen fertilizer typically result in an increase in stand, excessive vegetative growth, and canopy density, which raises a damp microclimate that is conducive to the spread of diseases. In order to lessen the harm caused by sheath blight, avoiding high planting rates and the excessive application of fertilizers, particularly nitrogen, are important methods of control (Uppala & Zhou, 2018). In addition, there are currently no rice variety completely resistant to *Rhizoctonia solani* (Zhang et al., 2017).

Rhizoctonia solani morphology, host range, and aggressiveness exhibit an extensive diversity. Using hyphal interactions, this pathogen has been divided into 14 anastomosis groups (AGs). Intraspecific groups are identified within a single AG group using morphology, pathology, pectinase isoenzymes, and DNA sequencing (Hanson & Minier, 2015). For this study we focused on the AG 4 (Gaire et al., 2020) and AG 9 (Wamishe et al, 2019), which cause seedling diseases in rice plants.

4.1.c. Rice blast fungus caused by Magnaporthe oryzae

Rice blast is one of the most devastating diseases of rice plants that is caused by the fungus *Magnaporthe oryzae*. This pathogen is an airborne filamentous ascomycete fungus, and it is considered the most destructive fungal pathogen in the world, because it is distributed in 85 countries of different environmental conditions and its infection contributes to 10–30% of the annual loss in rice yield (Campos-Soriano et al, 2013; Dean et al, 2012; Ryan et al, 2016). All of

the rice-growing regions in the United States have recorded cases of rice blast disease, including the state of Arkansas (Wang, et al, 2017;Wamishe et al, 2021). Rice blast can affect plants in any stage of growth, and it infects a variety of tissues, including leaves, stems, nodes, and panicles, with the typical symptom of diamond shaped lesions and necrosis (Wilson & Talbot, 2009). The optimum conditions for *Magnaporthe oryzae* are rainfall that last 12 hours or more, high levels of nitrogen fertilizer in the soil and mild temperatures (24 degrees Celsius) (Liu et al, 2021).

The infection cycle of the rice blast fungus begins when a three-celled conidium lands on a rice leaf surface. When conidia placed on rice tissues germinates to create a germ tube and an appressorium, rice becomes infected. Since the appressorium is a melanized structure, an infection peg grows there and enters the tissue. Once inside the vulnerable tissues, the original infection hypha multiplies quickly and promotes the hyphal ramification (Meng et al., 2019; Tan et al., 2023; Wilson & Talbot, 2009). The disease can persist in the air all year, and the grasses, volunteer plants, infested waste, infested seed on the soil surface can be the overwintering sources of spores that compose the primary inoculum. Within a few days of infection, lesions start to form on the young seedlings. These secondary lesions release more spores, which easily spread by the wind to surrounding healthy leaf tissues. Throughout the growing season, secondary cycles can occur, potentially causing very high levels of disease in the crop (Li et al, 2019; Liu et al, 2021).

Rice blast can be a difficult disease to control because of the pathogen genetic variability for virulence and its spread through the air. A thorough set of recommendations using various management techniques leads to the effective management of rice blast. Methods of control include the use of forecast models to determine whether using fungicides under the

circumstances would be harmful or cost-effective, using clean fungicide treated seeds, avoiding high rates of nitrogen fertilizer, using resistant cultivars mainly on fields with a history of blast fungus and periodically scouting fields to identify symptoms (Liu et al, 2021; Wamishe et al., 2014). Studies suggest that one of the best approaches to control rice blast is through the use of resistant varieties. Studies found more than 100 blast R genes in the rice genome, of which 35 have been cloned (Wang et al., 2017), some of which are associated with hormone pathways (Meng et al., 2019). However, resistant cultivars can be more expensive, these cultivars have lower yield potential compared with the susceptible ones and the resistance can be overcome by the pathogen within 2-3 years of growing the cultivar in the field (Meng et al., 2019; Nalley et al., 2016; Wilson & Talbot, 2009).

This study has the objective of evaluating the disease response in *snrk1αa+b* and *snrk1αc* mutants along with the WT by using the pathogens: *Burkholderia glumae*, *Magnaporthe oryzae* and *Rhizoctonia Solani*.

4.2. Materials and Methods

4.2.a. Bacterial panicle blight caused by Burkholderia glumae

Bacteria strain:

The bacteria strain used was UAPB 13. *Burkholderia glumae* strain UAPB13 is a virulent strain that has been used in earlier investigations and it was first isolated from rice (*Oryza sativa*) variety Wells in Arkansas County in 2014 (Gil et al., 2022). Bacterial strains were preserved in 30% sterile glycerol at -80 ˚C freezer in long-term storage. The *B. glumae* strain was grown in King's B (KB) media and incubated at 28 °C for 48 hours. Single colonies were transferred to 15

ml tubes with 3 ml of broth and incubate for 16-18 hours at 30 °C in the shaker. The bacterial suspension was centrifuged at 6,000 rpm for 10 minutes using Eppendorf Centrifuge 5417R (Eppendorf North America Inc.), the supernatant was discarded, and the bacterial pellet was washed two times using distilled water in the centrifuge as described above. The bacterial solution was diluted in dilution factor of 10. The optical density at 600nm (OD600) was measured using Synergy HT microplate reader (BioTek) and adjusted to an OD600= 1.0(1 x 108 CFU/ml) for spray inoculation. After that, this solution was put in a sprayer container, and it was sprayed 1 ml of the solution per panicle per plant. After spraying, the plants were covered and tied with an autoclave bag. After inoculation, the panicles were harvested to do the bacterial growth curve. Each panicle weight was recorded, cut into small pieces and grinded using the machine 1600 MiniG (SPEX sample Prep). It was put 500 µl of solution of each panicle of each genotype on 2 ml Eppendorf tubes. After that, each tube (repetition representing one panicle) was diluted 8 times. 10 µl of each dilution was added to King's B (KB) media. The plates were incubated in incubator at 28 ˚C for 48 hours counted the number of bacterial colonies using a microscope.

Plant inoculation:

The seeds of the WT and mutant lines were sterilized with 70% ethanol and 30% bleach and were grown on ½ Murashige and Skoog media (pH: 5.7) and 2g/L of phytagel in Petriplates. Seven days later, at V1-V2 stage, the seedlings were transferred to the greenhouse in pots filled with a mixture of sphagnum peat moss and perlite (9:1). The plants were grown in randomized block design in the greenhouse. Plants were fertilized with iron chelate and Osmocote fertilizer (15N-9P-12K) and insecticide (abamectin) when it was necessary. On R4-R5 stage, when one or

more florets on the main stem panicle has reached anthesis, the rice plants were ready to be inoculated with the bacteria.

The first experiment was done inoculating *snrk1αc* mutant 6-23 along with the WT cv. Kitaake and it was evaluated the bacterial growth 0, 3 and 5 days post inoculation (DPI). In the second experiment, the *snrk1αc* mutant 10-1 was inoculated with *B. glumae* along with the WT and the bacterial growth was measured 0 and 6 DPI. In the last experiment, it was used the *snrk1αc* mutant 6-23 and 10-1, the *snrk1αa+b* double mutants 1-1 and 2-4 along with the WT and the bacterial growth was measured 0 and 6 dpi Since the bacterial growth curve is a demanding protocol, on the last experiment we divided it into 2 parts: the first inoculation was done on the WT along with *snrk1αa+b* mutant 2-4 on October 4 of 2022 and the second part was inoculated the *snrk1αc* mutant 6-23 and 10-1 along with the *snrk1αa+b* mutant 1-1 on October 7. In all experiments, it was inoculated with bacteria a total of 4 panicles per genotype per dpi. The control (mock) was first done using only distilled water and it was used only one panicle.

Statistical analysis:

Differences in number of bacteria colonies per genotype was determined by Tukey–Kramer test (HSD) using JMP Statistical Discovery 17 from SAS (Version 13.2.1) software. Analyses were performed at P=0.05 level.

4.2.b. Sheath blight caused by Rhizoctonia solani

It was done a total of 2 experiments, in which one was used 5 genotypes: WT Kitaake, *snrk1αc* mutant 6-23 and 10-1, the *snrk1αa+b* double-homozygous mutants 1-1 and 2-4. The pathogens used in this test were *Rhizoctonia solani* (AG 1-IA) AG4 and AG9. The AG4 strain

was isolated from soybeans and the AG9 strain was isolated from rice in the state of Arkansas previously.

Inoculum preparation

For the inoculum preparation, in a 500 mL Erlenmeyer flask, 100 grams of prosso millet were soaked overnight in 100 mL of deionized water. The millet was autoclaved for 40 minutes at 121°C and 15 psi. The millet was autoclaved one more the following day under the identical circumstances after cooling down. The strains were cultivated on solid PDA. The bags containing the infected millet were periodically shaken. A gram of fully colonized millet was plated onto solid PDA, and the plates were incubated at room temperature for 5-7 days to check for contamination. The inoculum was kept in sterile plastic bags and kept in the refrigerator.

Plant inoculation:

Once the inoculum was prepared, the experiment was installed using sixteen-ounce (16 oz) foam cups with four draining holes in diameter were employed. Equal parts of Promix MP (Pro-mix, Quakertown, PA) and sterile vermiculite were combined. One hundred grams g of the soil media and the inoculum were mixed and used to fill the perforated foam. For the first experiment, it was used 1 tablespoon, or 6 grams of inoculum of AG 4 and AG 9. However, AG4 was highly aggressive in the genotypes, so for the second experiment it was used two volumes of AG 4 (1/2 tablespoon or 4.5 grams and 1 teaspoon or 1.5 grams) was used to determine the best one for future experiment. In the second experiment it was kept the same volume for AG 9. After mixing the soil and vermiculite with the inoculum and pouring it on the cups, it was used 5 cups per treatment per genotype and planted 5 seeds per cup for the control and AG 9 treatment and it was used 3 cups per treatment and planted 5 seeds per cup for the AG 4 ½ tbps and 1 tsp

treatment. It was also used 2 types of control: soil + vermiculite and soil + vermiculite with sterilized millet in case millet affects plant germination and growth. Plant emergence was recorded at 14 days pos inoculation and plants were harvested 5 weeks after inoculation. The plants were grown in the greenhouse in the same way as mentioned in the previous pathogens. During harvest, the number of plants per cup was recorded. The roots were washed, and it was measured plant fresh biomass and roots fresh biomass using a scale in grams.

Statistical analysis:

Statistical differences between genotypes and treatments were determined by Tukey–Kramer test (HSD) using JMP Statistical Discovery 17 from SAS (Version 13.2.1) software. Analyses were performed at P=0.05 level.

4.2.c. Rice blast fungus caused by Magnaporthe oryzae

The seeds were sterilized, and the plants were grown in the greenhouse in the same way as mentioned in the panicle blight disease test. The disease test was done on 3-4 weeks old plants. It was done a total of 4 experiments, in which one was used 6 genotypes: WT YT16, WT Kitaake, *snrk1αc* mutant 6-23 and 10-1, the *snrk1αa+b* double-homozygous mutants 1-1 and 2-4 and 6 replicates (leaves) per genotype. The pathogen used in this test was *Magnaporthe oryzae* strain Guy11.

Inoculum preparation:

First, the *M. oryzae* strain Guy 11 was grown in complete media agar plate for 10-14 days to allow sufficient sporulation. Once the fungi sporulated, 2 ml of 0.02% gelatin were pipetted onto the plate and a spatula was used to scrape the spores into the solution. The spores were

filtered using 1 layer of miracloth and collected in 1.5 ml Eppendorf tubes. The tubes were centrifuged at 5000xg centrifuge for 5 minutes. The supernatant was removed, and the spores were re-suspended in 1 ml gelatin solution. The spores were diluted and counted using a hemocytometer. The spore's solution was diluted for a final concentration of 1×10^5 per ml.

Plant inoculation:

Once the spore's solution was prepared, the youngest, fully expanded leaves of the plants were cut and placed on plates with 0.8% water agar media, allowing for better positioning of the leaf for pipetting. Once the leaves were placed on the plates, it was pipetted 5 drops of 20ul of spore/gelatin solution on each leaf. 5 days after inoculation, the leaves were scanned using a computer scanner and the area of each lesion of the leaf was calculated using auto threshold MaxEntropy of the ImageJ program.

Statistical analysis:

Differences in lesion areas per genotype was determined by Tukey–Kramer test (HSD) using JMP Statistical Discovery 17 from SAS (Version 13.2.1) software. Analyses were performed at P=0.05 level.

4.3 Results

4.3.a. Bacterial panicle blight caused by Burkholderia glumae

In the first experiment, bacterial growth on 0, 3 and 5 days post inoculation (DPI) of the panicles of *snrk1αc* mutant 6-23 line and the WT were evaluated. The results show that on 0 DPI, both of the genotypes have statistically similar numbers of bacteria (Figure 4.1a). However,

in 3DPI and 5DPI 6-23 line showed statistically reduced growth of *B. glumae* when compared to the WT. Corroborating with this, the WT panicles have more discoloration symptoms than the *snrk1αc* mutant in 5DPI (Figure 4.1b). Additionally, WT showed increased growth of *B. glumae* from 0DPI to 3DPI and both of the genotypes had reduced growth from 3DPI to 5DPI, but the 6-23 line showed a bigger decrease of growth from 3DPI to 5DPI.

In the next experiment, bacterial growth on 0 and 6 days post inoculation of panicles of *snrk1αc* mutant 10-1 line and the WT were evaluated. The results show that on 0 DPI, WT has statistically higher number of bacteria than 10-1 (Figure 4.2a). Both genotypes had decreased *B. glumae* growth from 0DPI to 6DPI, and the bacterial growth in WT is statistically similar with 10-1. In Figure 4.2b, we can see that both of the genotypes have similar discoloration symptoms.

In the third experiment, bacterial growth on 0 and 6 DPI was evaluated in the panicles of *snrk1αc* mutant 6-23 and10-1 line, the *snrk1αa+b* double mutants 1-1 and 2-4 and the WT (Figure 4.3). The first inoculation was done on the WT along with line 2-4 followed by inoculation of 6-23, 10-1 and 1-1 lines. The mock (control where no *B. glumae* was applied) showed no symptoms in the panicles (Figure 4.4). Bacterial growth assay on 0 DPI did not produce reliable data. The bacterial growth curve of 0DPI showed inconsistent growth in the genotypes, where only some panicles showed bacterial growth, and in the 6-23 line no bacteria was found. Therefore, we did not add 0 DPI to our statistical analysis. In the first inoculation on WT and 2-4 line on 6DPI, the WT and 2-4 line had statistically similar bacterial growth; however, 2-4 showed slightly reduced value (Figure 4.3). In the second inoculation (6-23, 10-1 and 1-1) on 6DPI, the *snrk1αa+b* mutant 1-1 and *snrk1αc* mutant 10-1 showed statistically higher bacterial growth, where 6-23 line had the lower values (Figure 4.3) and less symptoms (Figure 4.5). The bacterial growth curve on the 6–23 line was done twice to make sure the

measurements were more reliable. Figure 4.6 shows that the 6-23 had reduced bacterial growth compared to other mutants in the first and second trial, which is similar with the trend we observed in the first experiment (Figure 4.1).

4.3.b. Sheath blight caused by Rhizoctonia solani

In the first experiment, emergence rate after 14 days of sowing was evaluated in *snrk1αa+b* mutants 1-1 and 2-4, *snrk1αc* mutants 6-23 and 10-1, and the WT in the millet control (Figure 4.7a) or in presence of *Rhizoctonia solani* AG 9 (Figure 4.7b) or *R. solani* AG 4 (Figure 4.7c). The WT had the highest emergence rate in the control (millet) (Figure 4.7a). Treatment with *R. solani* AG 9 and AG 4 decreased the emergence in all genotypes, with the lowest emergence observed with *R. solani* AG 4. However, no statistical difference in the emergence was observed among genotypes in any of the treatments. A big variation in emergence can be observed in the genotypes in the presence of AG 9 and AG 4, with 0% germination in *snrk1αc* mutant 10-1 in the presence of *R. solani* AG 4 (Figure 4.7c). Figure 4.8 shows plant emergence and percentage decrease of emergence in the mutants and in the WT in *R. solani* AG 9 and *R. solani* AG 4 compared with millet (control). In all the genotypes *R. solani* AG 9 and AG 4 decreased emergence compared with the control (millet), and *R. solani* AG 4 caused the biggest decrease in emergence in all genotypes. The severe decrease in emergence was in 1-1 (74%) and 10-1 (100%) as compared to millet. On the other hand, *R. solani* AG 9 caused only a 24% decrease in emergence in 10-1 with a higher decrease in emergence in WT (52%).

After the experiment was harvested, the average plant and root weight in millet, *R. solani* AG 9 and *R. solani* AG 4 were measured in the mutants and the WT. In millet, WT had the highest average plant weight compared with the *snrk1* mutants; however, it was only 10-1 line statistically different from WT (Figure 4.9a). Similarly, the WT had the highest average root weight compared with other genotypes. However, no statistical difference was observed among the genotypes in the average plant and root weight in *R. solani* AG 9 and *R. solani* AG 4 treatment. Similarly with the emergence, a big variation was found in plant and root weight in the genotypes when inoculated with *R. solani* AG 9 (Figure 4.9b) and AG 4 (Figure 4.9c), mainly on 2-4 line. Figure 4.7a shows the average plant weight and the percentage decrease of plant weight in the mutants and in the WT in *R. solani* AG 9 and *R. solani* AG 4 treatments compared with millet (control). In all the genotypes, *R. solani* AG 9 and AG 4 decreased the plant weight compared with millet. The decrease of plant weight ranged from 5.5 to 56% in *R. solani* AG 9 treatment, with 10-1 showing the lowest percentage decrease. However, in *R. solani* AG 4, 10-1 had 96% decrease in plant biomass compared with the control. Figure 4.10b shows the average root weight and percentage decrease of root weight in the mutants and in the WT in *R. solani* AG 9 and *R. solani* AG 4 compared with millet (control). Unexpectedly, in the 2-4 line, the average root weight increased in *R. solani* AG 9 and AG 4 treatments by 20 and 24% respectively, and in 10-1 line, root biomass increased by 15% in *R. solani* AG 9 treatment when compared to millet. In addition, in WT and 6-23, *R. solani* AG 9 had a higher decrease of root weight than *R. solani* AG 4. In the WT inoculated with *R. solani* AG 4, root weight decreased by 8.3%, while 38% decrease in root weight occurred with the *R. solani* AG 9 treatment. In 1-1, *R. solani* AG 4 treatment decreased 75% of root weight, while *R. solani* AG 9 treatment caused 26% decrease.

In the second experiment, the emergence rate was evaluated in *snrk1αa+b* mutants 1-1 and 2-4, *snrk1αc* mutants 6-23 and 10-1 along with the WT in millet (control) (Figure 4.11a), *R. solani* AG 9 (Figure 4.11b), and *R. solani* AG 4 (Figure 4.11cd). Because *R. solani* AG 4 showed to be highly virulent, inoculum rate in the second experiment was reduced to ½ tbsp and 1 tsp. Again, millet (control) had the highest emergence among the genotypes (Figure 4.11a). Line 1-1 showed high variation in emergence in all treatments, and it had statistically lower emergence in millet compared with the other genotypes. *R. solani* AG 9 and AG 4 decreased the emergence in all genotypes, with the lowest emergence observed in *R. solani* AG 4 ½ tbsp (Figure 4.11c). However, no statistical difference in emergence was observed among genotypes in any of the treatments: *R. solani* AG 4 ½ tbsp, 1 tsp, and AG 9. As observed in Experiment 1, 10-1 showed no emergence in *R. solani* AG 4 ½ tbsp and showed 33% emergence in *R. solani* AG 4 1 tsp. Figure 4.12 shows plant emergence and percentage decrease of emergence in the mutants and in the WT in *R. solani* AG 9 and *R. solani* AG 4 ½ tbsp and AG 4 1 tsp compared with millet (control). With the exception of 1-1 line, all the genotypes decreased emergence on *R. solani* AG 9 and AG 4 as compared to the millet treatment, with *R. solani* AG 4 causing the biggest decrease in emergence among all genotypes, mainly with ½ tbsp treatment. In 1-1 line, AG 9 treatment increased the emergence by 11%. Except for 1-1, the decrease of emergence caused by *R. solani* AG 9 ranged from 7.4 to 40% between the genotypes, where the lowest percentage decrease was found in 10-1 (7.4%), which is similar with the first experiment. The decrease of emergence caused by *R. solani* AG 4 ½ tbps and AG 4 1 tsp ranged from 78 to 100% and 77 to 92%, respectively. Therefore, for future experiments we might need to decrease the *R. solani* AG 4 concentration even further.

After the experiment was harvested, the average plant and root weight were measured (Figure 4.13). In millet, 1-1 had statistically lower plant and root weight, while no differences were observed between the rest of the *snrk1* mutants and the WT (Figure 4.13a). In the *R. solani* AG 9 (Figure 4.13b) and *R. solani* AG 4 ½ tbsp (Figure 4.13c) treatments, no statistical difference was observed among the genotypes in the plant and root weight, which is similar to the first experiment. In *R. solani* AG 9 treatment, line 6-23 showed a big variation in plant and root weight, and 1-1 having lower plant and root biomass. Figure 4.14a shows the average plant weight and the percentage decrease of plant weight in the mutants and in the WT. As expected, in all the genotypes *R. solani* AG 9 and AG 4 treatments (½ tbsp and 1 tsp) decreased the plant weight compared with the millet. The 1-1 line had the lowest plant weight in millet and *R. solani* AG 9 treatment which can explain the lowest percentage decrease of plant biomass compared with the other genotypes. The decrease of plant weight ranged from 9.7 to 52% in *R. solani* AG 9 treatment with 2-4 having the lowest percentage decrease. Both *R. solani* AG 4 concentrations (½ tbsp and 1 tsp) showed high and similar decrease values in plant weight, which ranged from 60 to 100% in ½ tbsp and 64% to 87% in 1 tsp. Figure 4.14b shows the average root weight and percentage decrease of root weight in the genotypes with *R. solani* AG 9 and *R. solani* AG 4 ½ tbsp or 1 tsp treatments. Similarly to the trend in plant weight, all the genotypes decreased the root weight with *R. solani* AG 9 and AG 4, where *R. solani* AG 4 causing greatest decrease. The 1-1 line had the lowest root weight in millet and in *R. solani* AG 9 treatment. The decrease of root weight ranged from 6 to 53% in *R. solani* AG 9 treatment with 2-4 having the lowest percentage decrease. Both of *R. solani* AG 4 concentrations (½ tbsp and 1 tsp) showed high decrease in root weight, which ranged from 63 to 100% in AG 4 ½ tbsp and 67% to 90% in AG 4 1 tsp.

4.3.c. Rice blast fungus caused by Magnaporthe oryzae

The statistical analysis of four independent experiments was performed that showed statistical differences in the infection severity of *Magnaporthe oryzae* between WT Kitaake and *snrk1* mutants (Figure 4.15). As expected, the negative control (inoculating leaves only with gelatin) did not cause any infection (Figure 4.15a). Figure 4.15b shows disease symptoms in representative leaves inoculated with *Magnaporthe oryzae* strain Guy11 of the third experiment. As shown in Figure 4.15b, the positive control, YT16, developed a larger lesion area at the inoculated sites. Additionally, yellowing started around the YT16 lesions, indicating high susceptibility. The *snrk1αa+b* mutant 1-1 and 2-4 and *snrk1αc* mutant 10-1 and 6-23, although more tolerant as compared to YT16, they were statistically more susceptible to the infection compared to the WT Kitaake (Figure 4.15). In the representative leaf images (Figure 4.15b), the *snrk1* mutants show visually bigger leaf lesions. In other words, WT Kitaake was more resistant to *Magnaporthe* oryzae Guy11 as it showed statistically smallest lesion area (Figure 4.15), which is in accordance with its lesion images in Figure 4.13b, where WT Kitaake shows weaker and smaller lesions compared to the other genotypes.

4.4 Discussion

4.4.a. Bacterial panicle blight caused by Burkholderia glumae

Many studies have shown that mutation in *SnRK1* gene causes an increase in the susceptibility to pathogens, while overexpression of *SnRK1* enhances the resistance against pathogens (Filipe et al., 2018; Hao et al., 2003; Kim et al., 2015; Perochon et al., 2019). This is primarily attributed to SnRK1 signaling leading to the activation of plant defense and immune response (Baena-Gonzalez et al., 2007; Baena-Gonzalez & Sheen, 2008). However, in our

research, no increase in the susceptibility was observed in *snrk1* mutants when compared to WT Kitaake. In the first experiment, 5 days post inoculation (DPI), the panicles of *snrk1αc* mutant 6-23 showed statistically reduced growth of *B. glumae* when compared to the WT (Figure 4.1a). Accordingly, less discoloration was observed in 6-23 panicles (Figure 4.1b), which is a typical symptom of infections caused by *B. glumae* (Gunasena et al., 2022; Ortega & Rojas, 2021). *B. glumae* prevents fertilization and grain filling causing the grain to abort and the panicles to fail to fill (Nandakumar et al., 2009), and it is well-known that *B. glumae* survive mainly on the seeds (Ortega & Rojas, 2021). Therefore, a possible explanation for 6-23 to be less susceptible is that *snrk1αc* mutants have lower number of seeds per panicle and lower weight of seeds per plant when compared with the WT (Figure 2.3c and Figure 2.5c). With low seed filling rate, the bacteria would be less aggressive and less likely to cause symptoms in *snrk1αc* mutants.

Similarly in experiment 3, the 6-23 line had lower bacterial growth compared to the other genotypes (Figure 4.3). This can also be observed in Figure 4.6, where 6-23 line had lower *Burkholderia glumae* growth in media compared to the other genotypes. However, at 6 DPI, *snrk1αc* mutant 10-1 had statistically similar *B. glumae* growth compared to the WT in the second experiment (Figure 4.2a) and statistically similar bacterial growth compared to the 1-1 line in the third experiment (Figure 4.3). In experiment number 3, 2-4 had statistically similar bacterial growth and the disease symptoms as the WT (Figure 4.3, 4.5). We could not compare *snrk1αa+b* mutant 1-1 and WT, because the inoculation in these genotypes was done on different days. However, 1-1 had numerically lower growth of *B. glumae* when compared with the WT (Figure 4.3), which is reflected in reduced symptoms in 1-1 panicles compared with the WT (Figure 4.5). Again, this was not expected since previous literature had shown that mutation in *SnRK1* causes more susceptibility to pathogens.

More experiments are needed to explain the disease response of *snrk1* mutants to *B. glumae.* In addition, the fact that there is currently no complete rice resistant variety to *Burkholderia glumae* and little is known about its molecular mechanisms of infection in rice, comprehending the role of SnRK1 in this particular disease is challenging.

4.4.b. Sheath blight caused by Rhizoctonia solani

In this study, we evaluated the disease response of *snrk1αa+b* and *snrk1αc* mutants against *Rhizoctonia solani* that causes sheath blight disease in rice. Plant emergence, plant biomass and root weight were evaluated in the *snrk1* mutants and WT against *R. solani* AG 4 and AG 9 using the seedlings in the greenhouse. Plant emergence data was collected 2 weeks after inoculation and plants were harvested 5 weeks later to measure total plant weight, and the root weight. No statistical differences were observed regarding plant emergence in the first experiment in millet treatment (Figure 4.7a). In addition, in the first experiment, WT showed higher plant weight compared to *snrk1* mutants in millet treatment (Figure 4.8a), which corroborates with our phenotypic assessment that showed *snrk1* mutants had lower shoot biomass compared to the WT (Figure 2.7a). However, unexpectedly, in the second experiment, the 6-23 line had higher emergence rate (Figure 4.11a) and higher plant weight (Figure 4.13a) compared to the millet treatment.

No statistical difference was observed between *snrk1αa+b* mutants, *snrk1αc* mutants, and the WT for AG 9 and AG 4 for plant emergence (Figure 4.7bc and Figure 4.11bcd), and plant and root weight (Figure 4.9bc and Figure 4.13bcd) in both experiments. This is not consistent with previous studies, which demonstrated that mutation in *SnRK1* gene causes an increase in susceptibility to pathogens including *R. solani* (Filipe et al., 2018; Hao et al., 2003; Kim et al.,

2015; Perochon et al., 2019). Filipe et al (2018) did overexpression and silencing of *SnRK1αc* (LOC_Os05g45420) in rice cultivar Kitaake and observed enhanced resistance in the *SnRK1* overexpression line, and increased susceptibility to *R. solani* in snrk1αc silenced line. However, they used *R. solani* AG-1 IA, which is a different anastomosis group from AG4 and AG9, used in our experiments, and they performed detached leave assay in six-week-old plants, while we did *in planta* inoculations. *R. solani* has an extensive population diversity, and AG-1 IA has different morphology and aggressiveness compared to AG 9 and AG 4, which could explain the differences between our results and the ones of Filipe et al (2018). In addition, Filipe et al (2018) performed a detached leaf assay, while we inoculated the fungi in the soil and sowed seeds in it. In addition, *R. solani* AG-1 IA has not been reported as a seed or seedling pathogen in rice (Yang and Li, 2012), while AG4 and AG9 are the rice pathogens.

Figure 4.8 and Figure 4.9 show plant emergence and percentage decrease of emergence, and Figure 4.10 and Figure 4.14 show plant and root weight in the mutants and in the WT in *R. solani* AG 9 and *R. solani* AG 4 treatments compared with millet (control). As expected, in most of the genotypes, the *R. solani* AG 9 and AG 4 treatments decreased emergence and plant and root weight compared to millet treatment. Similar result was reported by previous studies which showed that *R. solani* causes root damage and lower biomass in crops (Gaire 2021; Lamichhane et al. 2017). In addition, *R. solani* AG 4 caused a bigger decrease in emergence than AG 9, which AG 4 is a very aggressive strain of *R. solani* (Gaire et al., 2020). Unexpectedly, the 2-4 line had an increase of root weight in AG 9 and AG 4 treatments when compared to the control in the first experiment (Figure 4.10). In the second experiment, we used 2 concentrations of AG 4 to determine the best concentration for the Kitaake cultivar. However, even the lowest

concentration (1 tsp) showed high virulence as indicated by 84% decrease in the emergence of WT (Figure 4.9).

In the second experiment, the 1-1 line, on AG 9 treatment, increased the emergence by 11%, which could be explained as an artifact due to the low emergence (60%) of 1-1 line in millet (Figure 4.9). The *snrk1αa+b* mutants show low germination in normal conditions when compared to the WT (data not shown). In order to determine whether the reduced germination is caused by the *snrk1* mutation or by the pathogenicity of *R. solani*, future experiments might use germinated seeds from ½ MS media and inoculation of germinated seedlings with the pathogen. In addition, no big difference between the decrease of emergence in WT and the mutants was observed in AG 9 and AG 4 treatments (Figure 4.8 and Figure 4.9). The *snrk1αc* mutant 10-1 line had no emergence in AG 4 treatment in experiment 1 (Figure 4.8) and in AG 4 (1/2 tbsp) in experiment 2 (Figure 4.9), which shows that this line is very susceptible to *R. solani* AG 4. In addition, our data shows a big variation in the emergence and the plant and root weights between the experiments for both *R. solani* AG 9 and AG 4 treatments. Therefore, more experiments are needed as well as make trails to see the ideal quantity of pathogen's inoculum for the Kitaake cultivar.

4.4.c. Rice blast fungus caused by Magnaporthe oryzae

In this study, we performed disease tests and evaluated disease response in *snrk1αa+b* and *snrk1αc* mutants along with the WT against rice blast fungus. As compared to YT16 cultivar, the leaf lesions in in Kitaake cultivar were smaller a.nd with less yellow region surrounding the lesion (Figure 4.16). This indicates that Kitaake is more resistant to rice blast fungus than the YT16. Previous studies showed that Kitaake has moderate resistance to *M. oryzae*, because it

contains rice blast resistance genes called Pi genes (Yang et al., 2021). Additionally, MAX effectors – effectors that determines virulence in the rice blast disease – have weak levels of expression in cultivar Kitaake (Vernet et al., 2023).

Combining the data of four independent experiments, we found that all *snrk1* mutants were more susceptible to *M. oryzae* Guy11 as compared with the WT Kitaake (Figure 4.15). As shown in Figure 4.16, the leaf lesions on WT Kitaake were smaller than the lesions of *snrk1* mutants. This finding is consistent with previous studies, where mutation in *SnRK1* genes was found to cause an increase in the susceptibility to pathogens (Filipe et al., 2018; Hao et al., 2003; Kim et al., 2015; Perochon et al., 2019). Filipe et al (2018) did overexpression and silencing of *SnRK1αc* (LOC_Os05g45420) in rice cultivar Kitaake and observed nonsporulating necrotic spots, a characteristic resistance phenotype, on the *snrk1* overexpression line, while while round necrotic and yellow lesions appeared on the *snrk1* silenced line, indicating increased susceptibility to rice blast fungus. This finding was also reported by Kim et al. (2015), who noted that *SnRK1αa* (LOC_Os03g17980) activation line had increased resistance against *M. oryzae*, while the *snrk1αa* knockout line showed increased susceptibility to the rice blast. Similarly, other studies demonstrated that SnRK1 is associated with plant defense response against fungal pathogens (Hulsmans et al., 2016; Perochon et al., 2019; Yuan et al., 2008). In accordance with these previous studies, our study also showed more susceptibility to rice blast fungus in the *snrk1* mutants than the WT.

An explanation for these results is that SnRK1 activates genes and processes related to plant immune response under stress conditions, such as hormone signaling pathways and defense genes. Our transcriptomics data showed downregulation of defense to other organisms and jasmonic acid metabolic process in *snrk1αa+b* mutant in dark conditions mimicking stress

(Figure 3.2). On the other hand, in dark condition, WT showed upregulation of jasmonic acid signaling and defense response to other organisms (Figure 3.1), which suggests that SnRK1 orchestrates defense genes and hormone signaling under stress conditions. Correspondingly, Filipe et al (2018) noted that during *M. oryzae* infection, *SnRK1αc* positively affects salicylic acid and jasmonic acid hormone signaling and upregulates defense genes such as pathogenesis-related genes.

In conclusion, we performed disease tests and evaluated disease response in *snrk1αa+b* and *snrk1αc* mutants along with the WT against three different pathogens. The diseases investigated were bacterial panicle blight caused by *Burkholderia glumae*, sheath blight caused by *Rhizoctonia solani*, and rice blast fungus caused by *Magnaporthe oryzae* with the goal to evaluate the susceptibility or resistance of the *snrk1* mutants compared to the WT. Previous studies have shown that mutation in the *SnRK1* genes increases susceptibility to pathogens, while overexpression of *SnRK1* enhances resistance. However, in our experiments we did not observe an increase in susceptibility in the *snrk1* mutants for the bacterial panicle blight and sheath blight diseases. Therefore, further experiments are essential to understand the role of *SnRK1* in bacterial panicle blight and sheath blight diseases. Regarding blast fungus caused by *M. oryzae*, we noted that *snrk1* mutants were more susceptible than the WT, which is in accordance with the literature and correlates with the transcriptomic data that showed that suppression of disease response and hormone signaling pathways in *snrk1* mutants.

References

Adamu, A., Ahmad, K., Siddiqui, Y., Ismail, I. S., Asib, N., Bashir Kutawa, A., Adzmi, F., Ismail, M. R., & Berahim, Z. (2021). Ginger Essential Oils-Loaded Nanoemulsions: Potential Strategy to Manage Bacterial Leaf Blight Disease and Enhanced Rice Yield. Molecules (Basel, Switzerland), 26(13), 3902–. https://doi.org/10.3390/molecules26133902

Adriana Pedraza, L., Bautista, J., & Uribe-Velez, D. (2018). Seed-born Burkholderia glumae Infects Rice Seedling and Maintains Bacterial Population during Vegetative and Reproductive Growth Stage. The Plant Pathology Journal, 34(5), 393–402. https://doi.org/10.5423/PPJ.OA.02.2018.0030

Birla, D. S., Malik, K., Sainger, M., Chaudhary, D., Jaiwal, R., and Jaiwal, P. K. (2017). Progress and challenges in improving the nutritional quality of rice (Oryza sativaL.).Crit. Rev. Food Sci. Nutr.57, 2455–2481. doi: 10.1080/10408398.2015.1084992

Bomford, M. . (2009). Integrated pest management: v.1: Innovation-development process [Review of Integrated pest management: v.1: Innovation-development process]. CHOICE: Current Reviews for Academic Libraries, 47(3), 525–. American Library Association CHOICE.

Broucke, E., Dang, T. T. V., Li, Y., Hulsmans, S., Van Leene, J., De Jaeger, G., Hwang, I., Van den Ende, W., & Rolland, F. (2023). SnRK1 inhibits anthocyanin biosynthesis through both transcriptional regulation and direct phosphorylation and dissociation of the MYB/bHLH/TTG1 MBW complex. The Plant Journal : for Cell and Molecular Biology. https://doi.org/10.1111/tpj.16312

Campos-Soriano, L.; Valè, G.; Lupotto, E.; Segundo, B.S. Investigation of rice blast development in susceptible and resistant ricecultivars using a gfp-expressingMagnaporthe oryzaeisolate.Plant Pathol.2013,62, 1030–1037.

Chaloner, T. M., Gurr, S. J., & Bebber, D. P. (2021). Plant pathogen infection risk tracks global crop yields under climate change. Nature Climate Change, 11(8), 710–715. https://doi.org/10.1038/s41558-021-01104-8

Dean, R.; Van Kan, J.A.; Pretorius, Z.A.; Hammond-Kosack, K.E.; Di Pietro, A.; Spanu, P.D.; Rudd, J.J.; Dickman, M.; Kahmann,R.; Ellis, J.; et al. The Top 10 fungal pathogens in molecular plant pathology.Mol. Plant Pathol.2012,13, 414–430.

Filipe, O., De Vleesschauwer, D., Haeck, A., Demeestere, K., & Höfte, M. (2018). The energy sensor OsSnRK1αa confers broad-spectrum disease resistance in rice. Scientific Reports, 8(1). https://doi.org/10.1038/s41598-018-22101-6

Fory, P. A., Triplett, L., Ballen, C., Abello, J. F., Duitama, J., Aricapa, M. G., Prado, G. A., Correa, F., Hamilton, J., Leach, J. E., Tohme, J., & Mosquera, G. M. (2014). Comparative Analysis of Two Emerging Rice Seed Bacterial Pathogens. Phytopathology, 104(5), 436–444. https://doi.org/10.1094/PHYTO-07-13-0186-R

Francis, F., Kim, J., Ramaraj, T., Farmer, A., Rush, M. C., & Ham, J. H. (2013). Comparative genomic analysis of two Burkholderia glumae strains from different geographic origins reveals a high degree of plasticity in genome structure associated with genomic islands. Molecular Genetics and Genomics : MGG, 288(3-4), 195–203. https://doi.org/10.1007/s00438-013-0744-x

Gaire, S. P. 2021. Seedling Blight of Rice in the Southern United States and Its Management. Available at: https://oaktrust.library.tamu.edu/handle/1969.1/193167

Gaire, S. P., Zhou, X. G., Jo, Y. K., & Shi, J. (2020). First report of rhizoctonia solani ag-4 causing seedling disease in Rice. In Plant Disease (Vol. 104, Issue 5). American Phytopathological Society. https://doi.org/10.1094/PDIS-07-19-1570-PDN

Gil, J., Ortega, L., Rojas, J. A., & Rojas, C. M. (2022). Genome Sequence Resource of Burkholderia glumae UAPB13. PhytoFrontiers™, 2(2), 140-142.

Gunasena, M. T., Rafi, A., Mohd Zobir, S. A., Hussein, M. Z., Ali, A., Kutawa, A. B., Abdul Wahab, M. A., Sulaiman, M. R., Adzmi, F., & Ahmad, K. (2022). Phytochemicals Profiling, Antimicrobial Activity and Mechanism of Action of Essential Oil Extracted from Ginger (Zingiber officinale Roscoe cv. Bentong) against Burkholderia glumae Causative Agent of Bacterial Panicle Blight Disease of Rice. Plants (Basel), 11(11), 1466–. https://doi.org/10.3390/plants11111466

Ham J H, Groth D E. 2011. Bacterial Panicle Blight, an Emerging Rice Disease. Baton Rouge, Louisiana, USA: Louisiana State University Agricultural Center: 16–17.

Ham J H, Melanson R A, Rush M C. 2011. Burkholderia glumae: Next major pathogen of rice? Mol Plant Pathol, 12(4): 329–339.

Hanson, L., & Minier, D. (2015). *RHIZOCTONIA SOLANI: UNDERSTANDING THE TERMINOLOGY*. http://arsftfbean.uprm.edu/bic/wpcontent/uploads/2018/05/BIC_2015_Annual_Report.pdf

Hao, L., Wang, H., Sunter, G., & Bisaro, D. M. (2003). Geminivirus AL2 and L2 proteins interact with and inactivate SNF1 kinase. Plant Cell, 15(4), 1034–1048. https://doi.org/10.1105/tpc.009530

Hikichi Y, Egami H, Oguri Y, Okuno T. Fitness for survival of Burkholderia glumae resistant to oxolinic acid in rice plants. Annals of the Phytopathological Society of Japan. 1998; 64:147-152

Hikichi Y, Tsujiguchi K, Maeda Y, Okuno T. Development of increased oxolinic acid-resistance in Burkholderia glumae. Journal of General Plant Pathology. 2001; 67:58-62

Hikichi Y. Relationship between population dynamics of Pseudomonas glumae on rice plants and disease severity of bacterial grain rot of rice. Journal of Pesticide Science. 1993; 18:319-324.

Hikichi, Y., Noda, C., & Shimizu, K. (1989). Oxolinic acid.

Hulsmans, S., Rodriguez, M., De Coninck, B., & Rolland, F. (2016). The SnRK1 Energy Sensor in Plant Biotic Interactions. Trends in Plant Science, 21(8), 648–661. https://doi.org/10.1016/j.tplants.2016.04.008

Karki H S, Shrestha B K, Han J W, Groth D E, Barphagha I K, Rush M C, Melanson R A, Kim B S, Han J H. 2012. Diversities in virulence, antifungal activity, pigmentation and DNA fingerprint among strains of Burkholderia glumae. PLoS One, 7: e45376.

Kim, C. Y., Vo, K. T. X., An, G., & Jeon, J. S. (2015). A rice sucrose non-fermenting-1 related protein kinase 1, OSK35, plays an important role in fungal and bacterial disease resistance. Journal of the Korean Society for Applied Biological Chemistry, 58(5), 669–675. https://doi.org/10.1007/s13765-015-0089-8

Kumar, K. V. K., Reddy, M. S., Kloepper, J. W., Lawrence, K. S., Groth, D. E. and Miller, M. E. 2009. Sheath blight disease of rice (Oryza sativa L.) - An overview. Biosci. Biotech. Res. Asia. 6: 465-480.

Kumar, V., Jain, P., Venkadesan, S., Karkute, S. G., Bhati, J., Abdin, M. Z., Sevanthi, A. M., Mishra, D. C., Chaturvedi, K. K., Rai, A., Sharma, T. R., & Solanke, A. U. (2021). Understanding rice-magnaporthe oryzae interaction in resistant and susceptible cultivars of rice under panicle blast infection using a time-course transcriptome analysis. *Genes*, *12*(2), 1–23. https://doi.org/10.3390/genes12020301

Lamichhane, J. R., Dürr, C., Schwanck, A. A., Robin, M.-H., Sarthou, J.-P., Cellier, V., et al. 2017. Integrated management of damping-off diseases. A review. Agron. Sustain. Dev. 37:10.

Lee, F. N. and Rush, M.C. 1983. Rice sheath blight: A major rice disease. Plant Dis. 67: 829-832.

Lee, Y. H., Ko, S. J., Cha, K. H., and Park, E. W. 2015. BGRcast: a disease forecast model to support decision-making for chemical sprays to control bacterial grain rot of rice. Plant Pathol. J. 31:350-362.

Li, L., Wang, L., Liu, L.-M., Hou, Y.-X., Li, Q.-Q., & Huang, S.-W. (2016). Infection Process of Burkholderia glumae Before Booting Stage of Rice. Journal of Phytopathology, 164(10), 825–832. https://doi.org/10.1111/jph.12502

Liu, L.-W., Hsieh, S.-H., Lin, S.-J., Wang, Y.-M., & Lin, W.-S. (2021). Rice Blast (Magnaporthe oryzae) Occurrence Prediction and the Key Factor Sensitivity Analysis by Machine Learning. Agronomy (Basel), 11(4), 771–. https://doi.org/10.3390/agronomy11040771

Liu, M., Zhang, S., Hu, J., Sun, W., Padilla, J., He, Y., Li, Y., Yin, Z., Liu, X., Wang, W., Shen, D., Li, D., Zhang, H., Zheng, X., Cui, Z., Wang, G.-L., Wang, P., Zhou, B., & Zhang, Z. (2019). Phosphorylation-guarded light-harvesting complex II contributes to broad-spectrum blast

resistance in rice. Proceedings of the National Academy of Sciences - PNAS, 116(35), 17572–17577. https://doi.org/10.1073/pnas.1905123116

Maeda Y, Horita M, Shinohara H, Kiba A, Ohnish K, Tsuchima S, et al. Analysis of sources of oxolinic acid-resistant field strains of Burkholderia glumae based on rep-PCR analysis and nucleotide sequences of gyrB and rpoD. Journal of General Plant Pathology. 2007;73:46-52

Maeda Y, Kiba A, Ohnish K, Hikichi Y. New method to detect oxolinic acid-resistant Burkholderia glumae infecting rice seeds using a mismatch amplification mutation assay polymerase chain reaction. Journal of General Plant Pathology. 2004;70:215-217

Marie Le Naour--Vernet, Florian Charriat, Jérôme Gracy, Sandrine Cros-Arteil, Sébastien Ravel, Florian Veillet, Isabelle Meusnier, André Padilla, Thomas Kroj, Stella Cesari, Pierre Gladieux bioRxiv 2023.03.16.532886; doi: https://doi.org/10.1101/2023.03.16.532886

Meng, Q., Gupta, R., Min, C. W., Kwon, S. W., Wang, Y., Je, B. Il, Kim, Y. J., Jeon, J. S., Agrawal, G. K., Rakwal, R., & Kim, S. T. (2019). Proteomics of Rice—Magnaporthe oryzae Interaction: What Have We Learned So Far? In *Frontiers in Plant Science* (Vol. 10). Frontiers Media S.A. https://doi.org/10.3389/fpls.2019.01383

Mizobuchi R, Fukuoka S, Tsushima S, Yano M, Sato H. QTLs for Resistance to Major Rice Diseases Exacerbated by Global Warming: Brown Spot, Bacterial Seedling Rot, and Bacterial Grain Rot. Rice. 2016; 9: 23. https://doi.org/10.1186/s12284-016-0095-4 PMID: 27178300

Nalley, L., Tsiboe, F., Durand-Morat, A., Shew, A., & Thoma, G. (2016). Economic and environmental impact of rice blast pathogen (Magnaporthe oryzae) alleviation in the United States. *PLoS ONE*, *11*(12). https://doi.org/10.1371/journal.pone.0167295

Nandakumar, R., Shahjahan, A. K. ., Yuan, X. ., Dickstein, E. ., Groth, D. ., Clark, C. ., Cartwright, R. ., & Rush, M. . (2009). Burkholderia glumae and B. gladioli Cause Bacterial Panicle Blight in Rice in the Southern United States. Plant Disease, 93(9), 896–905. https://doi.org/10.1094/PDIS-93-9-0896 Progress and challenges in improving the nutritional quality of rice (Oryza sativaL.).Crit.

Okubara, P. A., Dickman, M. B., & Blechl, A. E. (2014). Molecular and genetic aspects of controlling the soilborne necrotrophic pathogens Rhizoctonia and Pythium. In *Plant Science* (Vol. 228, pp. 61–70). Elsevier Ireland Ltd. https://doi.org/10.1016/j.plantsci.2014.02.001

Ortega, L., & Rojas, C. M. (2021). Bacterial Panicle Blight and Burkholderia glumae : From Pathogen Biology to Disease Control. Phytopathology, 111(5), 772–778. https://doi.org/10.1094/PHYTO-09-20-0401-RVW

Perochon, A., Váry, Z., Malla, K. B., Halford, N. G., Paul, M. J., & Doohan, F. M. (2019). The wheat SnRK1α family and its contribution to Fusarium toxin tolerance. Plant Science, 288. https://doi.org/10.1016/j.plantsci.2019.110217

Pinson SRM, Shahjahan AKM, Rush MC, Groth DE. Bacterial Panicle Blight Resistance QTLs in Rice and Their Association with Other Disease Resistance Loci and Heading Date. Crop Science. 2010; 50: 1287–1297. https://doi.org/10.2135/cropsci2008.07.0447

Rasband, W.S., ImageJ, U. S. National Institutes of Health, Bethesda, Maryland, USA, https://imagej.nih.gov/ij/, 1997-2018.

Rev. Food Sci. Nutr.57, 2455–2481. doi: 10.1080/10408398.2015.1084992

Ryan, J.R.Biosecurity and Bioterrorism: Containing and Preventing Biological Threats, 2nd ed.; Butterworth-Heinemann: Oxford, UK,2016; pp. 1–373.

Sayler R J, Cartwright R D, Yang Y N. 2006. Genetic characterization and real-time PCR detection of Burkholderia glumae, a newly emerging bacterial pathogen of rice in the United States. Plant Dis, 90(5): 603–610.

Shahjahan, A.K.M., Rush, M.C., Groth, D. and Clark, C.A. (2000) Panicle blight. Rice J. 15, 26–29.

Tan, J., Zhao, H., Li, J., Gong, Y., & Li, X. (2023). The Devastating Rice Blast Airborne Pathogen Magnaporthe oryzae—A Review on Genes Studied with Mutant Analysis. *Pathogens*, *12*(3), 379. https://doi.org/10.3390/pathogens12030379

Tsushima S, Naito H, Koitabashi M. Population dynamics of Pseudomonas glumae, the causal agent of bacterial grain rot of rice, on leaf sheaths of rice plants in relation to disease development in the field. Ann Phytopathol Soc Jpn. 1996;62:108–113. doi: 10.3186/jjphytopath.62.108.

Uppala, S. and Zhou, X.G. 2018. Field efficacy of fungicides for management of sheath blight and narrow brown leaf spot of rice. Crop Prot. 104: 72-77.

Wamishe YA, Belmar SB, Kelsey CD, Gebremariam TA, McCarty DL. Effects of excessive nitrogen fertilizer on rice diseases with emphasis to bacterial panicle blight. In: 35th Proceedings of Rice Technical Working Group (RTWG). New Orleans, Louisiana, USA; 2014. pp. 86-87

Wamishe, Y. A., Jia, Y., Singh, P., & Cartwright, R. D. (2007). Identification of field isolates of Rhizoctonia solani to detect quantitative resistance in rice under greenhouse conditions. *Frontiers of Agriculture in China*, *1*(4), 361–367. https://doi.org/10.1007/s11703-007-0061-4

Wamishe, Y., Cartwright, R., & Lee, F. (n.d.). *Arkansas Rice Production Handbook - MP192*.

Wamishe, Y., Gebremariam, T., Kelsey, S., Belmar, S., and Mulaw, S. 2019. Seed Dressing to Manage Seedling Diseases of Rice Caused by Rhizoctonia solani AG9, 2019. 14.

Wang, B. hua, Ebbole, D. J., & WANG, Z. hua. (2017). The arms race between Magnaporthe oryzae and rice: Diversity and interaction of Avr and R genes. In *Journal of Integrative Agriculture* (Vol. 16, Issue 12, pp. 2746–2760). Chinese Academy of Agricultural Sciences. https://doi.org/10.1016/S2095-3119(17)61746-5

Wang, X., Jia, Y., Wamishe, Y., Jia, M. H., & Valent, B. (2017). Dynamic Changes in the Rice Blast Population in the United States Over Six Decades. Molecular Plant-Microbe Interactions, 30(10), 803–812. https://doi.org/10.1094/MPMI-04-17-0101-R

Wilson, R. A., & Talbot, N. J. (2009). Under pressure: Investigating the biology of plant infection by Magnaporthe oryzae. In *Nature Reviews Microbiology* (Vol. 7, Issue 3, pp. 185–195). https://doi.org/10.1038/nrmicro2032

Yang G, Li C (2012) General description of Rhizoctonia species complex. In: Cumagun CJ (ed) Plant Pathology, pp 41–52

Yang, L., Zhao, M., Sha, G., Sun, Q., Gong, Q., Yang, Q., Xie, K., Yuan, M., Mortimer, J. C., Xie, W., Wei, T., Kang, Z., & Li, G. (2022). The genome of the rice variety LTH provides insight into its universal susceptibility mechanism to worldwide rice blast fungal strains. Computational and Structural Biotechnology Journal, 20, 1012–1026. https://doi.org/10.1016/j.csbj.2022.01.030

Yeshi Wamishe, Christy Kelsey, Scott Belmar, Tibebu Gebremariam, Danny McCarty. Bacterial Panicle Blight of Rice in Arkansas - FSA7580. Division of Agriculture, University of Arkansas System, 2021.

Yuan, J., Zhu, M., Lightfoot, D. A., Iqbal, M. J., Yang, J. Y., & Meksem, K. (2008). In silico comparison of transcript abundances during Arabidopsis thaliana and Glycine max resistance to Fusarium virguliforme. BMC Genomics, 9 Suppl 2(Suppl 2), S6–S6. https://doi.org/10.1186/1471-2164-9-S2-S6

Zaidi, S. S. e. A., Mukhtar, M. S., & Mansoor, S. (2018). Genome Editing: Targeting Susceptibility Genes for Plant Disease Resistance. In Trends in Biotechnology (Vol. 36, Issue 9, pp. 898–906). Elsevier Ltd. https://doi.org/10.1016/j.tibtech.2018.04.005

Zhang, J., Chen, L., Fu, C., Wang, L., Liu, H., Cheng, Y., Li, S., Deng, Q., Wang, S., Zhu, J., Liang, Y., Li, P., & Zheng, A. (2017). Comparative transcriptome analyses of gene expression changes triggered by Rhizoctonia solani AG1 IA infection in resistant and susceptible rice varieties. *Frontiers in Plant Science, 8*. https://doi.org/10.3389/fpls.2017.01422

Zhou, X. G. (2019). Sustainable strategies for managing bacterial panicle blight in rice. In Protecting rice grains in the post-genomic era. London, UK: IntechOpen.

Tables and figures

a) *Burkholderia glumae* growth curve (WT and 6-23)

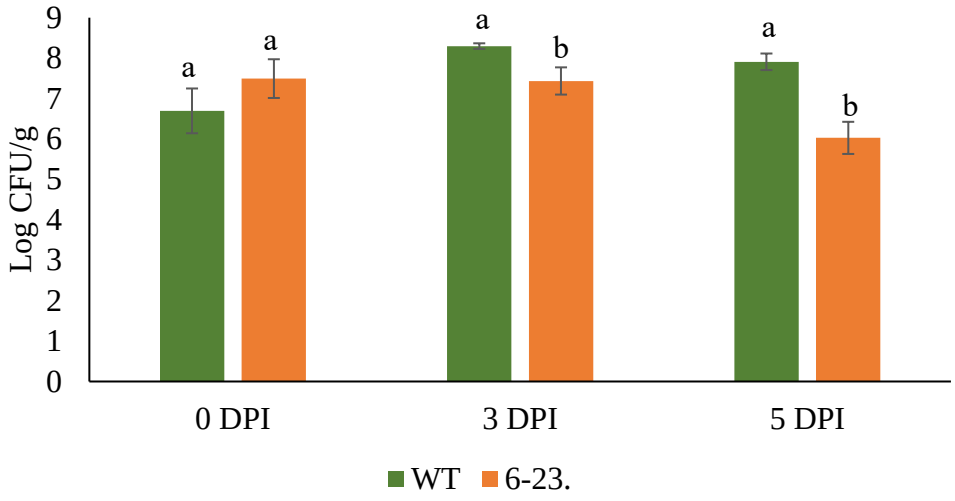

b) Symptoms panicles 5 DPI

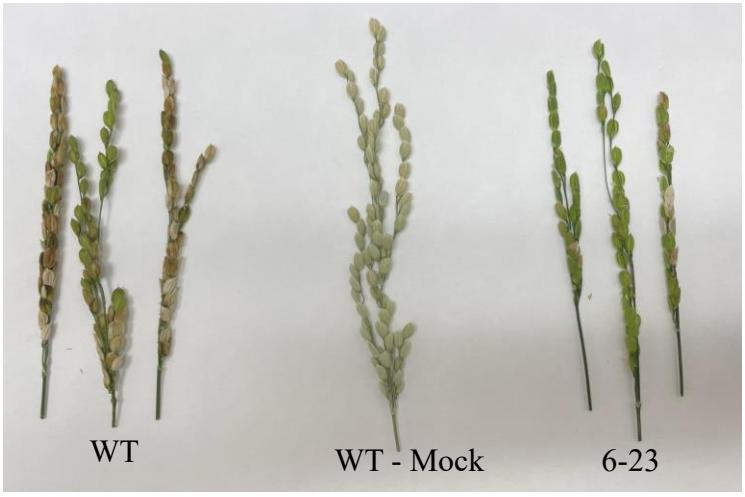

Figure 4.1. Disease response of *snrk1αc* mutant 6-23 against bacterial panicle blight pathogen. *snrk1αc* mutant 6-23 and WT cv. Kitaake were spray-inoculated with *B. glumae.* (a) *Burkholderia glumae* growth curve 0, 3 and 5 days post inoculation (DPI) in WT and *snrk1αc* mutant 6-23 panicles. Bars represent average bacterial numbers (Log CFU/g) for four replicates in each genotype. Data analyzed by Tukey HSD test and statistical differences are shown by letters on each box ($p \leq 0.05$). Values followed by the same letter are not significantly different. (b) Symptoms in panicles spray-inoculated with *B. glumae* of 5 DPI: WT, mock WT (negative control) and 6-23.

a) *Burkholderia glumae* growth curve (WT and 10-1)

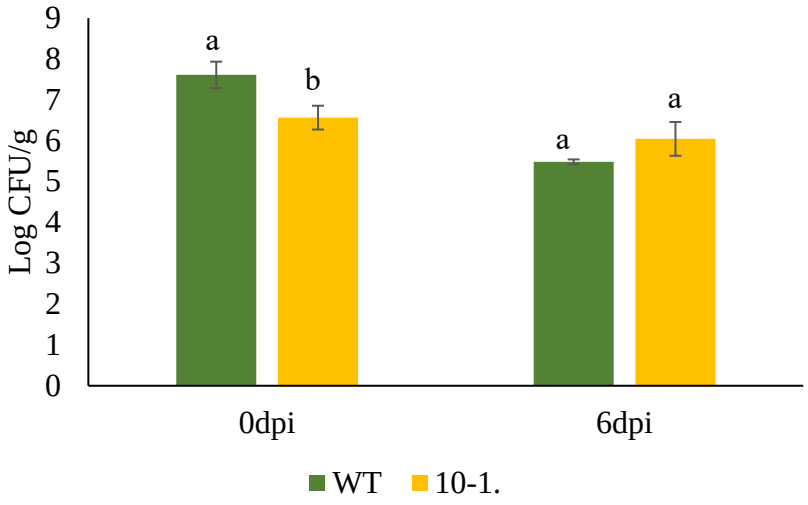

b) Symptoms panicles 6 DPI

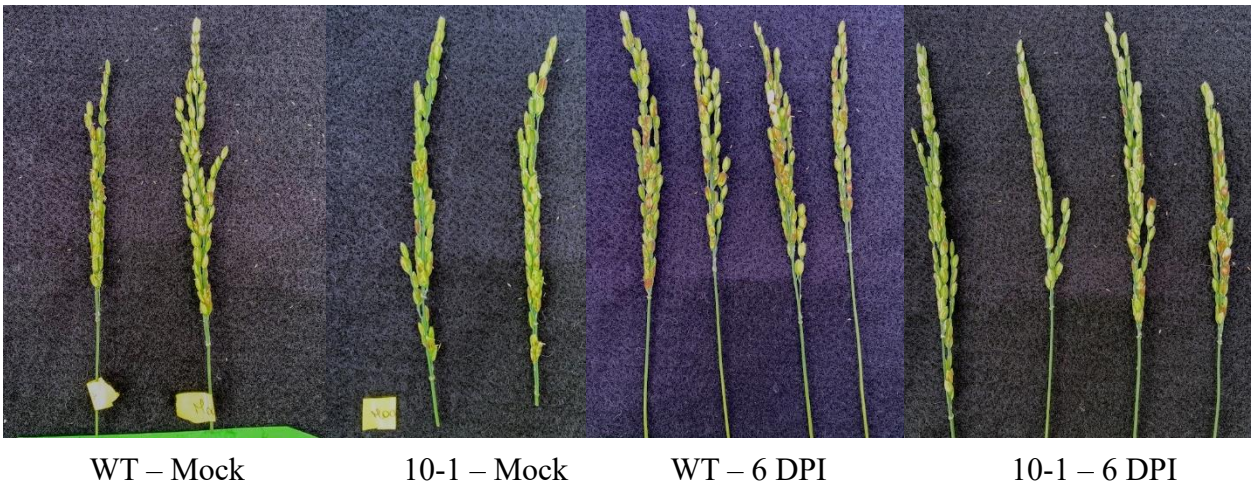

Figure 4.2. Disease response of *snrk1αc* mutant 10-1 against bacterial panicle blight pathogen. *snrk1αc* mutant 10-1 and WT cv. Kitaake were spray-inoculated with *B. glumae.* (a) *Burkholderia glumae* growth curve 0, 3 and 5 days pos inoculation (DPI) in WT and *snrk1αc* mutant 10-1 panicles. Bars represent average bacterial numbers (Log CFU/g) for four replicates in each genotype. Data analyzed by Tukey HSD test and statistical differences are shown by letters on each box ($p \leq 0.05$). Values followed by the same letter are not significantly different. (b) Symptoms in panicles spray-inoculated with *B. glumae* of 6 DPI and mock (negative control) in WT and 6-23.

***Burkholderia glumae* growth curve**

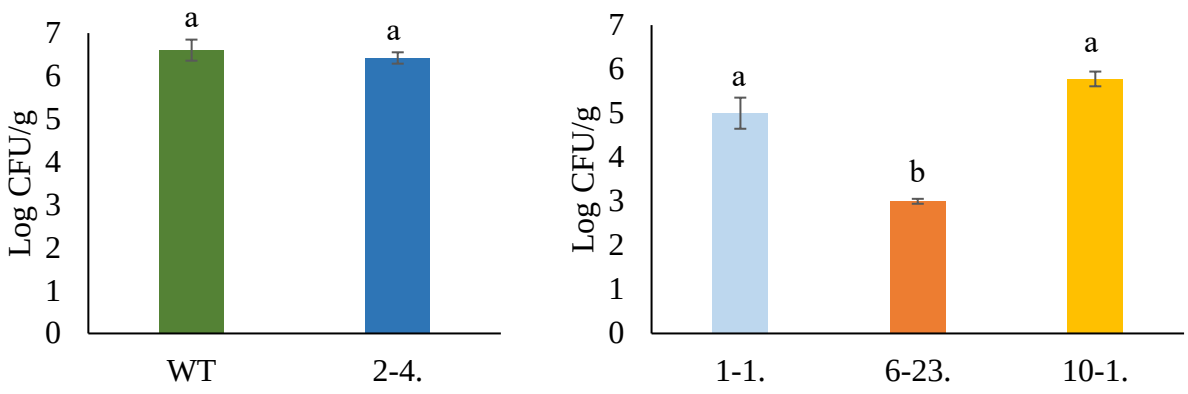

Figure 4.3 Disease response of *snrk1αa+b* and *snrk1αc* mutants against bacterial panicle blight pathogen. *Burkholderia glumae* growth curve 6 days post inoculation (DPI) in WT, *snrk1αc* mutants 10-1 and 6-23, *snrk1αa+b* mutants 1-1 and 2-4 panicles. Bars represent average bacterial numbers (Log CFU/g) for four replicates. Data analyzed by Tukey HSD test and statistical differences are shown by letters on each box ($p \leq 0.05$). Values followed by the same letter are not significantly different.

Mock (negative control) panicles

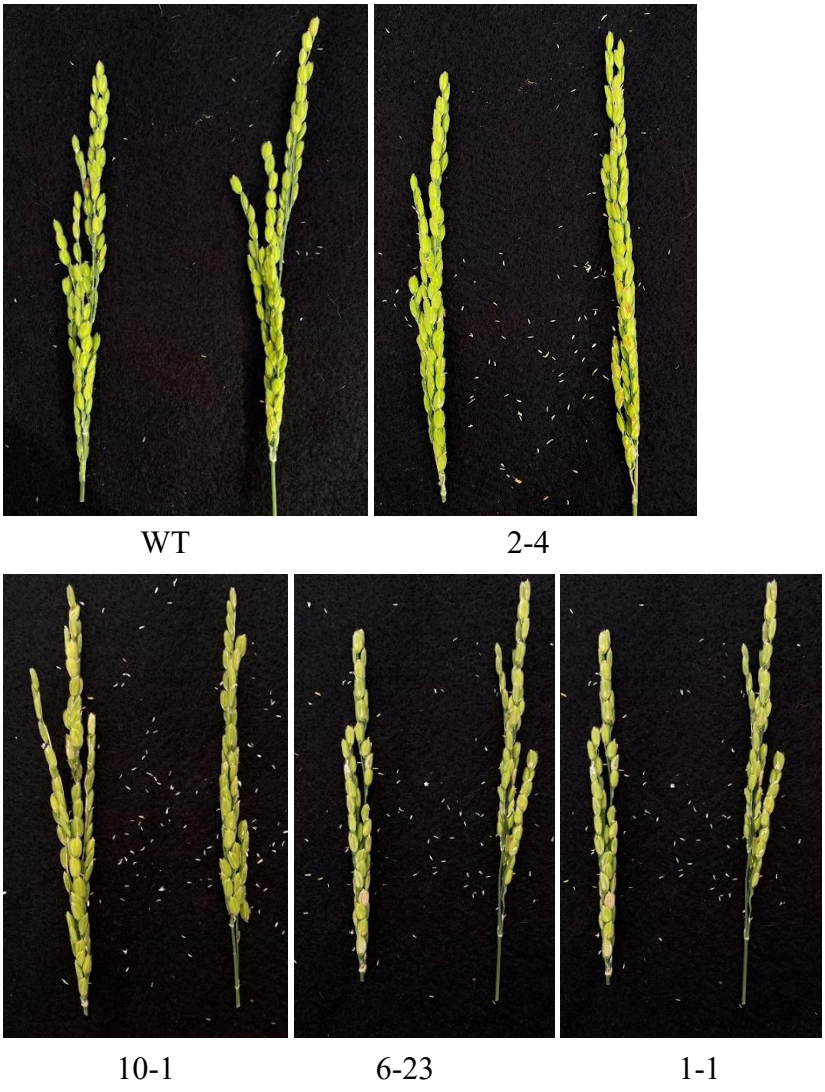

Figure 4.4 Mock treated panicles snrk1 mutants and the WT in panicles of 6DPI. Panicles of *snrk1αa+b* mutant lines 2-4 and 1-1 and *snrk1αc* mutant lines 10-1 and 6-23 along with the WT were mock-treated with water (negative control) and pictures were taken 6DPI.

Symptoms in panicles 6 DPI

WT 2-4

10-1 6-23 1-1

Figure 4.5 Symptoms in panicles inoculated with *Burkholderia glumae* of 6 DPI in WT and snrk1 mutants. Panicles of *snrk1αa+b* mutant lines 2-4 and 1-1 and *snrk1αc* mutant lines 10-1 and 6-23 along with the WT were spray-inoculated with *B. glumae* and pictures were taken 6DPI.

a) *Burkholderia glumae* growth in media

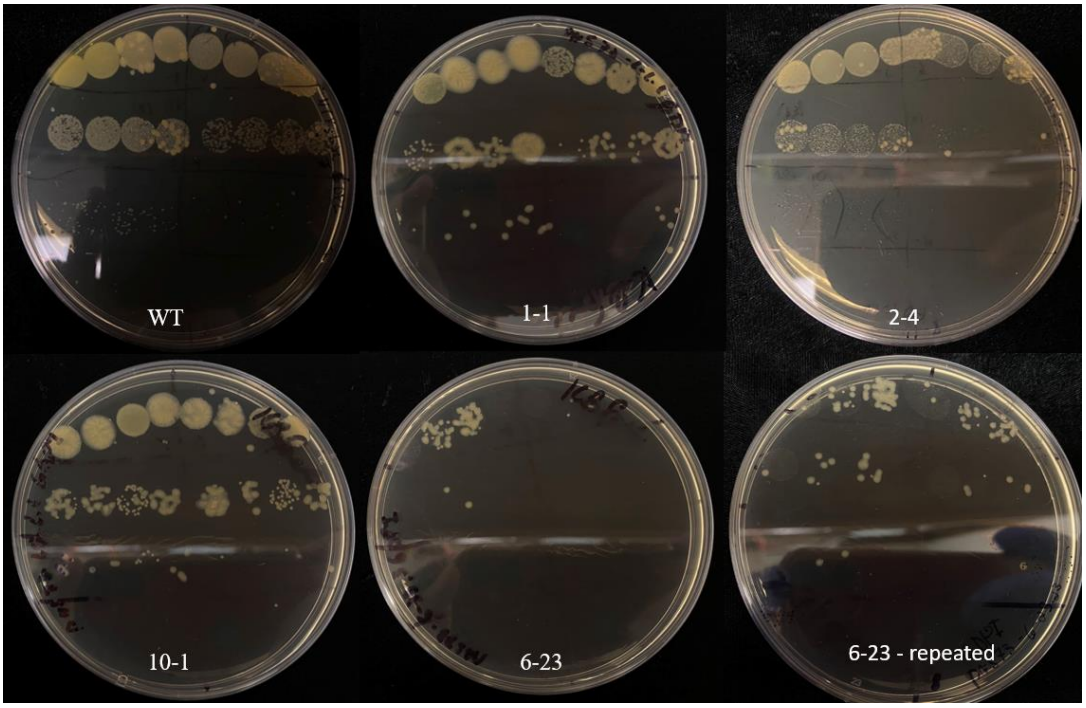

Figure 4.6 *Burkholderia glumae* growth in media in WT, 2-4, 10-1, 6-23 and 1-1 lines of 6DPI. At 6DPI the panicles were harvested for bacterial growth curve analysis. Each panicle was weighed, cut into small pieces, and ground using the 1600 MiniG machine (SPEX sample Prep). A 500 ml solution from each panicle of each genotype was transferred to 2 ml Eppendorf tubes. Each tube represented a repetition of one panicle and was diluted 8 times. Subsequently, 10 µl of each dilution was added to King's B (KB) media. The plates were incubated at 28 ˚C in an incubator for 48 hours, and the number of bacterial colonies was counted and used for statistical analysis. Picture shows KB media plates with *B. glumae* colonies.

a) Experiment 1: Emergence in Millet Control

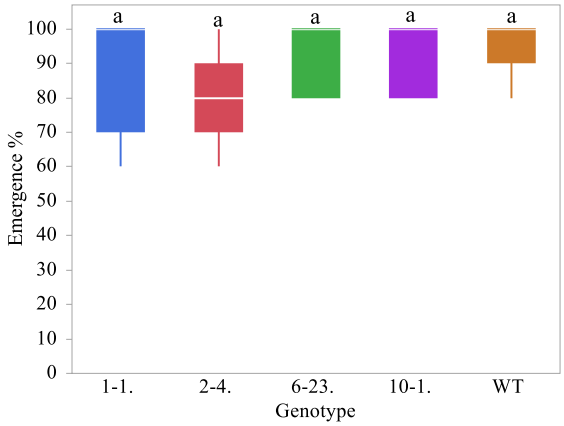

b) Experiment 1: Emergence in *R. solani AG 9*

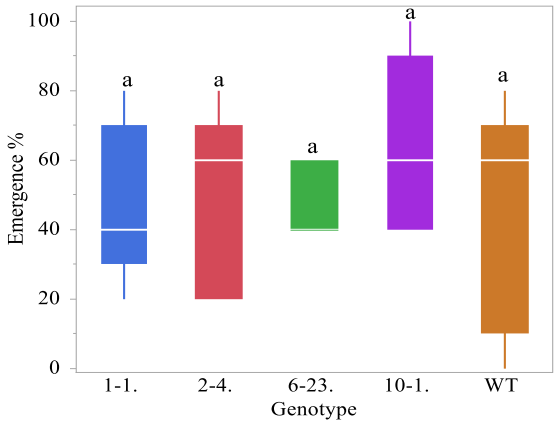

c) Experiment 1: Emergence in *R. solani* AG 4

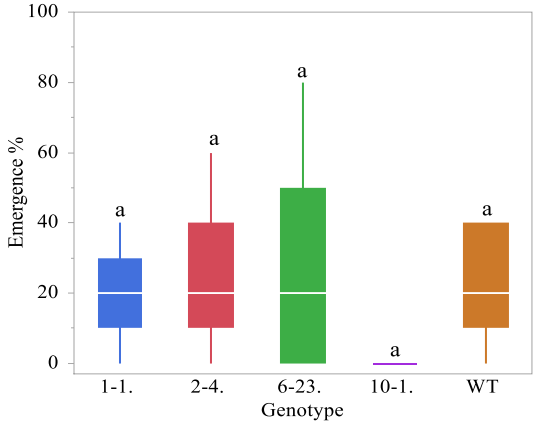

Figure 4.7 Evaluating plant emergence in *snrk1αa+b* mutants 1-1 and 2-4, *snrk1αc* mutants 6-23 and 10-1 along with the WT in millet (a) and against fungal pathogen *R. solani* AG 9 (b) and AG4 (c). It was planted a total of 25 seeds per genotype and treatment. Data was recorded 14 days post-planting. Letters above the error bars represent difference among emergence in genotypes. Values followed by the same letter are not significantly different at α=0.05 for comparisons of mean radius among treatments based on Tukey HSD test.

d) Experiment 1: Emergence in Millet, *R. solani* AG 9 and AG 4 and percentage decrease compared to Millet control

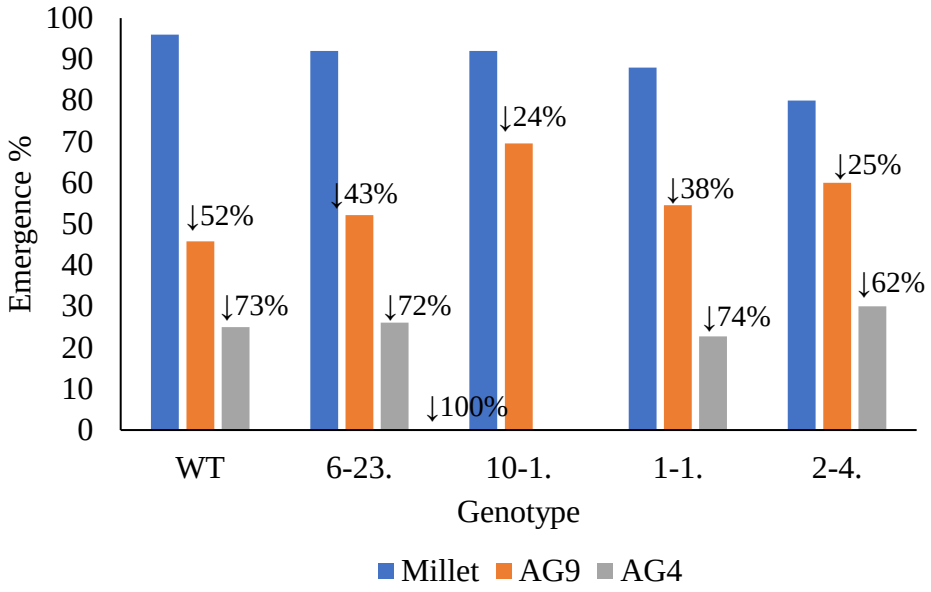

Figure 4.8 Comparison of plant emergence in *snrk1αa+b* mutants 1-1 and 2-4, *snrk1αc* mutants 6-23 and 10-1 along with the WT in millet (control) and in pathogen *R. solani* AG 9 and AG4. It was planted a total of 25 seeds per genotype and treatment. Data was recorded 14 days post-planting. Numbers above the bars represent percentage decrease of emergence compared with the millet control for each genotype.

a) Experiment 1: Average Plant and Root Weight in Millet Control

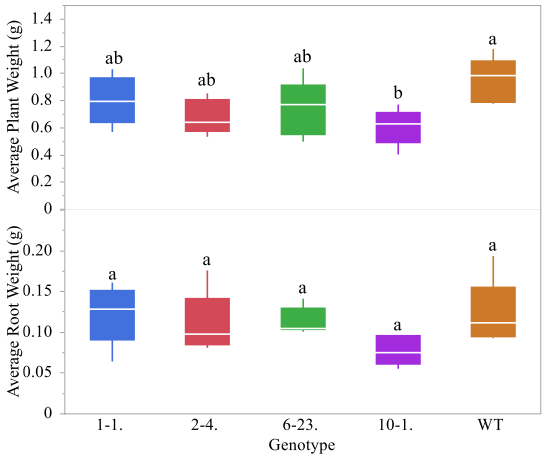

b) Experiment 1: Average Plant and Root Weight in *R. solani* AG 9

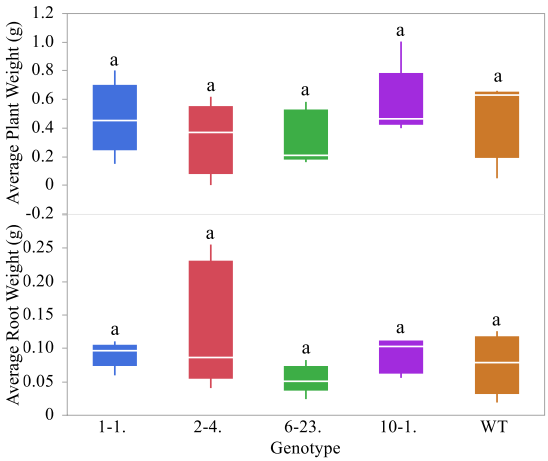

c) Experiment 1: Average Plant and Root Weight in *R. solani* AG 4

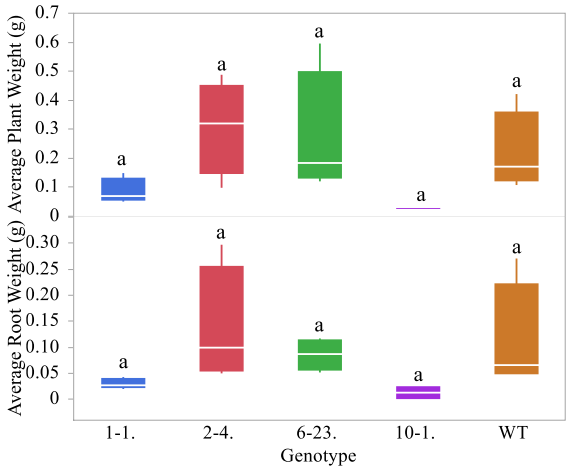

Figure 4.9 Evaluating average plant weight and root weight in *snrk1αa+b* mutants 1-1 and 2-4, *snrk1αc* mutants 6-23 and 10-1 along with the WT in millet (a) and against fungal pathogen *R. solani* AG 9 (b) and AG4 (c). Data was recorded 5 weeks post-planting. Letters above the error bars represent difference among emergence in genotypes. Values followed by the same letter are not significantly different at α=0.05 for comparisons of mean radius among treatments based on Tukey HSD test.

a) Experiment 1: Average Plant Weight (g) in Millet, *R. solani* AG 9 and AG 4 and percentage decrease compared to Millet control

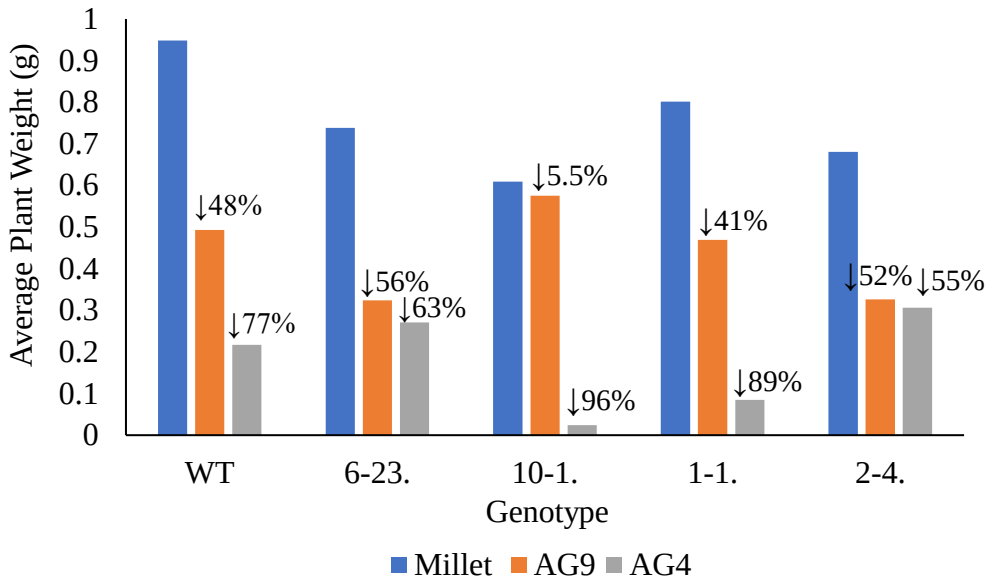

b) Experiment 1: Average Root Weight (g) in Millet, *R. solani* AG 9 and AG 4 and percentage decrease compared to Millet control

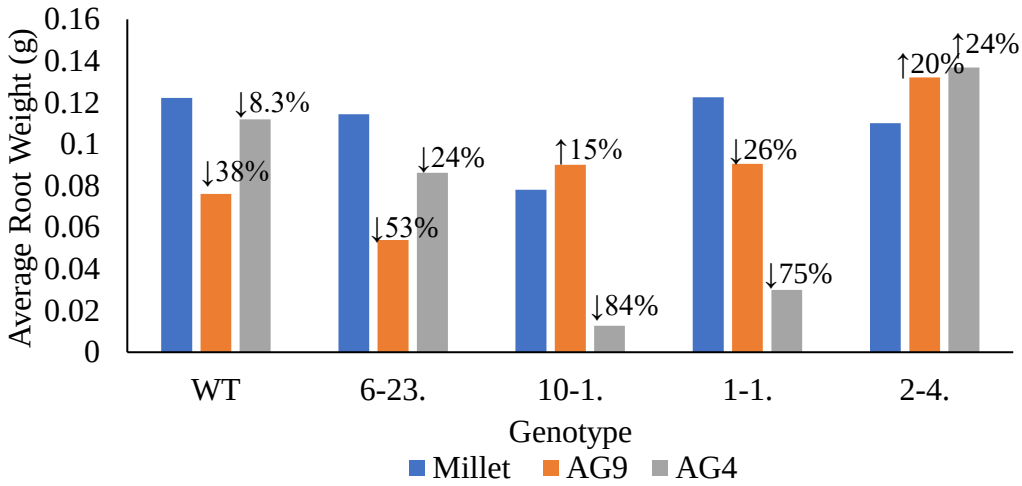

Figure 4.10 Comparison of plant weight (a) and root weight (b) in *snrk1αa+b* mutants 1-1 and 2-4, *snrk1αc* mutants 6-23 and 10-1 along with the WT in millet (control) and in pathogen *R. solani* AG 9 and AG4. Data was recorded 5 weeks post-planting. Numbers above the bars represent the percentage decrease of biomass compared with the millet control for each genotype.

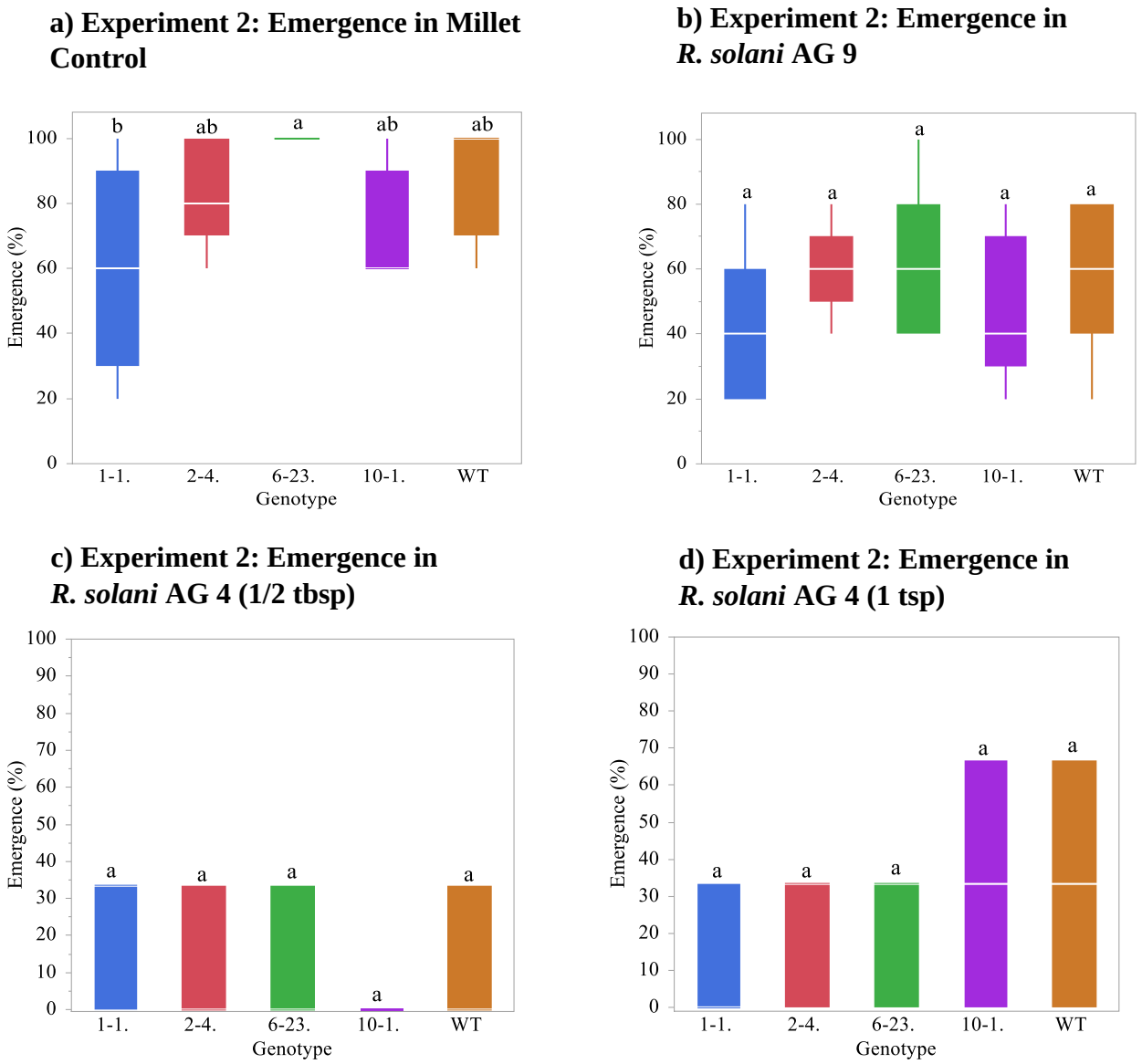

Figure 4.11 Evaluating plant emergence in *snrk1αa+b* mutants 1-1 and 2-4, *snrk1αc* mutants 6-23 and 10-1 along with the WT in millet (a) and against fungal pathogen *R. solani* AG 9 (b), AG 4 (1/2 tbsp) (c) and AG 4 (1 tsp) (d). It was planted a total of 25 seeds per genotype in millet and AG 9 treatment and it was planted a total of 15 seeds per genotype in AG 4 ½ tbsp and 1 tsp. Data was recorded 14 days post-planting. Letters above the error bars represent difference among emergence in genotypes. Values followed by the same letter are not significantly different at α=0.05 for comparisons of mean radius among treatments based on Tukey HSD test.

a) Experiment 2: Emergence in Millet, *R. solani* AG 9 and AG 4 and emergence percentage decrease compared to Millet control

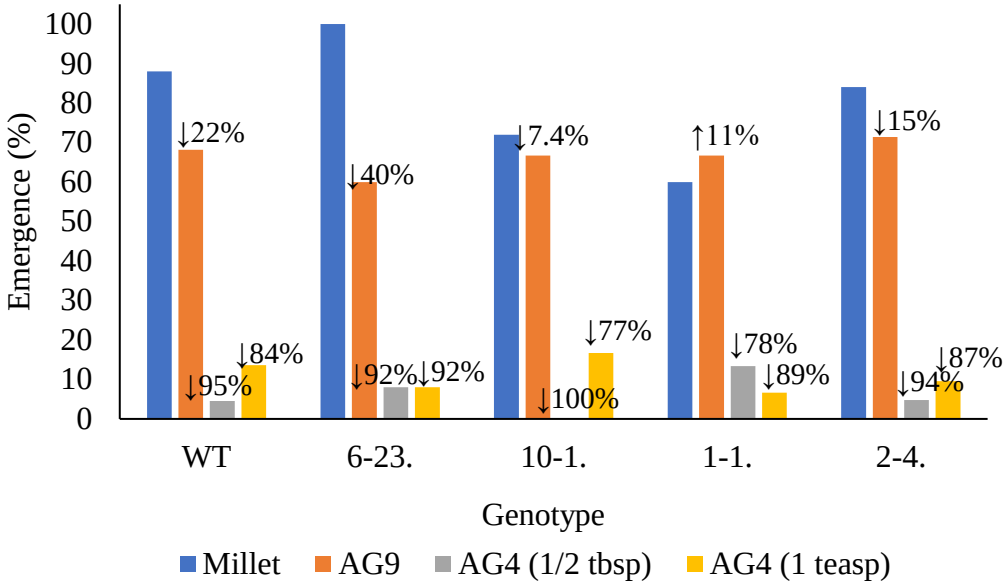

Figure 4.12 Comparison of plant emergence in *snrk1αa+b* mutants 1-1 and 2-4, *snrk1αc* mutants 6-23 and 10-1 along with the WT in millet (control) and in pathogen *R. solani* AG 9, AG 4 (1/2 tbsp) and AG 4 (1 tsp). It was planted a total of 25 seeds per genotype in millet and AG 9 treatment and it was planted a total of 15 seeds per genotype in AG 4 ½ tbsp and 1 tsp. Data was recorded 14 days post-planting. Numbers above the bars represent percentage decrease of emergence compared with the millet control for each genotype.

a) Experiment 2: Average Plant and Root Weight in Millet Control

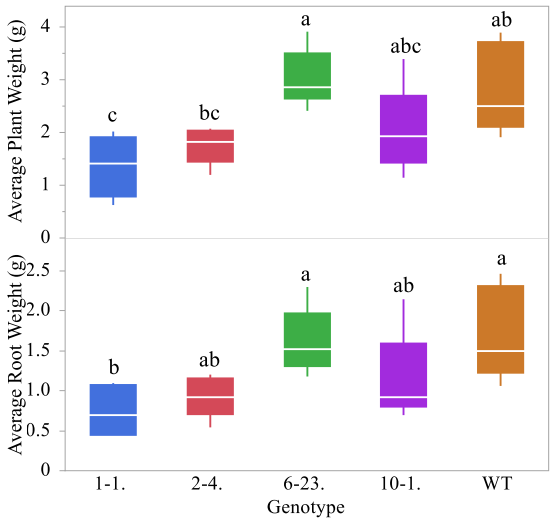

b) Experiment 2: Average Plant and Root Weight in *R. solani* AG 9

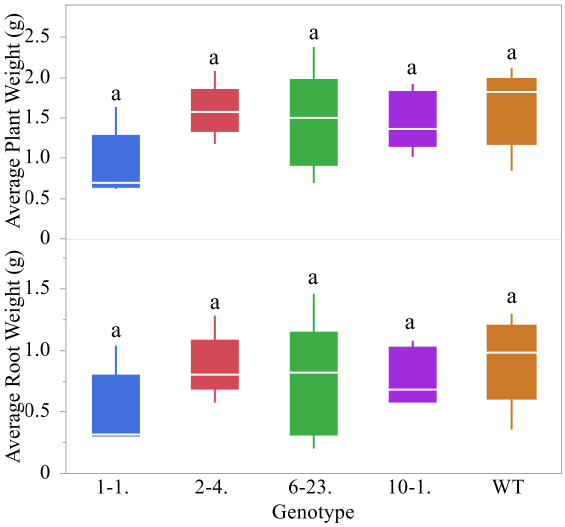

c) Experiment 2: Average Plant and Root Weight in *R. solani* AG 4 (1/2 tbsp)

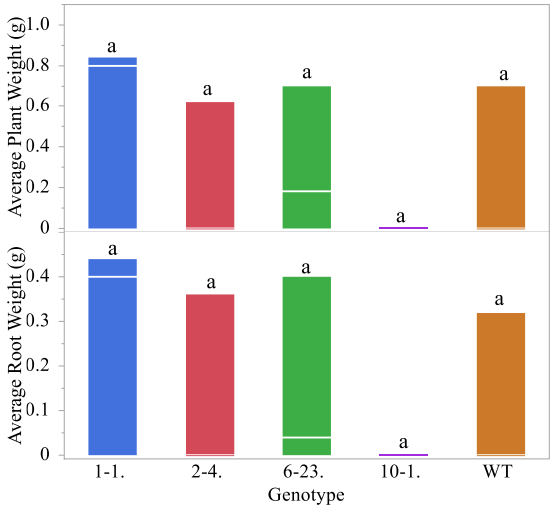

d) Experiment 2: Average Plant and Root Weight in AG 4 (1tsp)

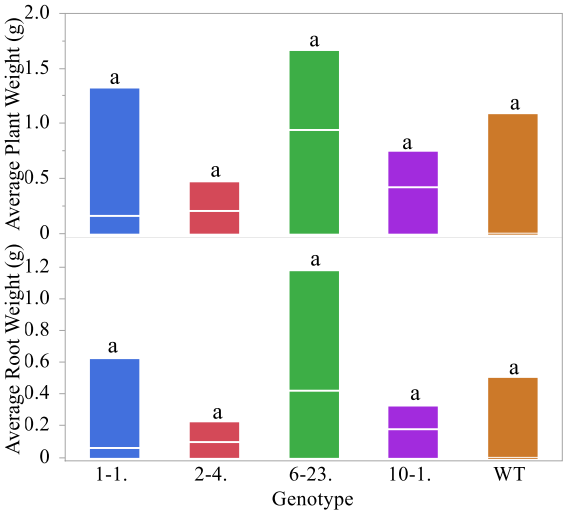

Figure 4.13 Evaluating average plant weight and root weight in *snrk1αa+b* mutants 1-1 and 2-4, *snrk1αc* mutants 6-23 and 10-1 along with the WT in millet (a) and against fungal pathogen *R. solani* AG 9 (b), AG 4 (1/2 tbsp) (c) and AG 4 (1 tsp) (d). Data was recorded 5 weeks post-planting. Letters above the error bars represent difference among emergence in genotypes. Values followed by the same letter are not significantly different at α=0.05 for comparisons of mean radius among treatments based on Tukey HSD test.

a) Experiment 2: Average Plant Weight (g) in Millet, *R. solani* AG 9, AG 4 (1/2 tbsp) and AG 4 (1tsp) and percentage decrease compared to Millet control

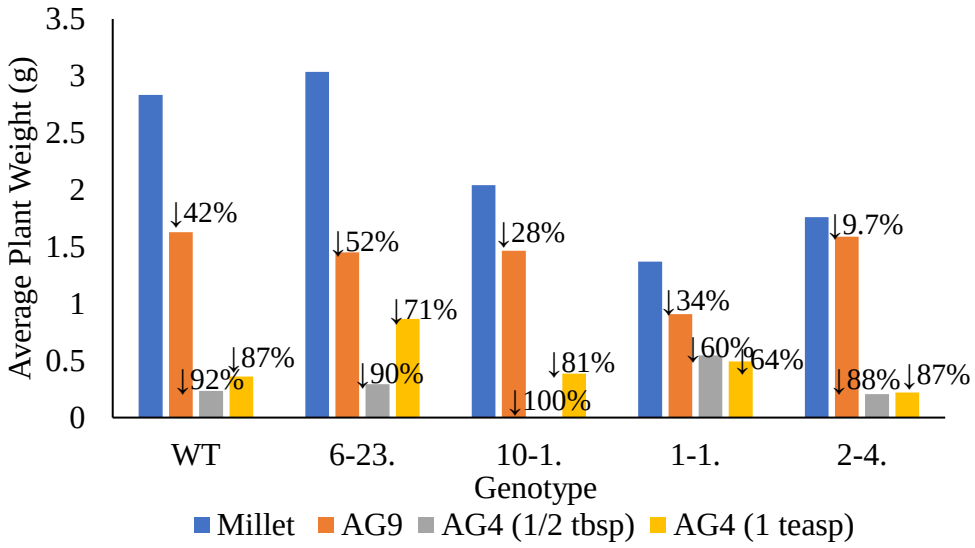

b) Experiment 2: Average Root Weight (g) in Millet, *R. solani* AG 9, AG 4 (1/2 tbsp) and AG 4 (1tsp) and percentage decrease compared to Millet control

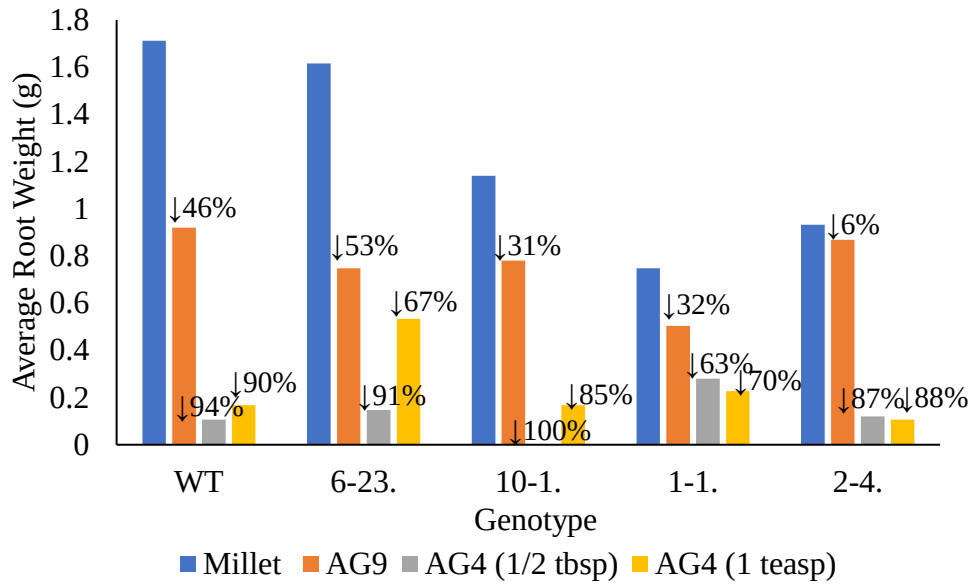

Figure 4.14 Comparison of plant weight (a) and root weight (b) in *snrk1αa+b* mutants 1-1 and 2-4, *snrk1αc* mutants 6-23 and 10-1 along with the WT in millet (control) and in pathogen *R. solani* AG 9, AG 4 (1/2 tbsp) and AG 4 (1 tsp). Data was recorded 5 weeks post-planting. Numbers above the bars represent the percentage decrease of biomass compared with the millet control for each genotype.

a) Lesion area (cm^2) in leaves inoculated with *Magnaporthe oryzae* strain Guy11

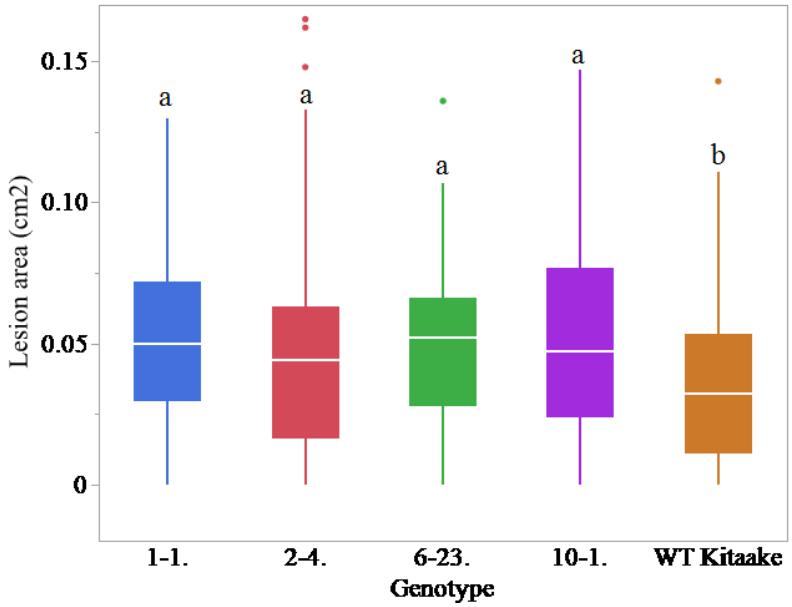

Figure 4.15 Lesion area (cm^2) in leaves inoculated with *Magnaporthe oryzae* strain Guy11 in *snrk1αa+b* mutants 1-1 and 2-4, *snrk1αc* mutants 6-23 and 10-1 along with the WT Kitaake. Combined data of four independent experiments were combined for analysis. Lesions were measured using auto threshold MaxEntropy of the ImageJ program. Data analyzed by Tukey HSD test and statistical differences are shown by letters on each box with 0.05 significance level ($p \leq 0.05$). Values followed by the same letter are not significantly different.

a) Gelatin control in leaves

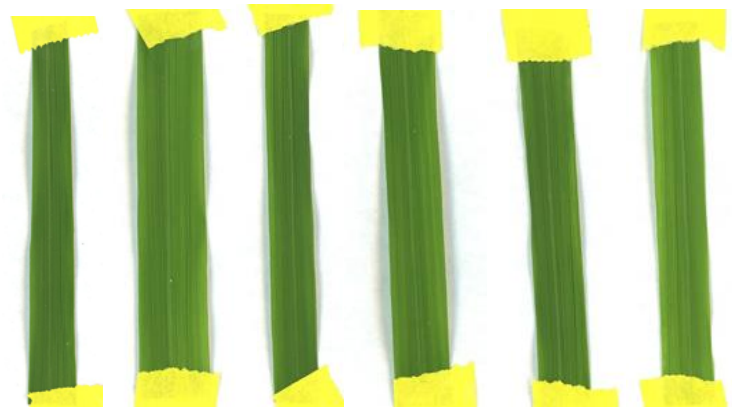

b) Lesion in leaves inoculated with *Magnaporthe oryzae* strain Guy11

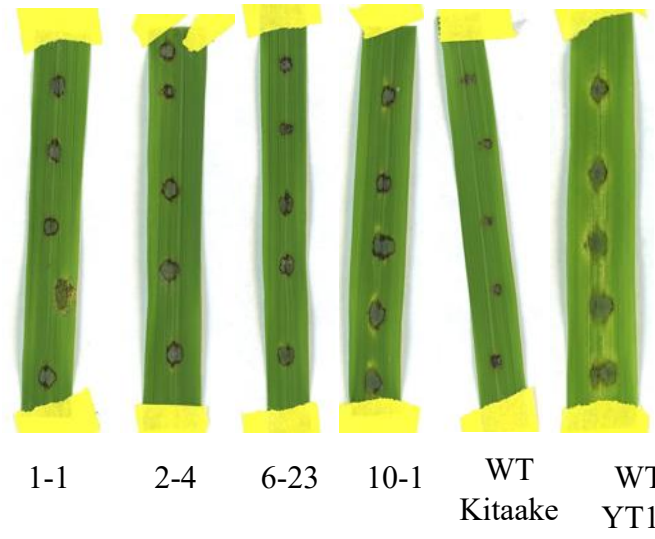

Figure 4.16 Evaluating disease symptoms in genotypes inoculated with *Magnaporthe oryzae* strain Guy11**.** (a) Gelatin (negative control) in WT Kitaake, WT YT16, 2-4, 10-1, 6-23 and 1-1 lines. (b) Symptoms in leaves of 5 days pos inoculation in each genotype.

Chapter V – Overall conclusions

SnRK1 is a global regulator of gene expression, orchestrating transcriptional networks involved in stress response and regulating genes associated with anabolic and catabolic processes. By regulating plant growth, development, and stress responses, SnRK1 acts as a central signaling pathway, triggering adaptive responses to promote plant survival.

This research focused on investigating the functions of SnRK1 paralogs through the evaluation of phenotypic and transcriptomic characteristics and disease responses in knockout mutants developed by CRISPR/Cas9-mediated targeted mutagenesis. The mutants consisted of double-mutant *snrk1αa+b* lines and single mutant *snrk1αc* lines. Phenotypic analysis of early-stage seedlings on ½ MS media revealed that *snrkαa+b* mutants exhibited reduced seedling length compared to the wild type (WT), while *snrk1αc* mutants showed no significant differences from the WT. However, in later developmental stages in the greenhouse, *snrk1αc* mutants displayed phenotypic variations in yield parameters, such as number of seeds per panicle and total weight of seeds per plant. These results indicate that *SnRK1αa* and *SnRK1αb* are predominantly expressed in early seedling stages, while *SnRK1αc* play a major role in later vegetative and reproductive phases.

Additionally, this study successfully validated the impact of SnRK1 mutations in two distinct rice lines, demonstrating similar transcriptomic changes as reported in previous studies on *snrk1* mutants. Transcriptomic analysis of 7-day-old seedlings shows that WT seedlings subjected to prolonged darkness to mimic starvation, exhibited upregulation in the defense response and secondary metabolic processes. Conversely, the dark-exposed *snrk1αa+b* mutant demonstrated downregulation in these biological processes, while showing an increase in light-induced processes like ribosome biogenesis, translation, and DNA replication. On the other hand,

dark-induced processes, such as catabolic process and regulation of hormone levels are upregulated in light grown *snrk1αa+b* mutant while biosynthesis processes are downregulated. The *snrk1αc* mutant showed minimal changes in the expression of biological processes, with few significant up or downregulations observed. Our results suggest that SnRK1 activity is essential for activating low energy, stress-induced transcriptional program under stress conditions and inhibiting it under energy-sufficient conditions.

Furthermore, this research investigated the response of *snrk1* mutants against three different diseases: rice blast caused by *Magnaporthe oryzae*, sheath blight caused by *Rhizoctonia solani*, and bacterial panicle blight caused by *Burkholderia glumae*. Previous research has demonstrated that pathogen susceptibility is increased by *SnRK1* mutation. In contrast, we found no evidence in our studies that the *snrk1αa+b* or *snrk1αc* mutants were more susceptible to sheath blight and bacterial panicle blight. However, we found that *snrk1* mutants were more susceptible to the blast fungus caused by *M. oryzae*, which is consistent with the literature and our transcriptomic findings that reveal downregulation of defense genes in *snrk1* mutants.

Overall, this study contributes to the understanding of the functions of SnRK1 in controlling energy homeostasis, regulating transcription factors and gene expression, as well as promoting plant growth, development, and plant defense against pathogens.

APPENDICES

Appendix Table 1. ANOVA for the shoot length of 2 days-old seedlings of *snrk1αa+b* line 1-1 and *snrk1αc* line 6-23

Analysis of Variance

Source	DF	Sum of Squares	Mean Square	F Ratio	Prob > F
SnRK line	2	44.581567	22.2908	53.9441	<.0001*
Error	50	20.660999	0.4132		
C. Total	52	65.242566			

Appendix Table 2. ANOVA for the root length of 2 days-old seedlings of *snrk1αa+b* line 1-1 and *snrk1αc* line 6-23

Analysis of Variance

Source	DF	Sum of Squares	Mean Square	F Ratio	Prob > F
SnRK line	2	37.44015	18.7201	12.1498	<.0001*
Error	47	72.41649	1.5408		
C. Total	49	109.85664			

Appendix Table 3. ANOVA for the shoot length of 7 days-old seedlings of *snrk1αa+b* line 1-1 and *snrk1αc* line 6-23

Analysis of Variance

Source	DF	Sum of Squares	Mean Square	F Ratio	Prob > F
SnRK line	2	74.00971	37.0049	4.6132	0.0189*
Error	27	216.58111	8.0215		
C. Total	29	290.59082			

Appendix Table 4. ANOVA for the shoot length of 3 days-old seedlings of *snrk1αa+b* line 2-4 and *snrk1αc* line 10-1

Analysis of Variance

Source	DF	Sum of Squares	Mean Square	F Ratio	Prob > F
SnRK line	2	14.958066	7.47903	10.2299	0.0002*
Error	46	33.630546	0.73110		
C. Total	48	48.588613			

Appendix Table 5. ANOVA for the root length of 3 days-old seedlings of *snrk1αa+b* line 2-4 and *snrk1αc* line 10-1

Analysis of Variance

Source	DF	Sum of Squares	Mean Square	F Ratio	Prob > F
SnRK line	2	0.801233	0.40062	0.2920	0.7481
Error	49	67.225539	1.37195		
C. Total	51	68.026772			

Appendix Table 4. ANOVA for the shoot length of 5 days-old seedlings of *snrk1αa+b* line 2-4 and *snrk1αc* line 10-1

Analysis of Variance

Source	DF	Sum of Squares	Mean Square	F Ratio	Prob > F
SnRK line	2	42.33685	21.1684	9.4928	0.0004*
Error	46	102.57728	2.2299		
C. Total	48	144.91413			

Appendix Table 7. ANOVA for the root length of 5 days-old seedlings of *snrk1αa+b* line 2-4 and *snrk1αc* line 10-1

Analysis of Variance

Source	DF	Sum of Squares	Mean Square	F Ratio	Prob > F
SnRK line	2	1.315560	0.65778	0.4653	0.6304
Error	55	77.751301	1.41366		
C. Total	57	79.066861			

Appendix Table 8. ANOVA for the shoot length of 4 days-old seedlings of *snrk1αa+b* lines 1-1 and 2-4 and *snrk1αc* lines 6-23 and 10-1

Analysis of Variance

Source	DF	Sum of Squares	Mean Square	F Ratio	Prob > F
SnRK line	4	8.23109	2.05777	1.0347	0.3937
Error	92	182.96558	1.98876		
C. Total	96	191.19667			

Appendix Table 9. ANOVA for the root length of 4 days-old seedlings of *snrk1αa+b* lines 1-1 and 2-4 and *snrk1αc* lines 6-23 and 10-1

Analysis of Variance

Source	DF	Sum of Squares	Mean Square	F Ratio	Prob > F
SnRK line	4	4.26921	1.06730	0.7506	0.5602
Error	91	129.39882	1.42197		
C. Total	95	133.66804			

Appendix Table 10. ANOVA for the shoot length of 9 days-old seedlings of *snrk1αa+b* lines 1-1 and 2-4 and *snrk1αc* lines 6-23 and 10-1

Analysis of Variance

Source	DF	Sum of Squares	Mean Square	F Ratio	Prob > F
SnRK line	4	53.50427	13.3761	2.1992	0.0752
Error	92	559.56974	6.0823		
C. Total	96	613.07401			

Appendix Table 11. ANOVA for the root length of 9 days-old seedlings of *snrk1αa+b* lines 1-1 and 2-4 and *snrk1αc* lines 6-23 and 10-1

Analysis of Variance

Source	DF	Sum of Squares	Mean Square	F Ratio	Prob > F
SnRK line	4	35.90611	8.97653	6.0649	0.0002*
Error	92	136.16743	1.48008		
C. Total	96	172.07354			

Appendix Table 12. ANOVA for the fresh biomass of 9 days-old seedlings of *snrk1αa+b* lines 1-1 and 2-4 and *snrk1αc* lines 6-23 and 10-1

Analysis of Variance

Source	DF	Sum of Squares	Mean Square	F Ratio	Prob > F
SnRK line	4	0.10045924	0.025115	15.9428	<.0001*
Error	92	0.14492839	0.001575		
C. Total	96	0.24538763			

Appendix Table 13. ANOVA for the shoot length of the greenhouse grown plants of *snrk1αc* mutants

Analysis of Variance

Source	DF	Sum of Squares	Mean Square	F Ratio	Prob > F
Genotype	3	1647.6742	549.225	11.0169	<.0001*
Error	51	2542.5101	49.853		
C. Total	54	4190.1843			

Appendix Table 14. ANOVA for the shoot biomass of the greenhouse grown plants of *snrk1αc* mutants

Analysis of Variance

Source	DF	Sum of Squares	Mean Square	F Ratio	Prob > F
Genotype	3	1333.0470	444.349	10.5560	<.0001*
Error	51	2146.8093	42.094		
C. Total	54	3479.8563			

Appendix Table 15. ANOVA for the root biomass of the greenhouse grown plants of *snrk1αc* mutants

Analysis of Variance

Source	DF	Sum of Squares	Mean Square	F Ratio	Prob > F
Genotype	3	17.29764	5.76588	3.2379	0.0296*
Error	51	90.81733	1.78073		
C. Total	54	108.11497			

Appendix Table 16. ANOVA for the root length of the greenhouse grown plants of *snrk1αc* mutants

Analysis of Variance

Source	DF	Sum of Squares	Mean Square	F Ratio	Prob > F
Genotype	3	116.77088	38.9236	3.1277	0.0336*
Error	51	634.68091	12.4447		
C. Total	54	751.45179			

Appendix Table 17. ANOVA for the number of seeds per panicle of the greenhouse grown plants of *snrk1αc* mutants

Analysis of Variance

Source	DF	Sum of Squares	Mean Square	F Ratio	Prob > F
Genotype	3	12127.557	4042.52	34.7404	<.0001*
Error	51	5934.547	116.36		
C. Total	54	18062.104			

Appendix Table 18. ANOVA for the weight of 100 seeds of the greenhouse grown plants of *snrk1αc* mutants

Analysis of Variance

Source	DF	Sum of Squares	Mean Square	F Ratio	Prob > F
Genotype	3	0.14616027	0.048720	2.6862	0.0625
Error	33	0.59853615	0.018137		
C. Total	36	0.74469642			

Appendix Table 19. ANOVA for the shoot length of the greenhouse grown plants of *snrk1αa+b* mutants

Analysis of Variance

Source	DF	Sum of Squares	Mean Square	F Ratio	Prob > F
Genotype	4	355.1075	88.7769	1.5079	0.2187
Error	39	2296.0308	58.8726		
C. Total	43	2651.1383			

Appendix Table 20. ANOVA for the shoot biomass of the greenhouse grown plants of *snrk1αa+b* mutants

Analysis of Variance

Source	DF	Sum of Squares	Mean Square	F Ratio	Prob > F
Genotype	4	306.78066	76.6952	5.1616	0.0020*
Error	39	579.49703	14.8589		
C. Total	43	886.27769			

Appendix Table 21. ANOVA for the root biomass of the greenhouse grown plants of *snrk1αa+b* mutants

Source	DF	Sum of Squares	Mean Square	F Ratio	Prob > F
Genotype	4	14.71373	3.67843	1.5313	0.2121
Error	39	93.68179	2.40210		
C. Total	43	108.39552			

Appendix Table 22. ANOVA for the root length of the greenhouse grown plants of *snrk1αa+b* mutants

Analysis of Variance

Source	DF	Sum of Squares	Mean Square	F Ratio	Prob > F
Genotype	4	253.0420	63.2605	2.2579	0.0804
Error	39	1092.6879	28.0176		
C. Total	43	1345.7299			

Appendix Table 23. ANOVA for the number of seeds per panicle of the greenhouse grown plants of *snrk1αa+b* mutants

Analysis of Variance

Source	DF	Sum of Squares	Mean Square	F Ratio	Prob > F
Genotype	4	825.2679	206.317	3.5203	0.0159*
Error	36	2109.8834	58.608		
C. Total	40	2935.1512			

Appendix Table 24. ANOVA for the weight of 100 seeds of the greenhouse grown plants of *snrk1αa+b* mutants

Analysis of Variance

Source	DF	Sum of Squares	Mean Square	F Ratio	Prob > F
Genotype	4	0.5962282	0.149057	9.3995	<.0001*
Error	27	0.4281648	0.015858		
C. Total	31	1.0243930			

Appendix Table 25. ANOVA for the shoot length of the greenhouse grown plants of *snrk1αa+b* lines 1-1 and 2-4 and *snrk1αc* lines 6-23 and 10-1

Analysis of Variance

Source	DF	Sum of Squares	Mean Square	F Ratio	Prob > F
Genotype	4	1958.5193	489.630	8.6776	<.0001*
Error	74	4175.4083	56.424		
C. Total	78	6133.9276			

Appendix Table 26. ANOVA for the shoot biomass of the greenhouse grown plants of *snrk1αa+b* lines 1-1 and 2-4 and *snrk1αc* lines 6-23 and 10-1

Analysis of Variance

Source	DF	Sum of Squares	Mean Square	F Ratio	Prob > F
Genotype	4	1775.0240	443.756	23.0651	<.0001*
Error	72	1385.2301	19.239		
C. Total	76	3160.2540			

Appendix Table 27. ANOVA for the root biomass of the greenhouse grown plants of *snrk1αa+b* lines 1-1 and 2-4 and *snrk1αc* lines 6-23 and 10-1

Analysis of Variance

Source	DF	Sum of Squares	Mean Square	F Ratio	Prob > F
Genotype	4	89.84682	22.4617	7.8680	<.0001*
Error	76	216.96608	2.8548		
C. Total	80	306.81289			

Appendix Table 28. ANOVA for the total weight of seeds per plant of the greenhouse grown plants of *snrk1αa+b* lines 1-1 and 2-4 and *snrk1αc* lines 6-23 and 10-1

Analysis of Variance

Source	DF	Sum of Squares	Mean Square	F Ratio	Prob > F
Genotype	4	547.08916	136.772	37.6064	<.0001*
Error	61	221.85364	3.637		
C. Total	65	768.94280			

Appendix Table 29. ANOVA for the number of seeds per panicle of the greenhouse grown plants of *snrk1αa+b* lines 1-1 and 2-4 and *snrk1αc* lines 6-23 and 10-1

Analysis of Variance

Source	DF	Sum of Squares	Mean Square	F Ratio	Prob > F
Genotype	4	8621.195	2155.30	89.2999	<.0001*
Error	75	1810.163	24.14		
C. Total	79	10431.358			

Appendix Table 30. ANOVA for the weight of 100 seeds of the greenhouse grown plants of *snrk1αa+b* lines 1-1 and 2-4 and *snrk1αc* lines 6-23 and 10-1

Analysis of Variance

Source	DF	Sum of Squares	Mean Square	F Ratio	Prob > F
Genotype	4	0.15345528	0.038364	2.8613	0.0345*
Error	43	0.57654264	0.013408		
C. Total	47	0.72999792			

Appendix Table 31. ANOVA for the lesion area (cm^2) in leaves inoculated with *Magnaporthe oryzae* strain Guy11 in *snrk1αa+b* mutants 1-1 and 2-4, *snrk1αc* mutants 6-23 and 10-1

Analysis of Variance

Source	DF	Sum of Squares	Mean Square	F Ratio	Prob > F
Genotype	4	0.02182996	0.005457	5.2845	0.0004*
Error	527	0.54425106	0.001033		
C. Total	531	0.56608102			